

7
5
8

V393
.R46

#1

3

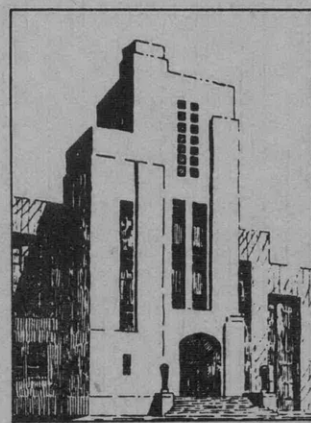


NAVY DEPARTMENT
THE DAVID W. TAYLOR MODEL BASIN
WASHINGTON 7, D.C.

THE WAVE RESISTANCE OF BODIES
OF REVOLUTION

by

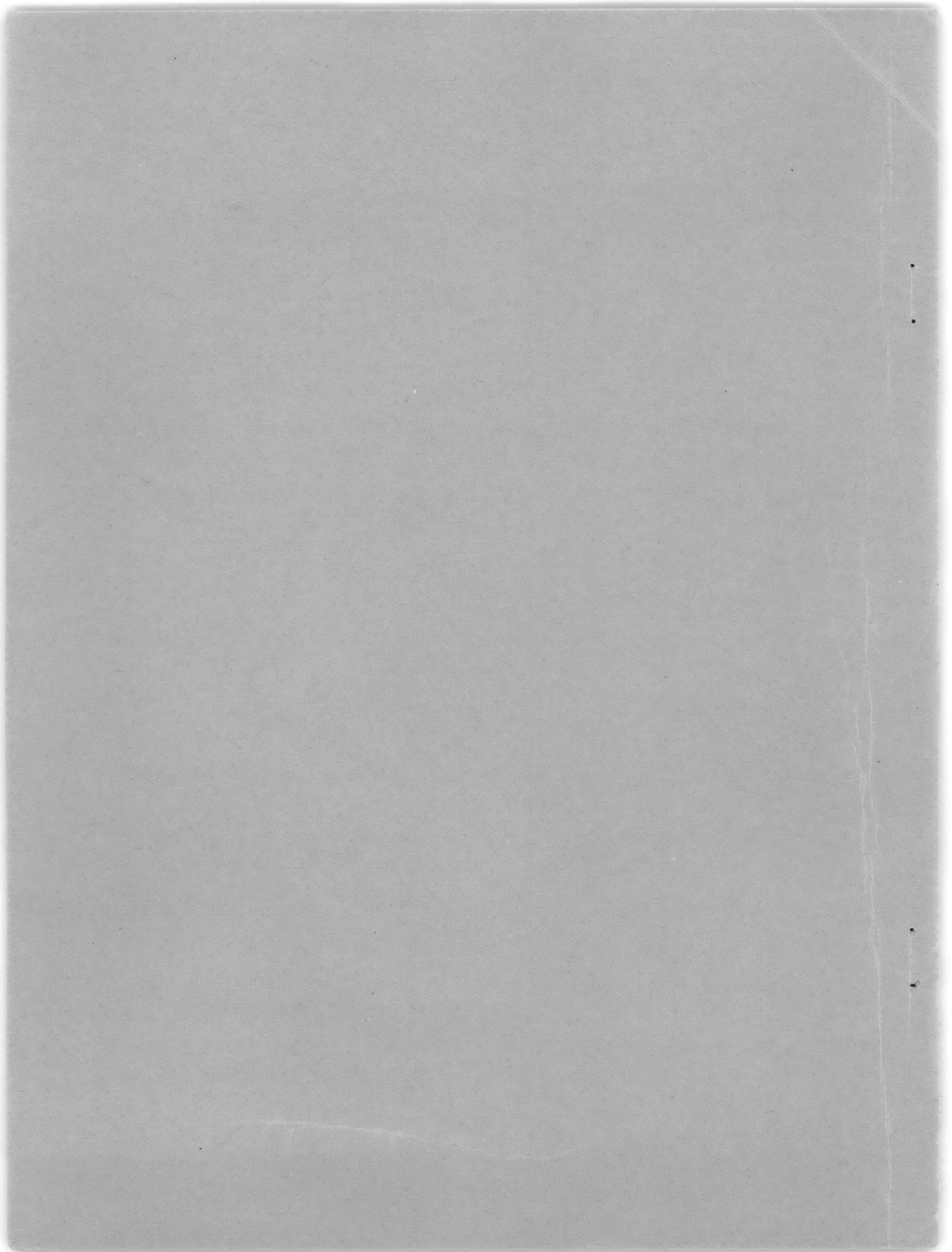
Georg P. Weinblum, D. Eng.
with a Contribution by
J. Blum, National Bureau of Standards



May 1951

Report 758

NS 715-084



INITIAL DISTRIBUTION

Copies

15 Chief, Bureau of Ships, Project Records (Code 324), for distribution:
5 Project Records
3 Research (Code 300)
2 Applied Science (Code 370)
1 Design (Code 410)
3 Preliminary Design (Code 420)
1 Technical Assistant to Chief of the Bureau (Code 106)

3 Chief, Bureau of Aeronautics, Aero and Hydrodynamics (DE-3)

5 Chief of Naval Research, for distribution:
3 Fluid Mechanics (N426)
2 Undersea Warfare (466)

4 Commander, U.S. Naval Ordnance Laboratory, Mechanics Division, White Oak, Silver Spring, Md.

1 Dr. J.H. McMillen, U.S. Naval Ordnance Laboratory, White Oak, Silver Spring, Md.

1 Commanding Officer and Director, U.S. Navy Underwater Sound Laboratory, Ft. Trumbull, New London, Conn.

1 Commanding Officer, U.S. Naval Torpedo Station, Design Section, Newport, R.I.

4 U.S. Maritime Administration, Washington, D.C.
1 Vice Admiral E.L. Cochrane, USN (Ret)
3 Director, Technical Division

4 British Joint Services Mission (Navy Staff)

2 British Joint Services Mission (Technical Services)

1 Australian Scientific Research Liaison Office, Washington, D.C.

1 Director, Hydrodynamics Laboratory, National Research Council, Ottawa, Canada

6 Director of Aeronautical Research, National Advisory Committee for Aeronautics, 1724 F St., N.W., Washington, D.C.

1 Capt. F.X. Forest, USN, Portsmouth Naval Shipyard, Portsmouth, N.H.

1 Director, Woods Hole Oceanographic Institution, Woods Hole, Mass.

Copies

- 2 Newport News Shipbuilding and Dry Dock Company, Newport News, Va., for distribution:
1 Senior Naval Architect
1 Supervisor, Hydraulic Laboratory
- 4 Director, Experimental Towing Tank, Stevens Institute of Technology, 711 Hudson St., Hoboken, N.J. Attn: Miss Jones
- 1 Dr. Hunter Rouse, Director, Iowa Institute of Hydraulic Research, State University of Iowa, Iowa City, Iowa
- 1 Dr. R.T. Knapp, Director, Hydrodynamic Laboratory, California Institute of Technology, Pasadena 4, Calif.
- 1 Dr. L.G. Straub, Director, St. Anthony Falls Hydraulic Laboratory, University of Minnesota, Minneapolis 14, Minn.
- 2 Director, Experimental Naval Tank, Department of Naval Architecture and Marine Engineering, University of Michigan, Ann Arbor, Mich.
- 2 Dr. V.L. Streeter, Illinois Institute of Technology, 3300 Federal Street, Chicago 16, Ill.
- 4 Head, Department of Naval Architecture and Marine Engineering, Massachusetts Institute of Technology, Cambridge 39, Mass.
- 1 Director, Applied Physics Laboratory, Johns Hopkins University, Silver Spring, Md.
- 1 Prof. W.S. Hamilton, Technological Institute, Northwestern University, Evanston, Ill.
- 2 Prof. G. Birkhoff, Harvard University, Cambridge, Mass.
- 1 Prof. K.E. Schoenherr, Dean, School of Engineering, University of Notre Dame, Notre Dame, Ind.
- 1 Prof. W. Spannhake, Armour Research Foundation, 35 West 33rd St., Chicago 16, Ill.
- 1 Dr. M.S. Plesset, California Institute of Technology, Pasadena 4, Calif.
- 1 Dr. Alexander Weinstein, Institute of Fluid Dynamics and Applied Mathematics, University of Maryland, College Park, Md.
- 1 Dr. J.V. Wehausen, Editor, Mathematical Review, Providence, R.I.
- 1 Librarian, American Society of Mechanical Engineers, 29 West Thirty-ninth Street, New York 18, N.Y.
- 5 Admiral S.M. Robinson, USN (Ret), Webb Institute of Naval Architecture, Crescent Beach Road, Glen Cove, Long Island, N.Y.

Copies

3 Mr. Tingey, Bethlehem Steel Corp., Shipbuilding Div., Quincy,
Mass.

2 Como. H.A. Schade, Director of Engineering Research, University
of California, Berkeley 4, Calif.

1 Prof. T.H. Havelock, 8 Westfield Drive, Gosforth, Newcastle-on-
Tyne 3, England

6 Commanding Officer, U.S. Naval Training Schools, Massachusetts
Institute of Technology, Cambridge 39, Mass.

1 Mr. C. Wigley, 6-9 Charterhouse Square, London EC-1, England

1 Prof. G. Schnadel, Ferdinandstr 58, Hamburg, West-Germany

1 Senior Naval Architect, Gibbs and Cox, Inc., 1 Broadway, New
York 4, N.Y.

1 Dr. J.F. Allen, Superintendent, Ship Division, National Physical
Laboratory, Teddington, Middlesex, England

1 Mr. R.W.L. Gawn, Superintendent, Admiralty Experiment Works,
Haslar, Gosport, England

1 Dr. A.G. Strandhagen, Head, Department of Engineering Mechanics,
University of Notre Dame, Notre Dame, Ind.

1 Dr. Max Schilhansl, Engineering Department, Brown University,
Providence, R.I.

1 Dr. W. Prager, Chairman, Graduate Division of Applied Mathematics,
Brown University, Providence, R.I.

2 Supervisor of Shipbuilding, USN, and Naval Inspector of Ordnance,
Electric Boat Company, Groton, Conn.

2 Prof. S.P. Timoshenko, Stanford University, Stanford University,
Calif.

1 Dr. C.H. Lee, U.S. Naval Postgraduate School, Annapolis, Md.

2 Librarian, Society of Naval Architects and Marine Engineers, 29
West 39th St., New York 18, N.Y.

: Mr. J. Blum, National Bureau of Standards, Washington 25, D.C.

TABLE OF CONTENTS

	Page
ABSTRACT	1
1. INTRODUCTION	1
2. THE REPRESENTATION OF SINGULARITY DISTRIBUTIONS AND SECTIONAL-AREA CURVES BY POLYNOMIALS	4
2.1. Connection between Body Form and Generating Hydrodynamic Singularities	4
2.2. Representation by Polynomials	6
2.2.1. General Remarks	6
2.2.2. The TMB (Landweber) Class of Bodies and Some Generalizations	7
2.3. Connection between Strength of Singularities and Body Shape	13
3. EVALUATION OF HAVELOCK'S INTEGRAL	14
3.1. General Considerations	14
3.2. Tabulation of Resistance Integrals for a Five-Parameter Class of Bodies	16
4. REPRESENTATION OF RESISTANCE CURVES	18
4.1. The Dimension Factor C_0 and Dimensionless Representations	18
4.2. Resistance Curves of Simple Symmetrical Bodies.	20
4.3. Resistance Curves of Asymmetrical Bodies	26
4.4. Limiting Depth of Immersion	37
5. BODIES OF REVOLUTION OF LEAST WAVE RESISTANCE	38
5.1. Two-Parameter Forms	38
5.2. Isoperimetric Problems, One-Parameter Forms	40
6. RESISTANCE CURVES OF THE FAMILY $(2, 4, 6; \phi; t)$	44
SUMMARY	45
APPENDIX I - APPROXIMATE CALCULATION OF THE SURFACE S OF A CLASS OF ELONGATED BODIES OF REVOLUTION	51
APPENDIX II - EVALUATION OF THE AUXILIARIES INTEGRALS*	53
APPENDIX III - AUXILIARY INTEGRALS FOR VARIOUS FROUDE NUMBERS.	55
REFERENCES	58

*By J. Blum, National Bureau of Standards

NOTATION

A	With index, a coefficient
A	Area
A_m	Area of meridian section
$A(x)$	Sectional-area curve
$A^*(\xi)$	Dimensionless sectional-area curve
a	Half length of distribution
a	As index, antisymmetry
b	Midship radius of body of revolution
C	Form parameter coefficient (Reference 7)
$C_o = 4\pi C^2 \rho g \frac{b^4}{a}$	Constant
$C_P = \phi$	Prismatic coefficient
$C_S = S/\pi DL$	Wetted surface coefficient
$D = 2b$	Midship diameter
$F = \frac{U}{\sqrt{gL}}$	Froude number
$F_f = \frac{U}{\sqrt{gf}}$	Depth Froude number
f	Depth of immersion
h	Wave amplitude
$K_o = \frac{g}{u^2}$	Wave number
L	Length of body
M	Auxiliary integral
M'	Auxiliary integral
m	Auxiliary integral
m'	Auxiliary integral
P	Intermediate integral
p	Intermediate integral
Q	Intermediate integral
q	Intermediate integral
R	Resistance, wave resistance
R_t	Total Resistance
R_v	Viscous resistance
R_w	Wave resistance
r_1	Resistance coefficient
r_o	Resistance coefficient

S	Wetted surface
s	As index, symmetry
U	Speed of advance
x	Longitudinal coordinate
x_0	Longitudinal distance of centroid
y	Ordinate of the meridian contour
η	Dimensionless ordinate of the sectional-area curve
$\eta_F \eta_A$	Dimensionless ordinate of the sectional-area curve fore and after body
$\eta_S \eta_a$	Dimensionless ordinate of the sectional-area curve even and odd part
θ	Variable of integration
$\mu(x), \mu^*(\xi)$	Doublet distribution
ξ	Dimensionless longitudinal coordinate
ξ_0	Dimensionless longitudinal distance of centroid
ρ	Density
$\sigma(x), \sigma^*(\xi)$	Source-sink distribution
ϕ_A	Prismatic coefficient; afterbody
ϕ_F	Prismatic coefficient; forebody

THE WAVE RESISTANCE OF BODIES OF REVOLUTION

by

Georg P. Weinblum, D.Eng.

ABSTRACT

Following a brief review of prior work on wave resistance of bodies of revolution carried out by Havelock and Weinblum a discussion is presented of the approximate relations between the shape of sectional-area curves and of hydrodynamic irregularity distributions. The latter are expressed by polynomials, which lend themselves to an evaluation of the basic resistance integrals by computing intermediate integrals. Values of the functions thus obtained are tabulated in an appendix. These functions are then used to calculate the resistance of some simple bodies of revolution. Also investigated is how the resistance is influenced by asymmetry with respect to midship section. Distributions leading to bodies of least wave resistance are calculated, assuming rather severe restrictions. A rather complete set of resistance curves is given for an important family of bodies.

1. INTRODUCTION

When a body moves uniformly and rectilinearly in an unbounded liquid the only resistance experienced by it is the viscous drag. Our knowledge as to how this drag depends upon the body form is very limited, but it is well-established that for streamlined, elongated hulls—with which we are only concerned—the drag is roughly proportional to the wetted surface and is rather insensitive to reasonable changes in the shape.^{1*} The well-known airship form with a rather blunt forebody and finer tail appears to be close to the minimum resistance attainable, although it must be emphasized that earlier resistance data obtained in wind tunnels at low Reynolds numbers are utterly unreliable. But that there is a slight advantage in introducing some asymmetry with respect to the midship section appears to be unquestioned, at least when larger end-radii are used. Matters become different when a body moves close to the free surface; see Figure 1. A wave pattern is then produced and therefore a wave resistance arises. The laws governing the wave resistance R_w are quite different from those valid

¹References are listed on page 58.

*Problems of cavitation are not considered here.

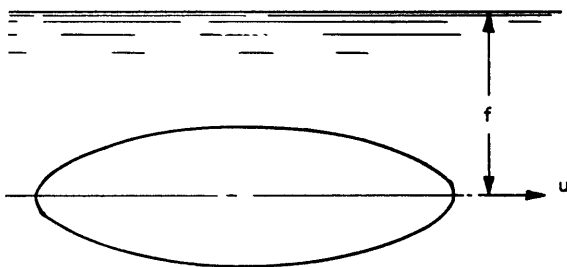


Figure 1 - Scheme of Submerged Body

elongated bodies of revolution, using an integral relation based on the work of Havelock.² The first classical solutions for the circular cylinder (Lamb)¹⁷ and the sphere (Havelock)¹⁸ have contributed much to the general understanding of the subject, but these solutions must be applied with great caution to problems connected with elongated bodies. The reason herein is the extreme simplicity of the cylinder and sphere; the resistance curves of these bodies do not show the characteristic interference effects which are peculiar for prolate bodies of revolution. From physical reasoning we infer at once that in the latter case two similarity parameters are involved: the common Froude number $F = U/\sqrt{gL}$ referred to the length L and a parameter characterising the depth of immersion f , say f/L or the depth Froude number $F_f = U/\sqrt{gf}$, while the shape of the wave-resistance curves for the circular cylinder and the sphere depend only upon F_f , and the parameter f/L appears as a scaling factor only. Thus, for instance, the peak of the resistance curve is located at $F_f = 1$ for the cylinder and just below $F_f = 1$ for the sphere. It can be easily shown that this unity value of the depth Froude number has no special significance for the wave resistance of a very elongated body of revolution.

Solutions for the spheroid and general ellipsoid due to Havelock^{3,4} lead to results which admit of qualitative and even of quantitative estimates of the resistance of "normal" bodies of revolution. The importance of the spheroid for general research on the subject cannot be overemphasized.

Using Havelock's general expression valid for a plane source-sink distribution,³ formulas were obtained which represent the wave resistance of a rather wide class of bodies of revolution.⁵ By these formulas the resistance of various forms has been investigated;⁶ especially, some endeavors were made to find forms of least wave resistance.⁵ These forms vary obviously with the Froude number and to a lesser degree with the depth parameter f/L . The rather striking results found in this way were checked experimentally and good agreement between theory and measurements was established as to the general trend.⁶

for the viscous drag R_v . Hence, in this case forms of least total resistance R_t must be derived from additional considerations and may differ, at least in principle, from the familiar streamlined forms.

In the present report it is intended to analyze the wave resistance of a rather wide class of

As with surface vessels, theoretical forms of least wave resistance are symmetrical with respect to the midship section. Any departure from symmetry causes an increase in wave resistance, and this increase can become appreciable in some ranges of Froude numbers when the asymmetry is pronounced. The degree of asymmetry can be described in the usual way, though roughly, by the location of the center of buoyancy x_0 , or the difference of the prismatic coefficients ϕ_F , ϕ_A of the fore and afterbody. For instance, a difference $\phi_F - \phi_A \cong 0.2$ means a large deviation from symmetry. Again, the resistance results are qualitatively supported by experiments.⁶

An extensive hydrodynamic study of bodies of revolution is underway at the Taylor Model Basin. It is based on a systematic variation of analytically defined forms.^{2, 11} As an extension of this work it was decided to make a more comprehensive theoretical investigation on the wave resistance of bodies of revolution. This is the subject of the present report.

In Section 1 of this report polynomials are discussed which are suitable for the representation of hydrodynamic singularity distributions (doublets, sources and sinks); to the first approximation the equation of the doublet distribution coincides with the equation of the sectional-area curve except for a scale factor.^{7, 8} A class of curves is selected which includes the TMB Series² generalized by one additional arbitrary parameter. For this family a set of auxiliary integrals covering a large range of Froude numbers has been tabulated. The values of these integrals furnish immediately the variable part of the wave resistance of the simplest forms (parabolas of the type $1 - \xi^n$). In the general case the wave resistance is given by a quadratic form of the parameters of the body in which the tabulated values appear as coefficients. Thus the computation of the wave resistance involves only some multiplications and an algebraic addition.

The auxiliary integrals mentioned have been computed by the Bureau of Standards. A short description of the work involved, contributed by Mr. Blum of that Bureau, and tables of functions are found in Appendices II and III.

As mentioned before, the resistance formula for a line distribution of singularities used throughout this report follows immediately from a more general expression due to Havelock^{3, 5} and therefore will be called Havelock's integral.

Using the tables annexed, resistance curves are plotted for various basic forms of sectional-area curves (doublet distributions); they cover three depths of immersion ratios f/L except for the spheroid where a fourth

f/L ratio has been added. Special investigations are made on the influence of asymmetry, and some examples of resistance curves refer to forms selected from the TMB Series.

Following an earlier attempt distributions of least wave resistance are investigated.⁵ Former results⁵ are checked and refined. Particularly, the distributions obtained lead to rather peculiar "swan-neck" forms, for higher Froude numbers. Finally it is shown how systematic sets of resistance curves can be obtained for families of sectional-area curves (doublet distributions).

2. THE REPRESENTATION OF SINGULARITY DISTRIBUTIONS AND SECTIONAL-AREA CURVES BY POLYNOMIALS

2.1. CONNECTION BETWEEN BODY FORM AND GENERATING HYDRODYNAMIC SINGULARITIES

In establishing a relationship between body form and generating hydrodynamic singularities two well-known problems can be formulated:

- a. Given a distribution, find the shape of the body (sectional-area curve $A(x)$).
- b. Given a body form (sectional-area curve $A(x)$), establish the appropriate distribution.

In the present report we disregard the complications connected with problem b and treat it in a very approximate way. The contemporary rudimentary state of knowledge on problems of wave resistance justifies this procedure to some extent; our investigation deals essentially with resistance properties of hydrodynamic distributions and merely some assumptions are made as to the probable shape of the bodies generated by these distributions.

Thus two essential sources of error are involved when investigating the wave resistance of bodies of revolution:

- a. The approximate character of the wave-resistance theory, and
- b. The generally admitted approximation that for a given body the deep-immersion distribution of singularities can be used instead of the actual distribution valid for near-surface conditions.

The second assumption (b) appears to be a serious one when the body is close to the surface. It has been proved by Havelock⁹ that it leads to inconsistent results with respect to added masses; however, by following numerous comparisons between theoretical and experimental results referring to surface ships it works reasonably well when applied to the resistance problem.

In the present report the assumption will be made that the shape of the body generated by singularities moving close to the surface is

identical with the shape of the corresponding body generated by the same singularities in an unbounded fluid.

It is well known that in the latter case one can construct the contour of a body of revolution for any given singularity distribution along the axis; auxiliary tables for this work are available,^{2,10} especially for cases in which the distribution is given by polynomials. Flat noses—as discussed by Weinstein¹⁶—will not be dealt with in the present report, although it is possible that such forms are advantageous from a point of view of wave resistance at high Froude numbers. When dealing with "normal" shapes, the important approximation developed by Weinig⁷ and Munk⁸ holds; i.e., for very elongated bodies the sectional-area curve of the generating body $A(x)$ is affine to the doublet distribution $\mu(x)$. This approximation will be used throughout the present report although its limitations should not be forgotten.

Some explanation—if not definition—must be given as to the concept of a "normal" shape of a doublet-distribution or a sectional-area curve. It means essentially a curve whose trend is similar to sectional-area curves of common ocean-going ships; these curves generally are monotonic with not more than one point of inflection in the fore and afterbody.

Since for closed bodies the source-sink distribution $\sigma(x)$ is the derivative of the doublet distribution $\mu(x)$ the latter is monotonic over the range of the forebody when $\sigma(x)$ consists only of sources in the same range. This condition (though not necessarily a required one) is sufficient to obtain bodies such that the circle of curvature at the nose lies inside of the meridian contour.

We mention some conditions under which the affinity between the doublet and the sectional-area curve becomes strained:

a. For larger values of the elongation D/L the divergence between the sectional-area curve $A(x)$ and the doublet distribution $\mu(x)$ becomes more pronounced even for "normal" shapes. This divergence can be roughly described. First, in the mutual relation of the prismatic (area) coefficients which are the decisive form parameters of the two curves—the one, ϕ_d , denoting the prismatic or area coefficient of the distribution, and the other, ϕ_s , the corresponding one for the sectional-area curve—the following statement holds for a wide class of normal bodies:^{5, 15}

for finite D/L

$$\phi_s > \phi_d \quad \text{when} \quad \phi_d < 2/3$$

$$\phi_s < \phi_d \quad \text{when} \quad \phi_d > 2/3$$

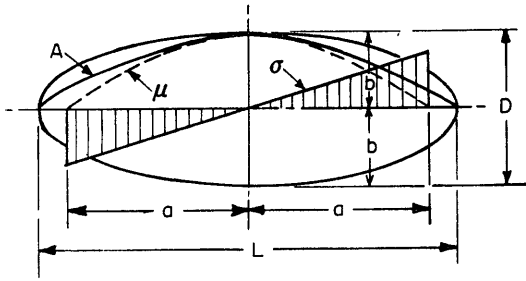


Figure 2 - Spheroid. Sectional-Area Curve A, Doublet and Source-Sink Distribution

The equality $\phi_d = \phi_s$ is valid only for the ellipsoid; see Figure 2. Second, in the prismatics a difference arises between the length of the body L and the distribution $2a$, $2a$ being smaller than L . For the spheroid the relative difference

$$\zeta = \frac{L-2a}{2a} \cong \frac{D^2}{2L^2} \cong \frac{b^2}{2a^2}$$

where ζ depends on the shape of the distribution, especially at the ends. (Since this problem is being thoroughly investigated by L. Landweber of the Taylor Model Basin, we confine ourselves to these brief remarks.)

b. When complicated "abnormal" distributions like "swan necks" or curves with very steep ends are investigated (for instance, Rankine's ovoid) the divergence between these distributions and the sectional-area curve can become appreciable even for smaller D/L .

2.2. REPRESENTATION BY POLYNOMIALS

2.2.1. General Remarks

In former reports polynomials have been used for the representation of the generating doublet (source and sink) distribution along the axis^{5,6,10,13}

The doublet and source-sink distributions $\mu(x)$, $\sigma(x)$ can be split up into dimensional factors μ_0 , σ_0 and variable dimensionless parts $\mu^*(\xi)$, $\sigma^*(\xi)$; $\mu(x) = \mu_0 \mu^*(\xi)$

$$\sigma(x) = \sigma_0 \sigma^*(\xi)$$

with $\xi = x/a$; see Figure 3b.

The dimensional factors will be established later; in the succeeding discussion the functions $\mu^*(\xi)$ and $\sigma^*(\xi)$ will be treated in the same way as ship lines and their derivatives. Generally following Munk and Weinig the doublet distribution $\mu^*(\xi)$ is identified with the sectional-area curve $A^*(\xi)$ and the symbol η is used for both of them. Actually the resistance computations refer to given distributions for which the corresponding sectional-area curves can be easily calculated^{2,10} when Munk's approximation is not accurate enough—as for instance in cases dealt with in Section 5.

The first adequate representation of ship lines by polynomials is due to Taylor;^{11,12} the equations obtained are, however, suitable for a separate description of the fore or afterbody only. Taylor locates the

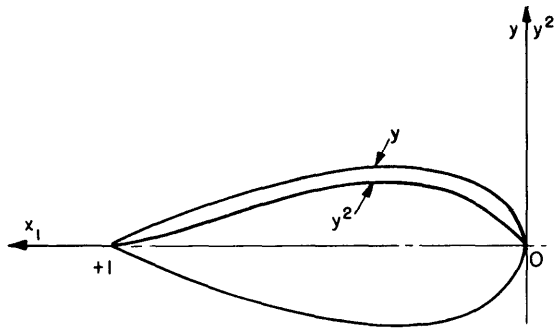


Figure 3a - Landweber's Axes

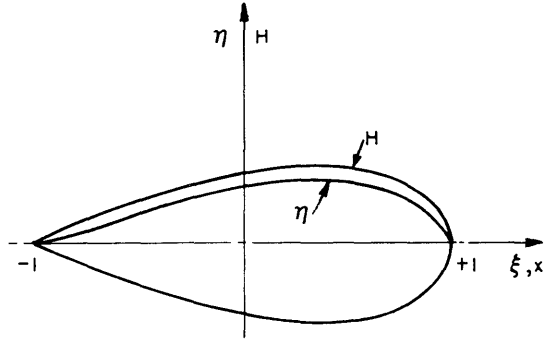


Figure 3b - Present Axes

Figure 3 - Systems of Axes

origin at the bow or stern. The present writer has proposed^{13,14} other sets of polynomials referred to a system of axes with an origin located midships. This approach has definite advantages when investigating the wave resistance.

Landweber² has generalized Taylor's equation by adding one more term and by introducing appropriate boundary conditions; he uses the expression obtained as the equation of the sectional-area curve of a four-parameter form.² The parameters are interpreted geometrically as the prismatic coefficient, the location of the maximum section along the axis and the nose and tail radii of curvature. It will be immediately shown that Landweber's equation transferred to an origin at the midship section can be split up into a two-parameter symmetrical and a two-parameter skew part with respect to this section; thus expressions are obtained for which the wave resistance can be calculated in a simple way.

2.2.2. The TMB (Landweber) Class of Bodies and Some Generalizations

The TMB (Landweber) class of bodies of revolution is given by the equation of the sectional-area curve

$$y^2 = a'_1 x_1 + a'_2 x_1^2 + a'_3 x_1^3 + a'_4 x_1^4 + a'_5 x_1^5 + a'_6 x_1^6 \quad [1]$$

referred to axes, as shown in Figure 3. We transform the equation of the body by shifting the origin to the midship section $x = 0.5$, reversing the direction of the axes, and putting the length of the body equal to 2.

Thus for

$$\begin{aligned} x_1 = 0 & & \xi = +1 \\ x_1 = 0.5 & & \xi = 0 \\ x_1 = +1 & & \xi = -1 \end{aligned}$$

The transformation is given by

$$\begin{aligned}\xi &= -2(x_1 - 0.5) \text{ or} \\ x_1 &= \frac{1 - \xi}{2}\end{aligned}\quad [2]$$

The resulting equation is

$$y^2 = A_0 + A_1 \xi + A_2 \xi^2 + A_3 \xi^3 + A_4 \xi^4 + A_5 \xi^5 + A_6 \xi^6 \quad [3]$$

where

$$\begin{aligned}A_0 &= \sum_1^6 \frac{a_n'}{2^n} & A_1 &= -\sum_1^6 \frac{na_n'}{2^n} & A_2 &= \sum_2^6 \frac{n(n-1)}{2} \frac{a_n'}{2^n} \\ A_3 &= -\sum_3^6 \frac{n(n-1)(n-2)}{2 \times 3 \times 2^n}, \text{ etc.}\end{aligned}$$

Equation [3] can be split up into a symmetrical and an antisymmetrical part

$$Y_s = A_0 + A_2 \xi^2 + A_4 \xi^4 + A_6 \xi^6 \quad [4a]$$

$$y^2 = Y = Y_s + Y_a$$

$$Y_a = A_1 \xi + A_3 \xi^3 + A_5 \xi^5 \quad [4b]$$

The obtained form [3] has definite advantages when calculating the wave resistance since the latter is the sum of the wave resistance corresponding to the symmetrical and antisymmetrical part computed independently.

Going further, we derive from [3] the following simple properties of the Landweber bodies:

$$\sum_1^6 a_n' x_1^n = \sum_1^6 A_0 \xi^n$$

The coefficient A_0 can be factored out and merged into a dimensional constant which defines the midship section. Thus, the normal form of our polynomial is obtained

$$\begin{aligned}\eta &= 1 - \sum_1^6 a_n \xi^n \\ \text{with } a_1 &= \frac{-A_1}{A_0}\end{aligned}\quad [4c]$$

The symmetrical part of [4c] is a two-parameter family

$$\eta_s(\xi) = 1 - a_2 \xi^2 - a_4 \xi^4 - a_6 \xi^6 = 1 - \xi^6 - a_2(\xi^2 - \xi^6) - a_4(\xi^4 - \xi^6)$$

because from the boundary condition

$$\begin{aligned}\eta_s(1) &= 0 \\ a_6 &= 1 - a_2 - a_4\end{aligned}$$

Such families have been called "basic forms" by the present writer¹³ and designated by $(2,4,6;\phi;t)$ since the arbitrary parameters a_2, a_4 can be determined by the prismatic coefficient $\phi = \int_0^1 \eta d\xi$ and by Taylor's tangent value $t = -\partial \eta(1)/\partial \xi$.

It is thought that the Landweber Series [1] meets almost all reasonable requirements as to wave-resistance properties presented by practice although only two arbitrary parameters ϕ, t are at our disposal for the main symmetric part. The reason for this assumption is that from investigations on surface ships it is well known that area curves of fine ships, based on the basic family equation $(2,4,6;\phi;t)$ are advantageous in the range of high and medium Froude numbers. At low Froude numbers other polynomials are preferable but there the wave resistance of submerged bodies becomes rather negligible.

We have, however, introduced an additional term $a_8 \xi^8$ for which auxiliary wave-resistance functions are also tabulated in this report; thus more elaborate investigations can be performed using the polynomial

$$\eta_s = 1 - \sum_{2,4,6,8} a_i \xi^i$$

The asymmetric (skew) part is the function

$$\eta_a = a_1 \xi + a_3 \xi^3 + a_5 \xi^5 \quad [4d]$$

factoring out a_1 , we write

$$\eta_a = a_1 \eta_a^* = a_1 (\xi + b_3 \xi^3 + b_5 \xi^5) \quad [4e]$$

Obviously the resultant curve $\eta = \eta_s + \eta_a$ can have its maximum section outside of $\xi = 0$ and the area of this section will generally differ from one. This slight complication does not involve any difficulties in actual work.

Let us investigate

$$\eta_a^* = \xi + b_3 \xi^3 + b_5 \xi^5 \quad [4f]$$

This trinomial has to comply with the conditions

$$\eta_a^*(0) = 0$$

$$\eta_a^*(+1) = \eta_a^*(-1) = 0$$

whence

$$b_5 = -(1 + b_3)$$

thus

$$\eta_a^* = \xi + b_3 \xi^3 - (1+b_3)\xi^5 \quad [4g]$$

The only arbitrary parameter b_3 can be fixed by one additional condition; as such we choose the tangent value t_a^* at the bow (at the stern the corresponding value is $-t_a^*$)

$$t_a^* = -\frac{\partial \eta_a^*(1)}{\partial \xi} = +4 + 2b_3$$

hence

$$b_3 = -2 + t_a^*/2 \quad [4h]$$

the corresponding tangent value t_a of η_a , Equation [4e], is obviously

$$t_a = a_1 t_a^*$$

The table below shows some examples of skew forms. The parameter $\phi_a^* = \int_0^1 \eta_a^* d\xi$ is an area coefficient referred to the unit square. Plots of $\xi - \xi^3$, $\xi - \xi^5$ and some other "skew" forms used in the TMB Series are shown on Figure 5. The actual skew part η_a contains additionally the "strength parameter" a_1 ; see Equation [4e].

t_a^*	0	1	2	4
η_a^*	$\xi(1 - \xi^2)^2$	$\xi - 1.5\xi^3 + 0.5\xi^5$	$\xi - \xi^3$	$\xi - \xi^5$
$\partial \eta_a^*/\partial \xi$	$1 - 6\xi^2 + 5\xi^4$	$1 - 4.5\xi^2 + 2.5\xi^4$	$1 - 3\xi^2$	$1 - 5\xi^4$
ϕ_a^*	$1/6 = 0.166\dots$	$5/24 = 0.2083\dots$	$1/4$	$1/3$

Our numeric evaluations are primarily based on Equations [4c] and [5]—which are stated below—but the theoretical treatment will be carried out along more general lines.

Extended investigations have been made by Landweber and Gertler² on the influence of an additional term $a_7 x^7$ on the form of the body when the geometric parameters are kept constant.

Using our system of axes it is easy to perform similar investigations for the symmetric and asymmetric part of [4c]

$$\eta_0 = \eta_s + \eta_a = 1 - \sum_{2,4,6} a_n \xi^n + a_1 (\xi + b_3 \xi^3 + b_5 \xi^5).$$

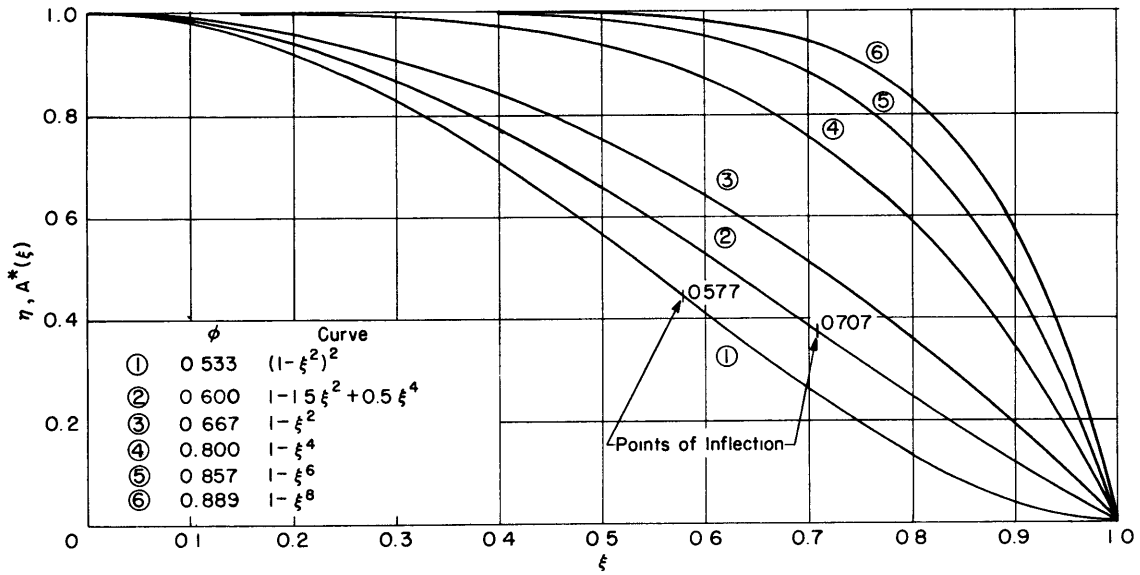


Figure 4 - Dimensionless Sectional-Area Curves $A^*(\xi)$ (Doublet Distributions $\mu^*(\xi)$) of Some Simple Bodies Symmetric with Respect to the Midship Section

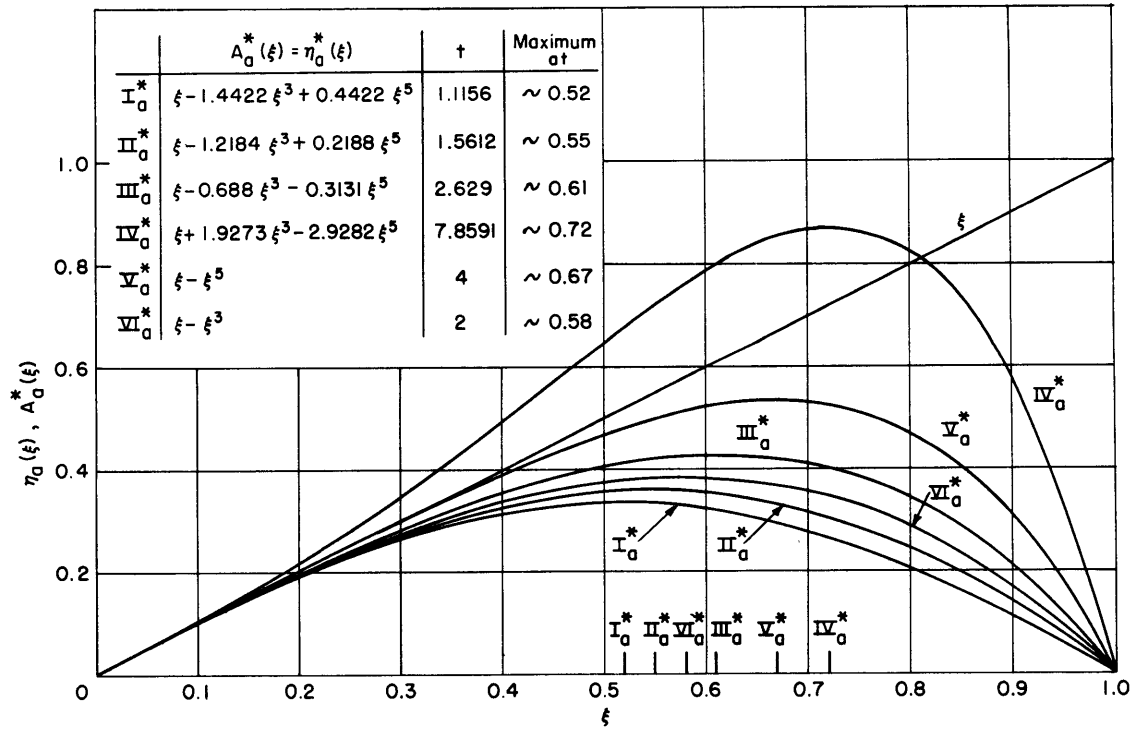


Figure 5 - Examples of the Antisymmetrical (Skew) Parts of Sectional-Area Curves $A_a^*(\xi)$ (Doublet Distributions $\mu^*(\xi)$) Belonging to the Family $\xi + b_3 \xi^3 - (1 + b_3) \xi^5$

By adding to η_0 terms with arbitrary parameters $a_7 \xi^7$ and $a_8 \xi^8$, a manifold $\eta_1 = \eta_0 + a_7 \xi^7 + a_8 \xi^8$ is obtained.

The polynomial [4c] is completely defined by the four geometrical parameters

$$\left. \begin{array}{l} 1) \quad \phi \\ 2) \quad t_s = -\frac{\partial \eta_s(1)}{\partial \xi} \\ 3) \quad \frac{\partial \eta_a(0)}{\partial \xi} = a_1 \\ 4) \quad \frac{\partial \eta_a(1)}{\partial \xi} = -a_1 t_a^* = -t_a \end{array} \right\} \quad [5]$$

When η_1 has to comply with the four equations [5] it can be expressed by

$$\eta_1 = \eta_0 + C_s \Delta_3 \eta(\xi) + C_a \Delta_4 \eta(\xi) \quad [6]$$

where

$$\Delta_3 \eta(\xi) = \xi^2 - 5\xi^4 + 7\xi^6 - 3\xi^8 \quad [6a]$$

complies with the conditions

$$\int_0^1 \Delta_3 \eta(\xi) d\xi = 0;$$

$$\Delta_3 \eta(0) = \Delta_3 \eta(1) = \frac{\partial \Delta_3 \eta(0)}{\partial \xi} = \frac{\partial \Delta_3 \eta(1)}{\partial \xi} = 0$$

and

$$\Delta_4 \eta(\xi) = \xi^3(1 - \xi^2)^2 \quad [6b]$$

satisfies

$$\Delta_4 \eta(0) = \Delta_4 \eta(1) = \frac{\partial \Delta_4 \eta(0)}{\partial \xi} = \frac{\partial \Delta_4 \eta(1)}{\partial \xi} = 0$$

Thus, an addition of the functions Δ_3 , Δ_4 to η_0 does not influence the boundary conditions, [5]. The shape of the curves $\Delta_3 \eta(\xi)$ and $\Delta_4 \eta(\xi)$ is shown in Figure 13. The advantage of this representation is obvious.

While in the equations

$$\eta = \eta_s + \eta_a$$

or

$$\mu^*(\xi) = \mu_s^*(\xi) + \mu_a^*(\xi)$$

the symmetrical (even) terms η_s, μ_s^* are the main parts, obviously in

$$\frac{\partial \eta}{\partial \xi} = \frac{\partial \eta_s}{\partial \xi} + \frac{\partial \eta_a}{\partial \xi}$$

or

$$\sigma^*(\xi) = \sigma_a^*(\xi) + \sigma_s^*(\xi)$$

the odd terms $\partial \eta_s / \partial \xi, \sigma_s^*$ become the main part.

2.3. CONNECTION BETWEEN STRENGTH OF SINGULARITIES AND BODY SHAPE

The next consideration is to establish the dimension factors μ_0 and σ_0 . The flux through the midship section may be written as

$$Q = C\left(\frac{b}{a}, \mu^*\right) \pi b^2 U \quad [7]$$

Here the coefficient $C(b/a, \mu^*)$ is, as indicated, a function of the elongation ratio $b/a \cong D/L$ and of the shape of the distribution μ^* . For very large elongations $C(b/a, \mu^*) \rightarrow 1$, but for shapes and values b/a used in actual operation C differs from one.

A closer investigation of the coefficient C will be given elsewhere by L. Landweber; for the present purpose we introduce C as a correction factor which improves the accuracy of Munk's or Weinig's approximate affinity theorem mentioned on page 5. The dependence of C upon μ^* , although apparently negligible within the range of presently used submarine hull forms, shows some interesting features. Earlier brief investigations lead to the following table for $C(b/a, \mu^*)$ (Reference 5).

		b/a \cong D/L				
		1/4	1/6	1/8	1/10	0
$\mu^*(\xi)$	ϕ_d	C(b/a, μ^*)				
$(1 - \xi^2)^2$	0.533	1.172	1.093	1.060	1.043	1
$1 - \xi^2$	0.660	1.192	1.092	1.054	1.036	1
$1 - 3.0825\xi^8 + 0.165\xi^{10} + 1.9175\xi^{12}$	0.820	-		1.0124	1.008	1

From these results we gather that $C(b/a, \mu^*)$ values for normal submarine shapes apparently can be estimated from the spheroid; an empirical

formula $C(b/a) \cong 1 + 3b^2/a^2$ may fit the facts reasonably well. For fuller bodies lower values seem to be suitable.

The constant

$$\mu_o = \frac{1}{4\pi} Q$$

is therefore obtained as

$$\mu_o = \frac{1}{4} C\left(\frac{b}{a}, \mu^*\right) b^2 U \quad [7a]$$

The flux [7] or the strength of the doublet distribution at the midship section must be somewhat higher than the product of the cross section times the speed of advance.

For the source, we have

$$\sigma_o = \frac{1}{4} C\left(\frac{b}{a}, \mu^*\right) \frac{b^2}{a} U \quad [8]$$

3. EVALUATION OF HAVELOCK'S INTEGRAL

3.1. GENERAL CONSIDERATIONS

The wave resistance experienced by a continuous doublet sheet μ , distributed over a vertical plane and moving uniformly on a straight horizontal path, has been calculated by Havelock.³ Concentrating the distribution $\mu(x)$ along a horizontal straight line we obtain immediately

$$R = 16\pi\rho K_o^4 \int_0^{\pi/2} \left\{ P_1^2 + Q_1^2 \right\} \sec^5 \theta d\theta; K_o = \frac{g}{U^2} \quad [9]$$

with

$$P_1 = \exp(-K_o f \sec^2 \theta) \int_{-a}^{+a} \mu(x) \cos(K_o x \sec \theta) dx = \exp(-K_o f \sec^2 \theta) p_1 \quad [9a]$$

$$Q_1 = \exp(-K_o f \sec^2 \theta) \int_{-a}^{+a} \mu(x) \sin(K_o x \sec \theta) dx = \exp(-K_o f \sec^2 \theta) q_1 \quad [9b]$$

hence

$$R = 16\pi\rho K_o^4 \int_0^{\pi/2} (p_1^2 + q_1^2) \exp(-2K_o f \sec^2 \theta) \sec^5 \theta d\theta \quad [9c]$$

Using a source-sink distribution we obtain similarly

$$R = 16\pi\rho K_o^2 \int_0^{\pi/2} (p^2 + q^2) \exp(-2K_o f \sec^2 \theta) \sec^3 \theta d\theta \quad [10]$$

$$p = \int_{-a}^{+a} \sigma(x) \sin(K_o x \sec \theta) dx \quad [10a]$$

$$q = \int_{-a}^{+a} \sigma(x) \cos(K_o x \sec \theta) dx \quad [10b]$$

Introducing dimensionless coordinates $x = a\xi$ and the expressions

$$\mu(x) = \mu_0 \mu^*(\xi)$$

$$\sigma(x) = \sigma_0 \sigma^*(\xi)$$

various forms of the integral for R can be derived for purposes of numerical evaluation.

We confine ourselves to the source-sink integral.¹⁰ Splitting up $\sigma^*(\xi)$ into a main antisymmetrical and a symmetrical part

$$\sigma^*(\xi) = \sigma_a^*(\xi) + \sigma_s^*(\xi)$$

and remembering that an integral taken over an odd integrand between limits of equal absolute value but opposite sign vanishes, we obtain with the designation

$$\gamma_0 = K_0 a = \frac{ga}{U^2} = \frac{1}{2F^2}$$

$$R = 4C^2 \pi \rho g \frac{b^4}{a} \gamma_0 \int_0^{\pi/2} \exp[-4 \frac{f}{L} \gamma_0 \sec^2 \theta] \sec^3 \theta. \quad [11]$$

$$\left[\left\{ \int_0^1 \sigma_a^*(\xi) \sin(\gamma_0 \xi \sec \theta) d\xi \right\}^2 + \left\{ \int_0^1 \sigma_s^*(\xi) \cos(\gamma_0 \xi \sec \theta) d\xi \right\}^2 \right] d\theta =$$

$$\text{const} \int_0^{\pi/2} \exp[-4 \frac{f}{L} \gamma_0 \sec^2 \theta] \sec^3 \theta [p^{*2} + q^{*2}] d\theta \quad [12]$$

We introduce further polynomials for

$$\mu^*(\xi) = 1 - \sum_n a_n \xi^n \quad [13]$$

hence

$$\sigma^*(\xi) = -\sum_n n a_n \xi^{n-1} \quad [14]$$

or

$$\sigma^*(\xi) = \sigma_a^*(\xi) + \sigma_s^*(\xi) = -\sum_k 2k a_{2k} \xi^{2k-1} - \sum_m (2m+1) a_{2m+1} \xi^{2m} \quad [14a]$$

with k, m as integers.

For the main antisymmetrical part the intermediate integral p^* becomes

$$p^* = \int_0^1 \sigma_a^*(\xi) \sin(\gamma_0 \xi \sec \theta) d\xi = -\sum_k 2k a_k \int_0^1 \xi^{2k-1} \sin(\gamma_0 \xi \sec \theta) d\xi$$

$$= -\sum_k 2k a_k M_{2k-1}(\gamma_0 \sec \theta) \quad [15]$$

with

$$M_{2k-1}(\gamma_0 \sec \theta) = M_{2k-1}(\gamma) = \int_0^1 \xi^{2k-1} \sin(\gamma_0 \xi \sec \theta) d\xi = \int_0^1 \xi^{2k-1} \sin(\gamma \xi) d\xi \quad [16]$$

Here for brevity the designation $\gamma = \gamma_0 \sec \theta$ has been introduced, [16].

For the symmetrical (even) part

$$q^* = \int_0^1 \sigma_S^*(\xi) \cos(\gamma_0 \xi \sec \theta) d\xi = - \sum_m (2m+1) a_{2m+1} M'_{2m}(\gamma_0 \sec \theta) \quad [17]$$

with

$$M'_{2m}(\gamma_0 \sec \theta) = M'_{2m}(\gamma) = M'_{2m} = \int_0^1 \xi^{2m} \cos(\gamma_0 \xi \sec \theta) d\xi = \int_0^1 \xi^{2m} \cos \gamma d\xi \quad [18]$$

inserting [15] and [16] into [12] one obtains

$$R = 4C^2 \pi \rho g \frac{b^4}{a} \gamma_0 \int_0^{\pi/2} \exp\left[-4 \frac{f}{L} \gamma_0 \sec^2 \theta\right] \left\{ \left(\sum_k 2k a_{2k} M_{2k-1} \right)^2 + \left(\sum_m (2m+1) a_{2m+1} M'_{2m} \right)^2 \right\} \sec^3 \theta d\theta \quad [19]$$

This formula is suitable for numerical computations above in special cases, since tables of the functions $M_{2k-1}(\gamma)$, $M'_{2m}(\gamma)$ are available and will be published in a TMB Report.

3.2. TABULATION OF RESISTANCE INTEGRALS FOR A FIVE-PARAMETER CLASS OF BODIES

As mentioned before, auxiliary integrals have been prepared for the three-parameter symmetric distributions of Equation [5], $\mu_S^*(\xi)$ (asymmetric in $\sigma_a^*(\xi)$).

$$\mu_S^*(\xi) = 1 - \sum_{2,4,6,8} a_n \xi^n \quad \text{and} \quad \sigma_a^*(\xi) = - \sum_{2,4,6,8} n a_n \xi^{n-1}$$

and the one-parameter skew distribution $\mu_a^*(\xi)$ (symmetric in $\sigma_S^*(\xi)$)

$$\mu_a^*(\xi) = \xi + b_3 \xi^3 - (1+b_3) \xi^5 \quad \text{and} \quad \sigma_S^*(\xi) = 1 + 3b_3 \xi^2 - 5(1+b_3) \xi^4$$

The computations are based on a slightly different form of R (see Appendix II). Substituting

$$\gamma = \gamma_0 \sec \theta \quad \sec \theta = \gamma/\gamma_0 \quad \text{tg } \theta = \sqrt{(\gamma/\gamma_0)^2 - 1}$$

one obtains

$$d\gamma = \gamma_0 \sec^2 \theta \sin \theta d\theta; \quad \gamma_0 \sec^3 \theta d\theta = \frac{(\gamma/\gamma_0)^2 d\gamma}{\sqrt{(\gamma/\gamma_0)^2 - 1}}$$

hence

$$R = 4C^2 \pi \rho g \frac{b^4}{a} \int_{\gamma_0}^{\infty} \exp\left[-4 \frac{f}{L} \frac{\gamma^2}{\gamma_0}\right] \frac{(\gamma/\gamma_0)^2}{\sqrt{(\gamma/\gamma_0)^2 - 1}} \left\{ \left(\sum_k 2k a_{2k} M_{2k-1}(\gamma) \right)^2 + \left(\sum_m (2m+1) a_{2m+1} M'_{2m}(\gamma) \right)^2 \right\} d\gamma \quad [20]$$

putting for abbreviation

$$4C^2 \pi \rho g \frac{b^4}{a} = \text{const} = C_0$$

$$\frac{(\gamma/\gamma_0)^2}{\sqrt{(\gamma/\gamma_0)^2 - 1}} = f(\gamma)$$

$$R = C_0 \int_{\gamma_0}^{\infty} \exp\left[-\frac{4f}{L} \frac{\gamma^2}{\gamma_0}\right] f(\gamma) \left\{ \sum_{i,j} 2i 2j a_{2i} a_{2j} M_{2i-1} M_{2j-1} + \sum_{r,s} (2r+1)(2s+1) a_{2r+1} a_{2s+1} M'_{2r} M'_{2s} \right\} d\gamma \quad [21]$$

with i, j, s, r integers. R can be built up of terms of the type

$$\int_{\gamma_0}^{\infty} \exp\left[-\frac{4f}{L} \frac{\gamma^2}{\gamma_0}\right] f(\gamma) M_{2i-1}(\gamma) M_{2j-1}(\gamma) d\gamma = m_{2i-1, 2j-1} \quad [22]$$

for the symmetrical part of the sectional-area curve

and

$$\int_{\gamma_0}^{\infty} \exp\left[-\frac{4f}{L} \frac{\gamma^2}{\gamma_0}\right] f(\gamma) M'_{2r}(\gamma) M'_{2s}(\gamma) d\gamma = m'_{2r, 2s} \quad [23]$$

for the skew part. The final result is therefore obtained as a quadratic form in the parameters a or, better, a_n

$$R = C_0 \left\{ \sum_{i,j} 2i 2j a_{2i} a_{2j} m_{2i-1, 2j-1} + \sum_{r,s} (2r+1)(2s+1) a_{2r+1} a_{2s+1} m'_{2r, 2s} \right\} \quad [24]$$

with the tabulated integral values $m_{2i-1, 2j-1}, m'_{2r, 2s}$ as main parts of the coefficients $2i 2j m_{2i-1, 2j-1}$, etc.

We mention again the fortunate circumstance that the contributions to the wave resistance due to the symmetrical and antisymmetrical parts can be calculated independently and added.

Returning now to a family of distribution curves given by Equation [4c] but generalized by one additional term $a_8 \xi_8$:

$$\eta = 1 - \sum_1^6 a_n \xi^n + a_8 \xi^8, \quad \frac{\partial \eta}{\partial \xi} = - \sum_1^6 n a_n \xi^{n-1} + 8a_8 \xi^7 \quad [41]$$

The wave resistance can be calculated by the functions

$$m_{11} \quad m_{13} \quad m_{15} \quad m_{17} \quad m'_{00} \quad m'_{02} \quad m'_{04}$$

$$m_{33} \quad m_{35} \quad m_{37} \quad m'_{22} \quad m'_{24}$$

$$m_{55} \quad m_{57} \quad m'_{44}$$

$$m_{77}$$

tabulated in the Appendix III. The integral R and the functions \mathcal{M} and \mathcal{M}' depend upon the two parameters $\gamma_0 = 1/2F^2$ and f/L . The tables have been prepared for a range $0.5 \leq \gamma_0 \leq 10$ and $f/L = 0.125, 0.25, 0.50$. Additionally, for \mathcal{M}'_{11} an intermediate depth of immersion ratio $f/L = 0.1875$ has been introduced. From the wave resistance integral it follows immediately that the ratio depth of immersion over length f/L is theoretically preferable to the more commonly used ratio f/D , since f/L appears explicitly as factor of the exponent of the e -function under the integral. With elongated bodies the ratio b/a or D/L influences primarily the constant $C_0 = 4C^2 \pi \rho g b^4/a$ only, though in a very decisive way. Although the lower speed limit $\gamma_0 = 10$ ($F = 0.224$)—up to which the auxiliary integrals have been computed—is rather high, it is thought that for normal hulls with $\phi < 2/3$ moving at greater depths than D , the wave resistance becomes unimportant when $F < 0.224$. The low-speed range may, however, be interesting in connection with other research problems.

In principle the wave-resistance equation, [24], solves the problem for any sets of a_n within the family following [41]. Actually since the relative error of the tabulated functions is approximately 0.0001, a loss of accuracy may occur—when the coefficients a_n reach high absolute values with alternating signs. It is not probable that difficulties of this kind will be important in connection with submarine work; besides, they can be overcome to some extent by plotting suitable simpler resistance curves and by interpolating.

4. REPRESENTATION OF RESISTANCE CURVES

4.1. THE DIMENSION FACTOR C_0 AND DIMENSIONLESS REPRESENTATIONS

The dimension factor in Equation [20], $C_0 = 4C^2 \pi \rho g b^4/a$, has a rather unusual form, but it will be widely used throughout this report because of its theoretical merits and the comparative ease with which it can be connected with more familiar expressions. We rewrite, in terms of the displacement Δ ,

$$C_0 = \phi \pi b^2 2a \rho g \frac{2b^2}{\phi a^2} C^2 = \Delta \frac{2b^2}{\phi a^2} C^2 \quad [25]$$

$$\frac{R}{C_0} = r_0 = \frac{R}{\Delta} \frac{\phi a^2}{2b^2 C^2} \quad \text{or} \quad \frac{R}{\Delta} = r_0 \frac{2b^2 C^2}{\phi a^2}$$

Hence we can immediately derive the resistance per unit displacement for a given b/a and shape when r_o is known.

The introduction of the displacement Δ in [20] is open to objection since so far we have not distinguished between the length of the body and the distribution. We repeat the definitions:

2a is the length of the distribution along the axis

L is the length of the generated body

2b = D is the diameter of the generated body

Obviously for the displacement of the body we must use $L = 2l$. Then

$$C_o = 4\pi\rho g C^2 b^4/a = \Delta \frac{2C^2 b^2 a}{\phi a^2 l} \quad [25a]$$

Further, the ratio $b/l = D/L$ is technically more important than b/a ; hence

$$r_o = \frac{R}{\Delta} \frac{\phi}{2C^2} \frac{l^2}{b^2} \frac{a}{l} \quad [25b]$$

or

$$\frac{R}{\Delta} = \frac{2C^2 (D/L)^2}{\phi} \frac{l}{a} r_o \quad [25c]$$

Later we shall use another coefficient

$$r_1 = \frac{r_o}{\phi} = \frac{R}{\Delta} \frac{1}{2C^2} \left(\frac{L}{D}\right) \frac{a}{l} \quad [26]$$

One should not, however, overestimate the influence of the length correction. For the spheroid

$$\frac{a}{l} \frac{1}{C^2} \cong \frac{1}{\left(1 + \frac{1}{2} \left(\frac{b}{a}\right)^2\right) \left(1 + \sigma \left(\frac{b}{a}\right)^2\right)}$$

i.e., influences the C^2 correction by less than 10 percent. Further, even the introduction of the more important C factor does not lead to an exhaustive correction since we know that not only the midship section but the whole trend of the curves changes with increasing b/a . Thus within the limited accuracy of the present wave-resistance theory we generally can put $l/a \cong 1$. It is of course important to use all approximations in a consistent and clearly defined way, so that fair comparisons can be made.

We note particularly, that for the spheroid

$$\frac{R}{\Delta} = r_o 3C^2 b^2/a^2$$

For comparison with experiments the coefficients c_w referred to the wetted surface S is advantageous.

We write

$$c_w = \frac{R}{\rho/2 U^2 S} = r_o \frac{4\pi C^2 b^2}{SF^2} \left(\frac{b}{a}\right)^2 \quad [27]$$

or introducing a surface coefficient S (Reference 17)

$$C_S = S/\pi DL$$

$$c_w = r_o \frac{C^2}{C_S} \left(\frac{b}{a}\right)^2 \frac{b}{C} \frac{1}{F^2} \cong r_o \frac{2C^2}{C_S} \left(\frac{b}{a}\right)^3 \gamma_o \quad [28]$$

with $\gamma_o = 1/2F^2$. For elongated spheroids $C_S \cong 0.79$.

The importance of the resistance coefficient c_w referred to the wetted surface S justifies a short digression on the calculation of S for bodies of revolution. Solutions of the exact expression (Equation [29]) can be obtained in a closed form in exceptional cases only, as for the spheroid. Of course it presents no difficulties to evaluate the integral numerically, but a simple approximate formula can be derived at least for the surface area of a restricted class of very elongated bodies of revolutions complying with the condition that the end tangents of their meridional contour do not become vertical; it is similar to the well-known expression for the length of a slightly curved arc, see Appendix I.

4.2 RESISTANCE CURVES OF SIMPLE SYMMETRICAL BODIES

Since the presentation and the discussion of resistance curves is the main subject of the present report, various sets of such curves have been computed. Essentially, the resistance properties of the following three groups of body forms (distributions) have been investigated:

(a) A set embracing a wide range of prismatic coefficients, which furnishes a general review of the resistance as function of the form (IV,2).

(b) A set dealing with four TMB models. This raises the problem of the influence of asymmetry with respect to the midship section (IV,3).

(c) A group consisting of systematically chosen forms belonging to the two-parameter family $(2, 4, 6; \phi; t)$ (VI); for the same family some calculations of shapes of least resistance are presented (V).

The procedure adopted leads to repetitions which, having in view the importance of the subject, have been thought to be advisable. Because of the complicated dependencies involved the interested reader can more

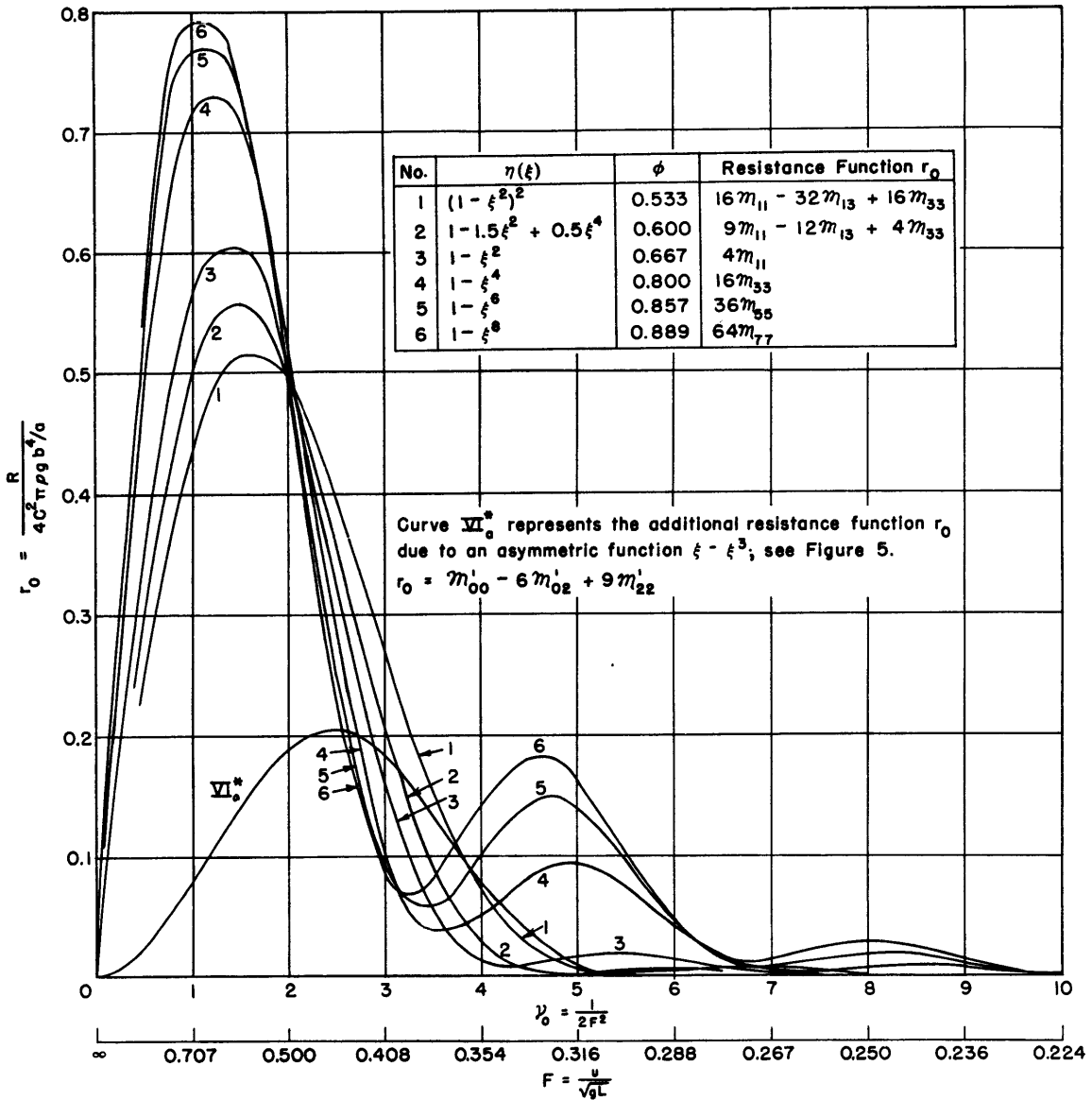


Figure 6 - Wave-Resistance Coefficients $r_0 = \frac{R}{4\pi C^2 \rho g b^4/a}$ of Symmetrical Bodies as Defined on Figure 4, $f/L = 0.125$

easily draw conclusions from the rather comprehensive plots than from any text.

We are mainly interested in the range of Froude numbers F below and at the maximum of the large hump in the resistance curve; see, for instance, Figures 6, 7 and 8. Above the maximum the absolute value of wave resistance decreases comparatively slowly with growing F , but the ratio wave resistance to frictional resistance drops quickly. Therefore, at high speeds

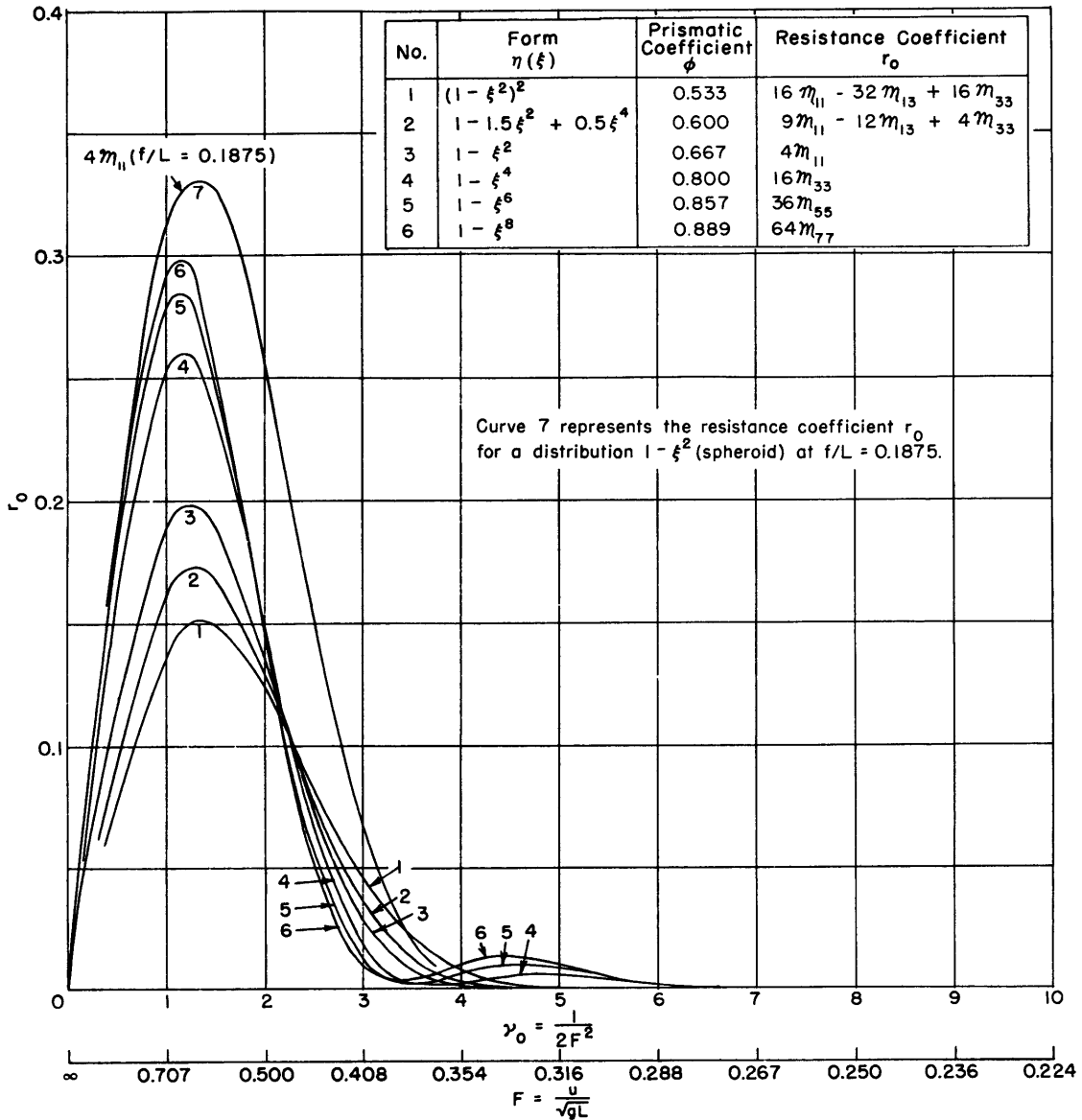


Figure 7 - Wave-Resistance Coefficients of Symmetrical Bodies as Defined on Figure 4, $f/L = 0.25$

the wave resistance of elongated bodies such as torpedoes represents only a small part of the total drag. It has been shown in References 4 and 5 that in the limit of very large Froude numbers the wave resistance becomes proportional to the square of the displacement or r_0 to ϕ^2 .

In general, throughout the present report calculations have been extended to $F = 1$ ($\gamma_0 = 0.5$), and to $F \cong 1.58$ ($\gamma_0 = 0.2$) for the parabolic distributions $1 - \xi^2$, $1 - \xi^4$, $1 - \xi^6$ only. From an approximate investigation

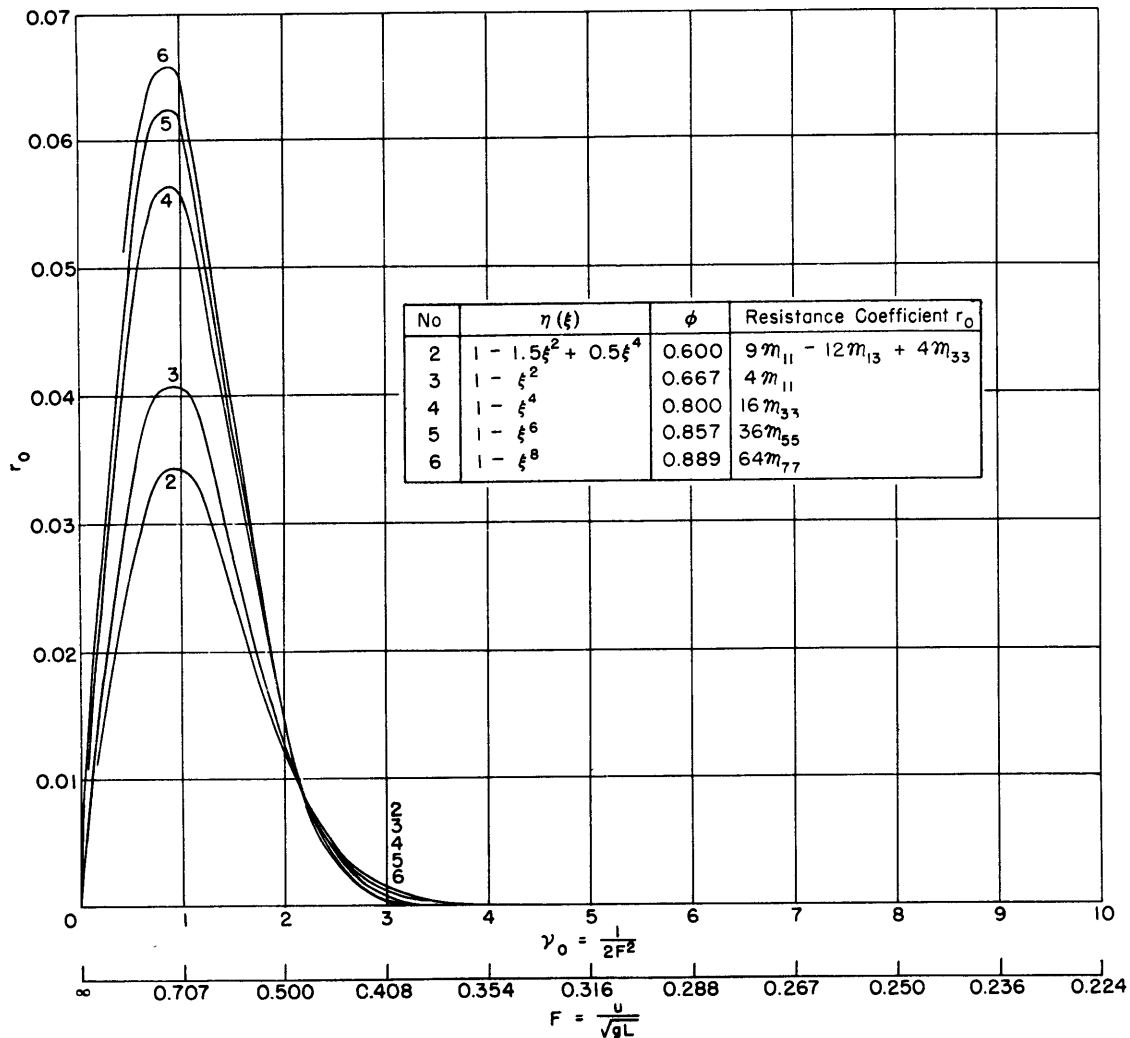


Figure 8 - Wave-Resistance Coefficients of Symmetrical Bodies as Defined on Figure 4, $f/L = 0.5$

it appears that the resistance curves $R(\gamma_0)$ plotted over γ_0 have a vertical tangent at $\gamma_0 = 0$, but no attempt has been made to draw accurately the range of curves below $\gamma_0 = 0.5$.

To obtain a general idea of the wave resistance for various symmetric distributions $\mu(\xi)$ (sectional-area curves $A^*(\xi)$) graphs have been plotted for following simple cases:*

*As before, by symmetry we mean symmetry with respect to the midsection.

	$\mu(\xi)$	ϕ	t
1)	$(1 - \xi^2)^2$	0.533	0
2)	$1 - 1.5 \xi^2 + 0.5 \xi^4$	0.6	1
3)	$1 - \xi^2$	2/3	2
4)	$1 - \xi^4$	0.8	4
5)	$1 - \xi^6$	6/7 = 0.857	6
6)	$1 - \xi^8$	8/9	8

Figure 4 shows these sectional-area curves and Figures 6, 7 and 8 the corresponding resistance coefficients as functions of $\gamma_0 = 1/2F^2$, with an additional non-equidistant scale for F. The choice of γ_0 as independent variable yields an appropriate picture of the wave-resistance values at high speeds.

From the Figures 6, 7 and 8 a rather complete understanding of the wave-resistance properties of various symmetrical forms can be derived. Reference is also made to Figure 12 and the pertaining discussions in the text. The influence of the depths of immersion follows immediately from a comparison of Figures 6 through 8; also, cross curves can be plotted over f/L as the independent variable. Figure 11 shows this dependency for $4\eta_{11}$, which is the resistance function of a spheroid $A^*(\xi) = 1 - \xi^2$, with $\gamma_0 = 1/2F^2$ as parameter. We note that with increasing depth the resistance drops more quickly at small than at large Froude numbers F. This is rather obvious; it will be discussed later more thoroughly that the most indicative parameter is the ratio f/λ , where λ the length of the free wave is $\lambda = 2\pi F^2 L$.

In Figures 9 and 10 the resistance curves for three depths of immersion have been reduced to approximately the same maximum ordinates. This rather artificial approach yields a clear idea about the shift of the last hump (of its steep rise as well as of the position of its maximum) to higher Froude numbers with increasing depth of immersion; it further emphasizes again that the rate of decay of the wave resistance with increasing depth is much higher for low Froude numbers than for high ones.

Figure 12 represents a coefficient $r_1 = R/\Delta a^2/2C^2b^2 = r_0/\phi$. For approximately constant C^2 (very elongated bodies) and given a^2/b^2 ratio, $r_1 \sim R/\Delta$, i.e., the figure yields a comparison of the resistance per unit displacement for various forms.

The discussion of the various graphs leads to the following summary results:

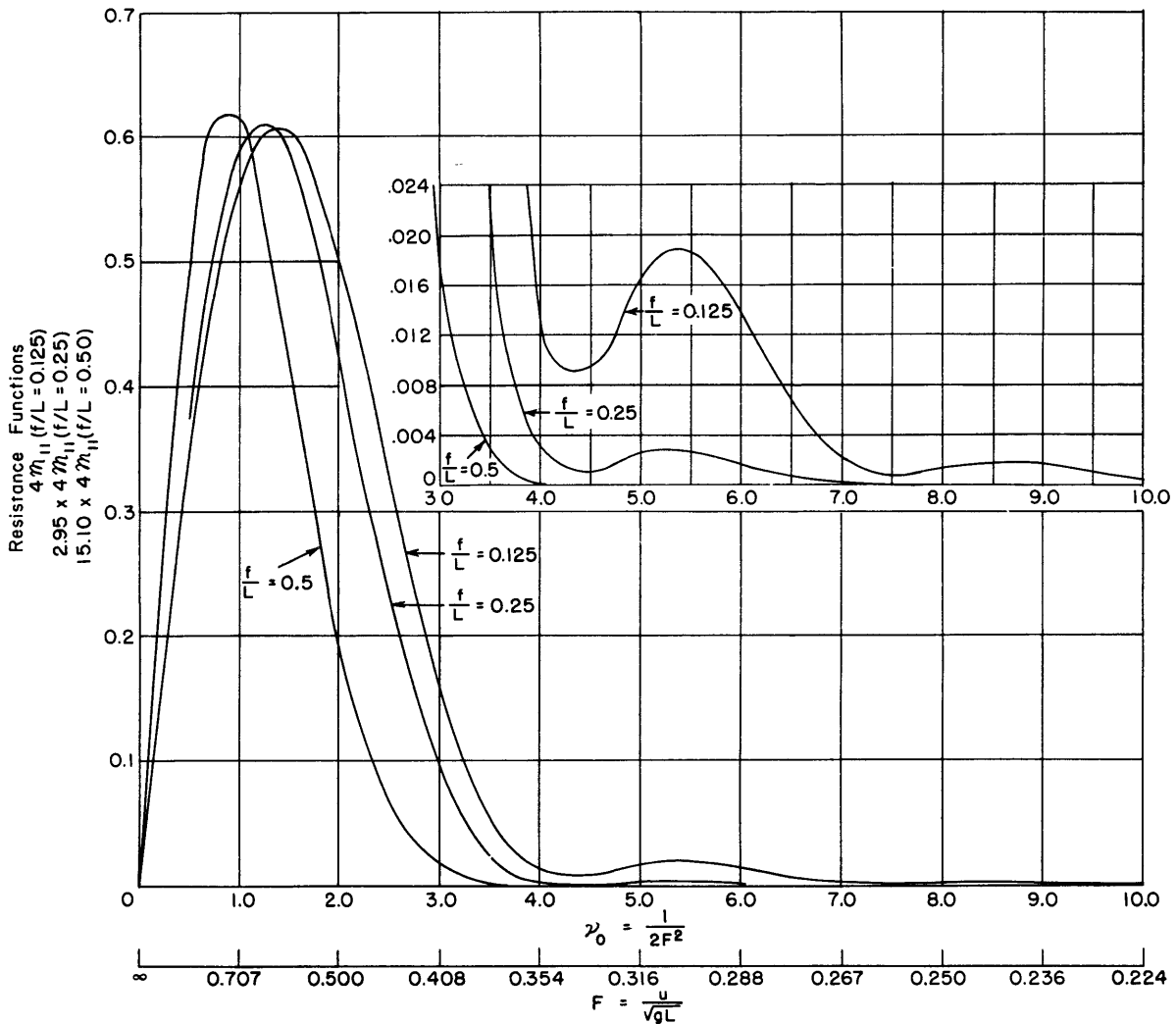


Figure 9 - Comparison of the Shape of Wave-Resistance Curves for the Spheroid $\eta(\xi) = 1 - \xi^2$; the Curves are Reduced to Approximately Equal Maxima

A. Small depths of immersion

1) Within reasonable limits, the peak value of the R/Δ curve does not depend too much on the shape of the body,* especially upon the prismatic coefficient.

2) The merits of full forms, over a wide and possibly important range of Froude numbers $0.35 \leq F \leq 0.50$, are clearly emphasized, as well as

3) The heavy penalty which has to be paid for high prismatics at lower F .

*If more elaborate results are desired they can be derived from Figures 28 through 35.

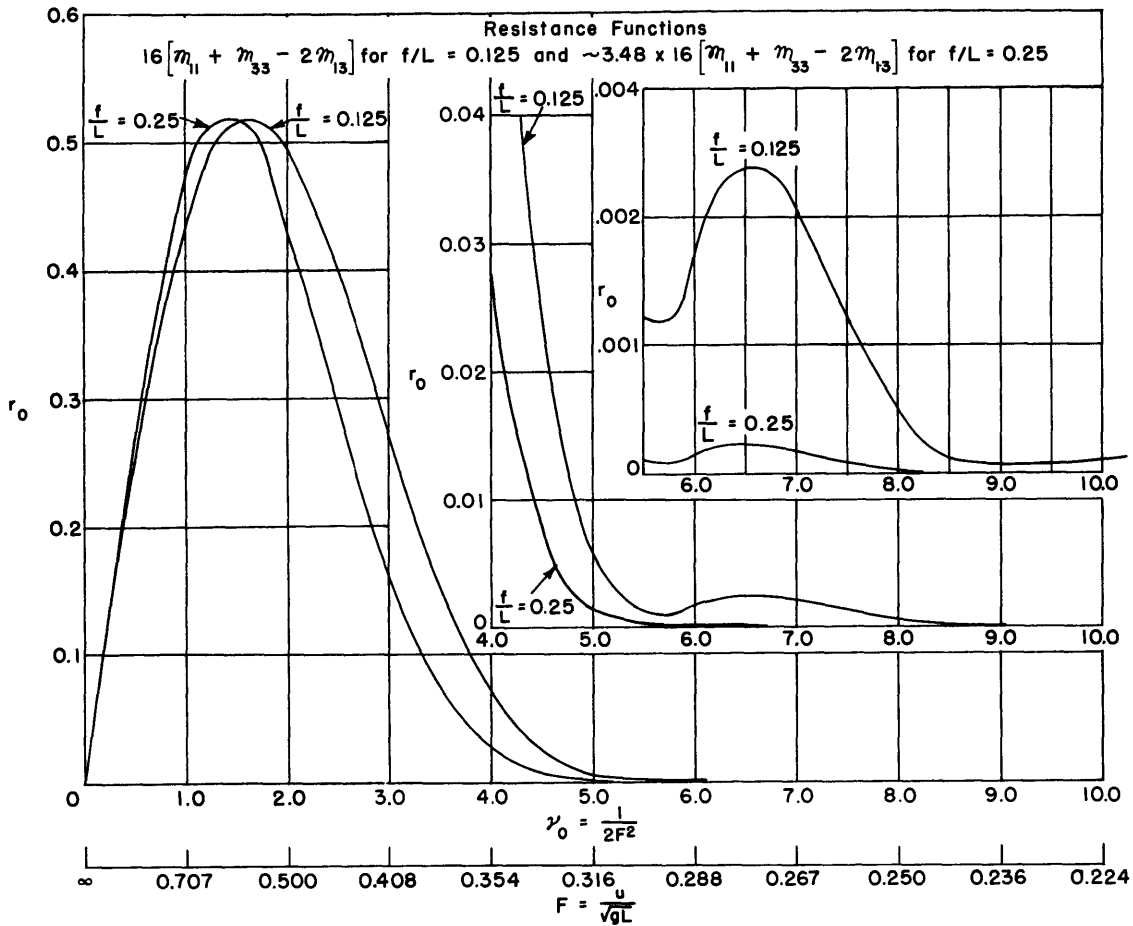


Figure 10 - Comparison of the Shape of Wave-Resistance Curves for $\eta = (1 - \xi^2)^2$ Reduced as by Figure 9

B. For larger depths of immersion the dependence of the peak values of R/Δ upon ϕ becomes more pronounced; the advantage of high prismatics in the range mentioned in A(2) is, on the average, reduced.

4.3. RESISTANCE CURVES OF ASYMMETRICAL BODIES

Further curves representing the wave-resistance coefficients of the four TMB models represented in Figures 14 and 15 are shown in Figures 16, 17 and 18. Before discussing these particular asymmetric models, however, an investigation must be made of the influence of asymmetry on the resistance.

Figure 5 represents examples of asymmetrical lines belonging to the family $\eta_a^* = \xi + b_3 \xi^3 - (1 + b_3) \xi^5$, Equation [4g].

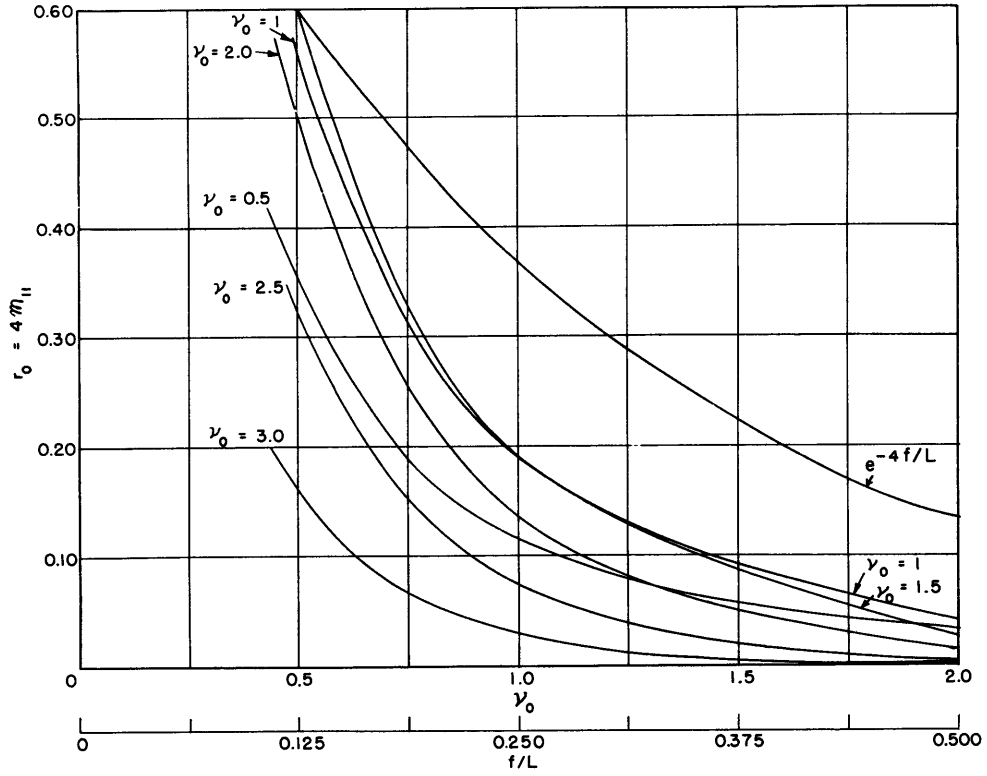


Figure 11 - Wave-Resistance Coefficients of the Spheroid as Functions of f/L with $\gamma_0 = 1/2F^2$ as Parameter

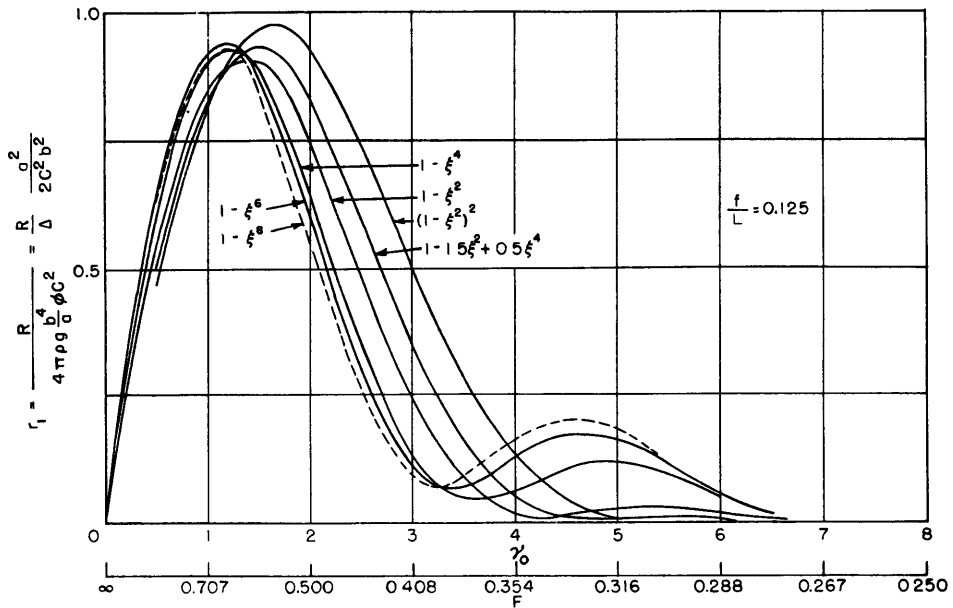


Figure 12 - Wave-Resistance Coefficients $r_1 = \frac{r_0}{\phi} = \frac{R}{\Delta} \frac{a^2}{2C^2 b^2}$ of Symmetrical Bodies Shown on Figure 4, $f/L = 0.125$

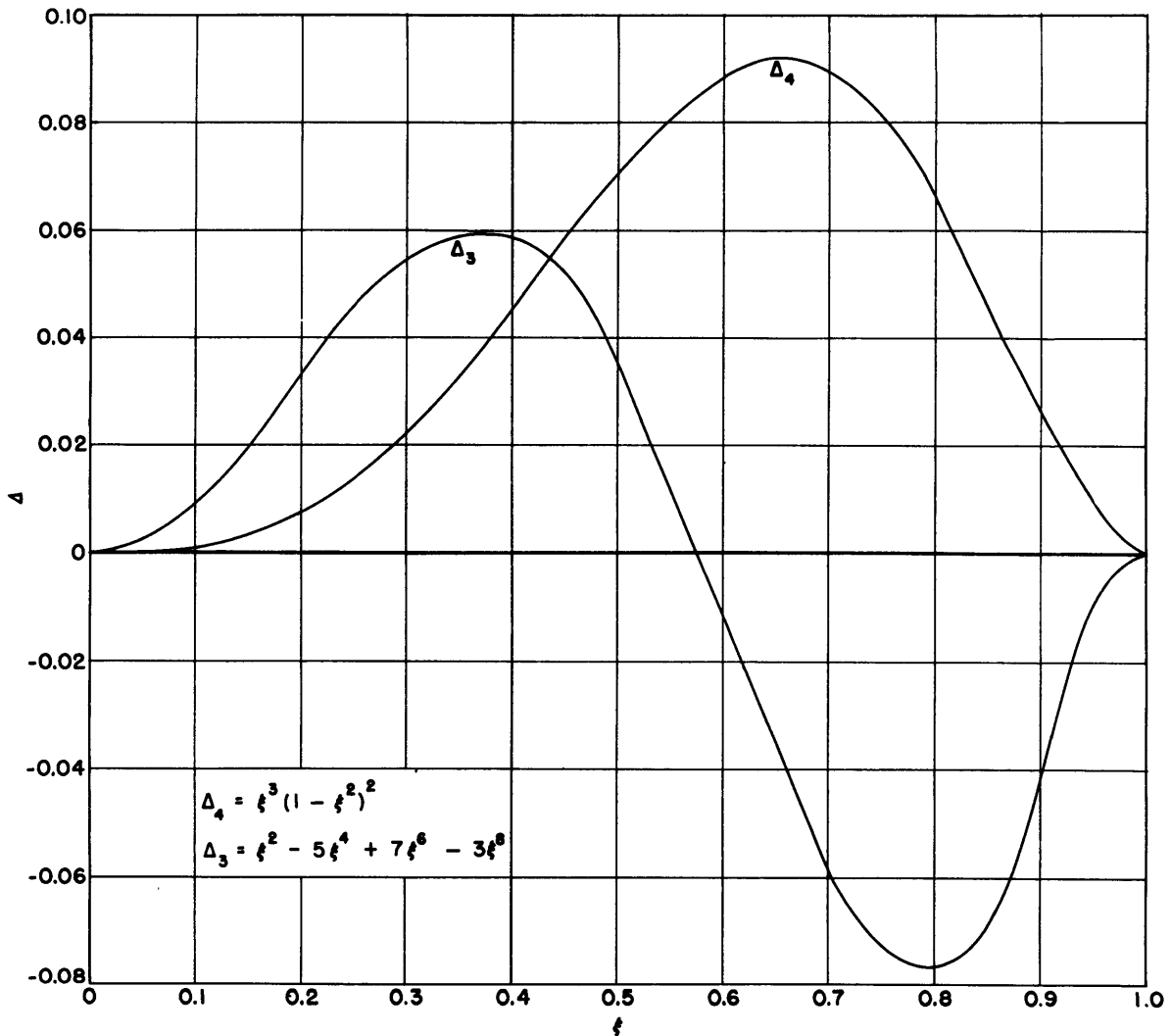


Figure 13 - Distribution Functions Following Equations [6a] and [6b]

The curves I_a to IV_a have been derived from the TMB models (Figures 14 and 15) by reducing the coefficient of ξ to unity. The procedure of obtaining the symmetric and the skew part from graphs is obvious: The first one is the arithmetic mean of the fore and afterbody ordinates $\eta_m = \frac{\eta_F + \eta_A}{2}$ and the latter one the difference $\frac{\eta_F - \eta_m}{2}$ or $\frac{\eta_m - \eta_A}{2}$ respectively.

The computation of the wave resistance due to asymmetry is based on Equation [24]:

For the trinomial

$$\eta_a = a_1 (\xi + b_3 \xi^3 + b_5 \xi^5)$$

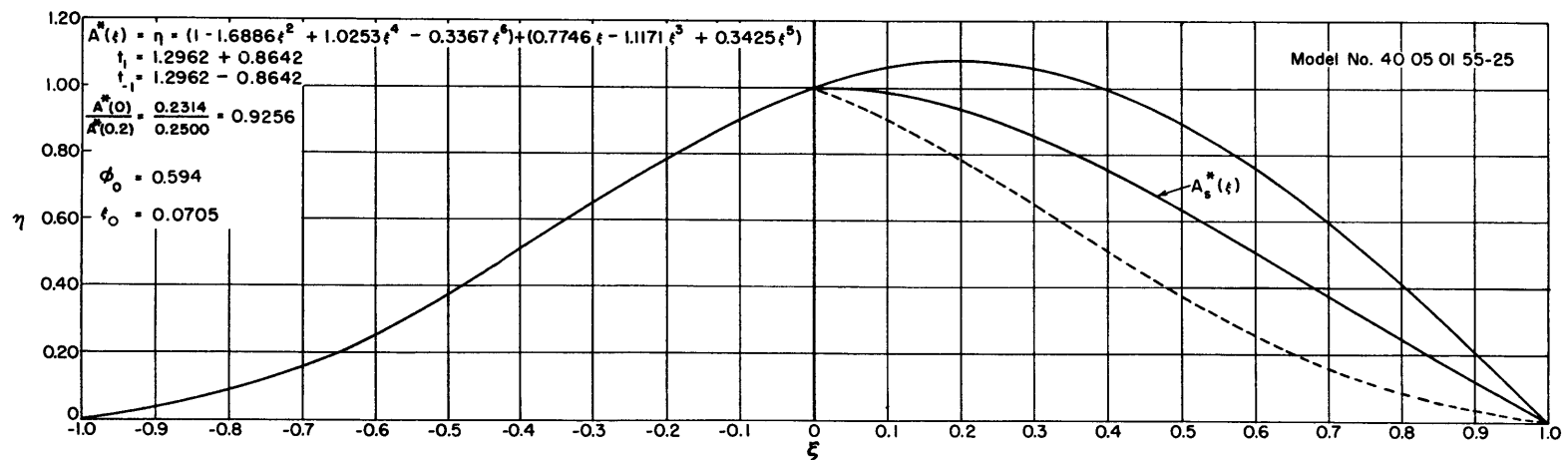
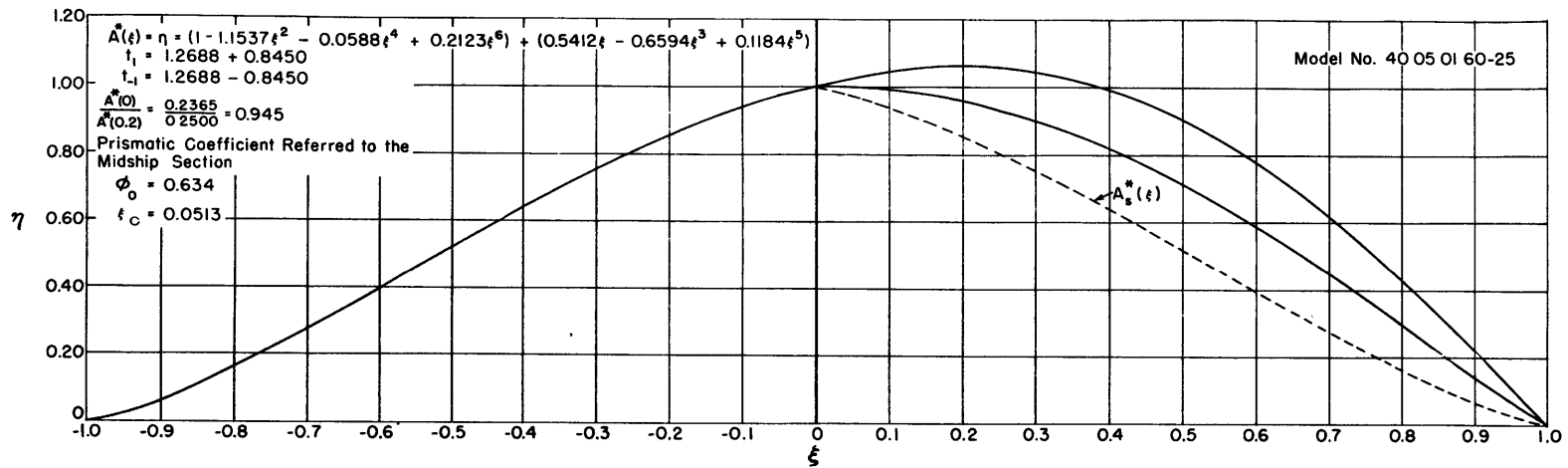


Figure 14 - Sectional-Area Curves of TMB Models

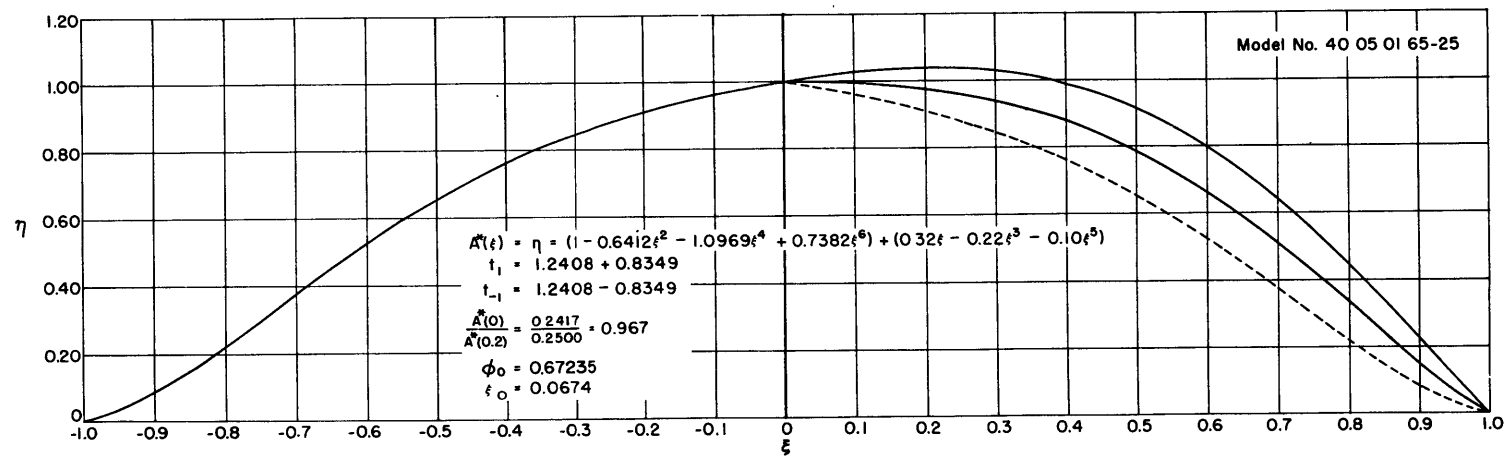
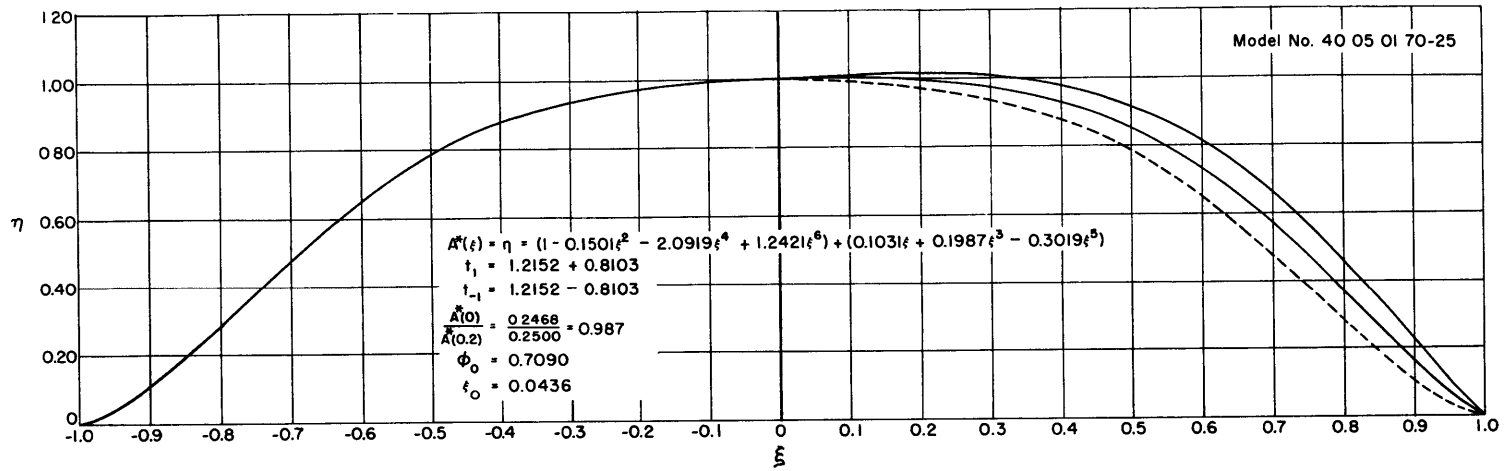


Figure 15 - Sectional-Area Curves of TMB Models

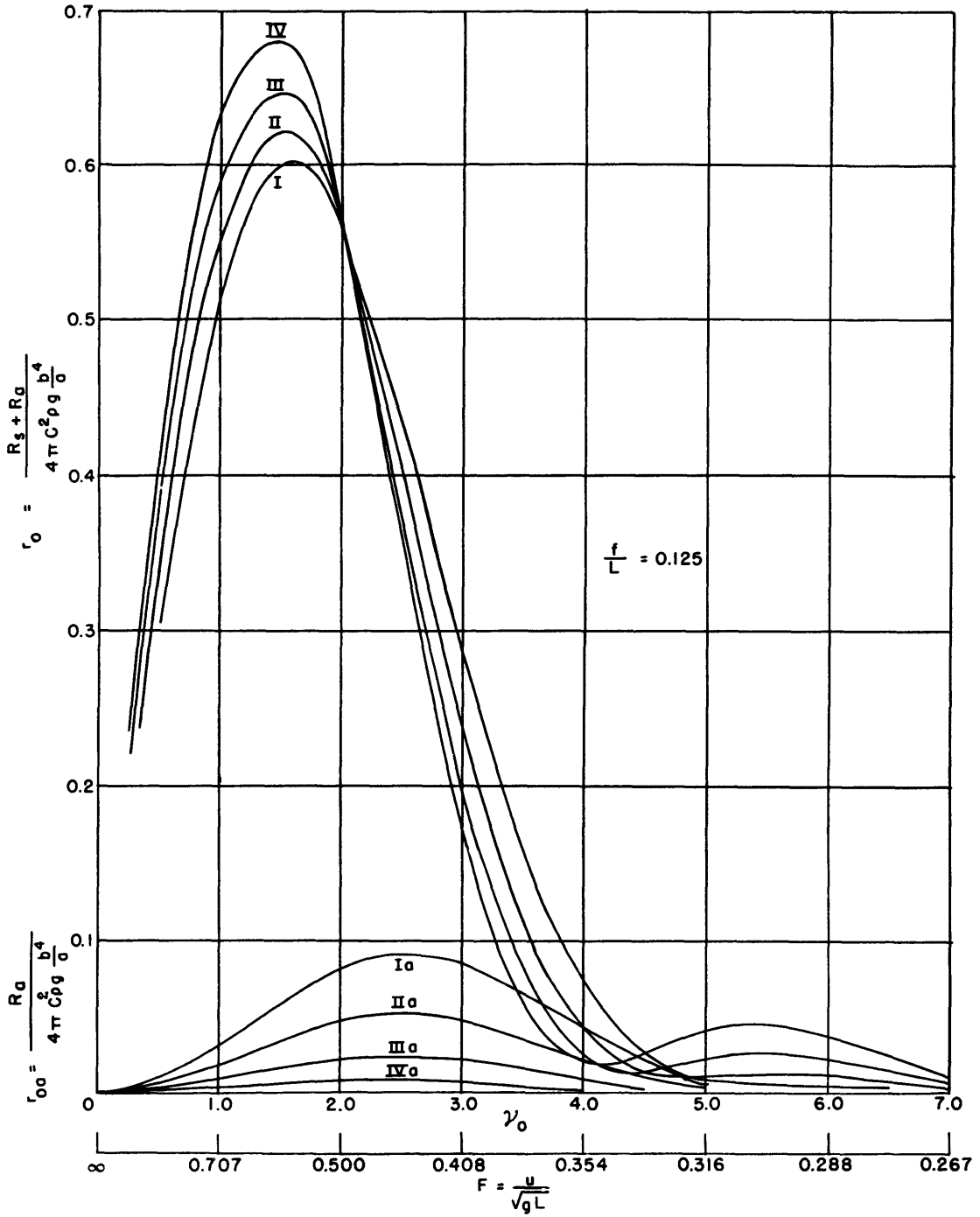


Figure 16 - Total Wave-Resistance Coefficients and Coefficients Due to Asymmetry of the Four TMB Models Shown in Figure 14 and Figure 15, $f/L = 0.125$

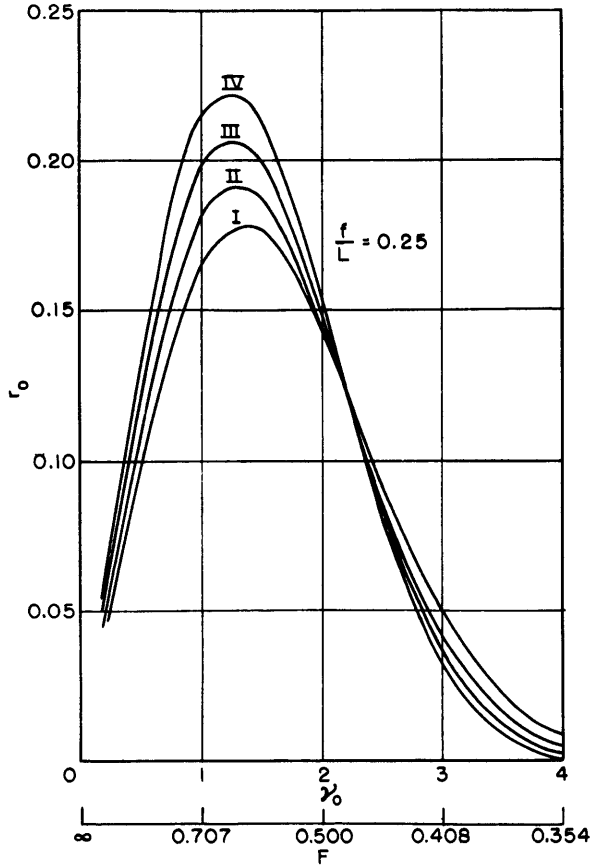


Figure 17 - Total Wave-Resistance Coefficients r_o of the TMB Models Shown in Figures 14 and 15, $f/L = 0.25$

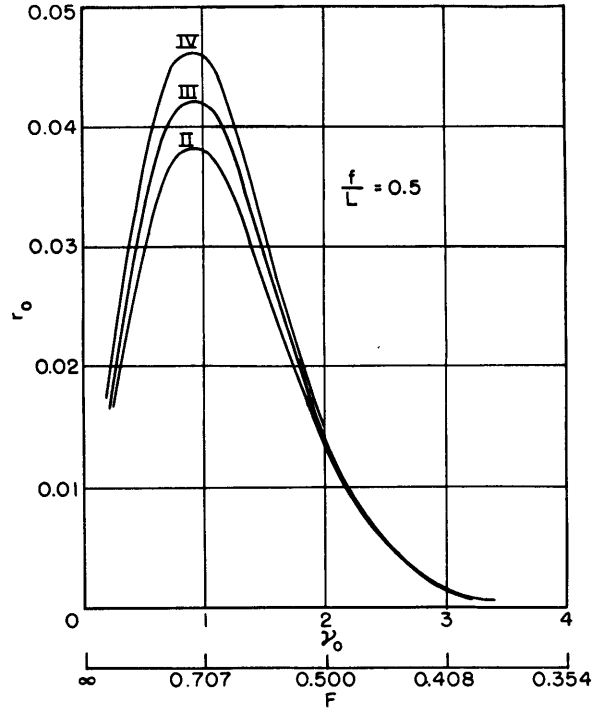


Figure 18 - Total Wave-Resistance Coefficients r_o of the TMB Models Shown in Figures 14 and 15, $f/L = 0.5$

with the derivative

$$\frac{\partial \eta_a}{\partial \xi} = a_1 (1 + 3b_3 \xi^2 + 5b_5 \xi^4)$$

we obtain

$$R_a = C_o a_1^2 \left[m'_{00} + 9b_3^2 m'_{22} + 25b_5^2 m'_{44} + 6b_3 m'_{02} + 10b_5 m'_{04} + 30b_3 b_5 m'_{24} \right] \quad [33]$$

Figure 19 shows the functions

$$r_{oa} = \frac{R_a}{4\pi\rho g C^2 b^4/a}$$

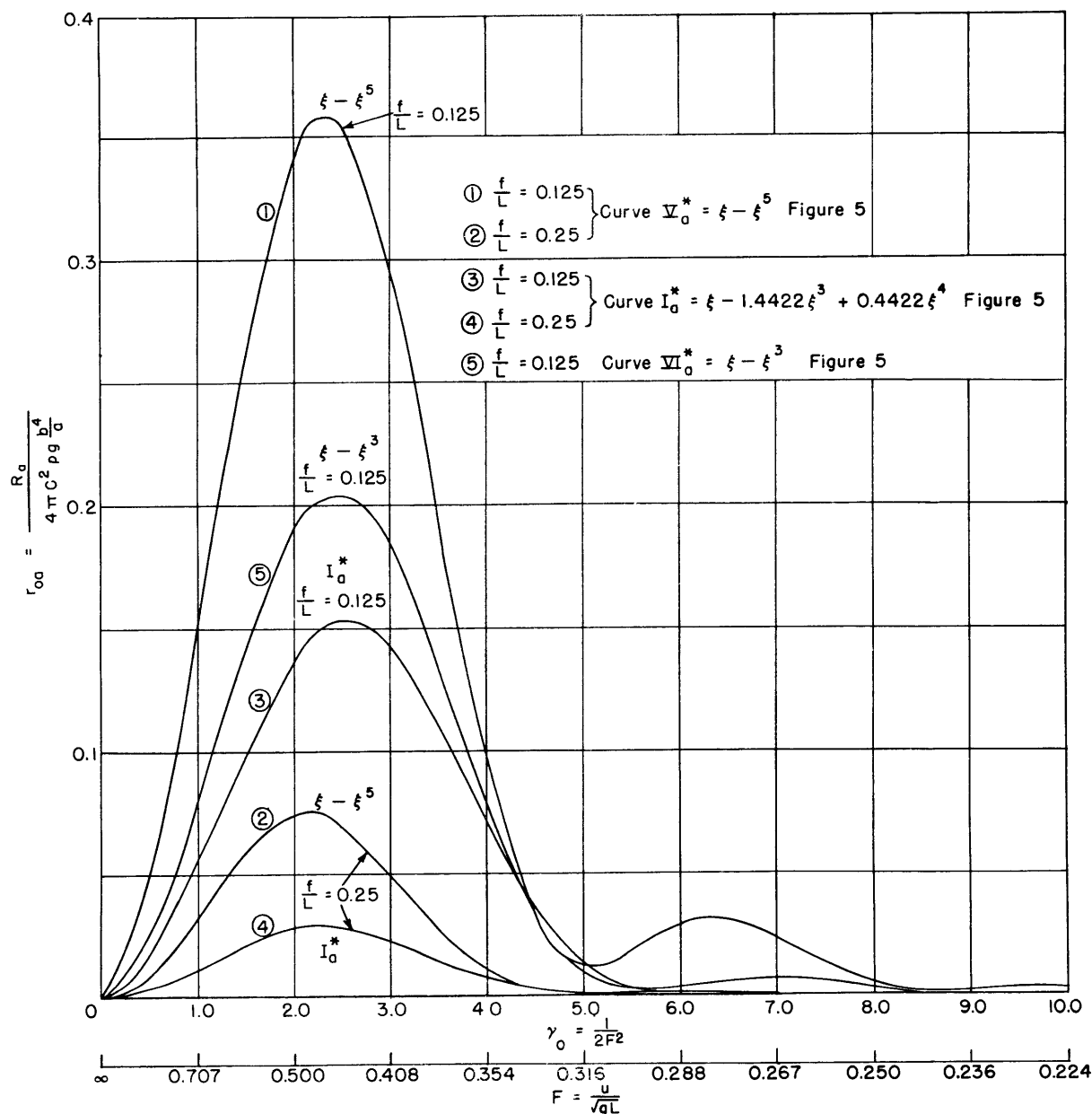


Figure 19 - Wave-Resistance Coefficients r_{0a} Due to Antisymmetrical Distributions Following Figure 5

corresponding to the distributions $\xi - \xi^5$, $\xi - \xi^3$ and I_a^* shown in Figure 5, where curve I_a^* is derived from the TMB body, Figure 14.

The "amount" of asymmetry which corresponds to the equation $\eta_a = \xi - \xi^5$ is very large, but by assuming the strength parameter $a_1 < 1$ (Equation [4e]) more usual distributions are reached; for these asymmetric terms the wave-resistance curves are obtained simply by multiplying the ordinates of Figure

19 by a_1^2 .

The resistance curves in Figure 19 corresponding to $\xi - \xi^5$ and I_a^* are somewhat similar in the range of the large hump and the ratios of their absolute values are of the order of 0.5. In the range of the second hump the ordinates of both curves are small, but it is characteristic that here a much lower resistance corresponds to the finer line I_a^* , rather than to $\xi - \xi^5$.

We return now to the four TMB models designated by I, II, III, IV shown in Figures 14 and 15. In these figures the line $A_s^*(\xi)$ shows the symmetrical part of a body. The resistance results are plotted on Figures 16, 17 and 18;* in them the lower set represents the contribution due to antisymmetry

$$r_{oa} = \frac{R_a}{4\pi\rho g C^2 b^4/a},$$

the upper set the total wave-resistance coefficient

$$r_o = \frac{R_a + R_s}{4\pi\rho g C^2 b^4/a}.$$

The computations are made under the assumption that the doublet distribution $\mu^*(\xi) = A^*(\xi)$. With the model number rising from I to IV the prismatic increases and the asymmetry decreases. In the important range of Froude numbers $0.50 \geq F \geq 0.35$ the finer models are extremely unfavorable because of the low prismatic as well as because of the very pronounced asymmetry.

When comparing the total resistance values a slight departure from symmetry generally is advantageous because of viscous effects. It has also been pointed out that small asymmetric terms do not increase appreciably the wave resistance even in the most sensitive range of Froude numbers, say $0.45 \geq F \geq 0.35$; this is well supported by our present results, for instance by Curve IV. Further, the obvious fact must be once more emphasized that an immediate comparison between symmetrical and asymmetrical bodies—as to their wave-resistance properties—is only feasible when the sectional area of the former $A_s^*(\xi)$ is the even part of the sectional area of the latter

$$A^*(\xi) = A_s^*(\xi) + A_a^*(\xi)$$

It is entirely possible to obtain asymmetrical forms with wave-resistance properties which are superior to the corresponding ones of a poorly chosen symmetrical form, equal prismatics and principal dimensions being assumed.

Similar computations have been performed for other depths of immersion; some results are listed in Table 2 of Appendix III. Obviously it is not difficult to investigate the wave resistance corresponding to any curve of the family defined by Equation [4e] at the three depths of immersion for which the integrals have been tabulated.

*There is a slight error in the resistance curves R_a of Model III due to inaccuracy in computations, but it does not invalidate the comparison.

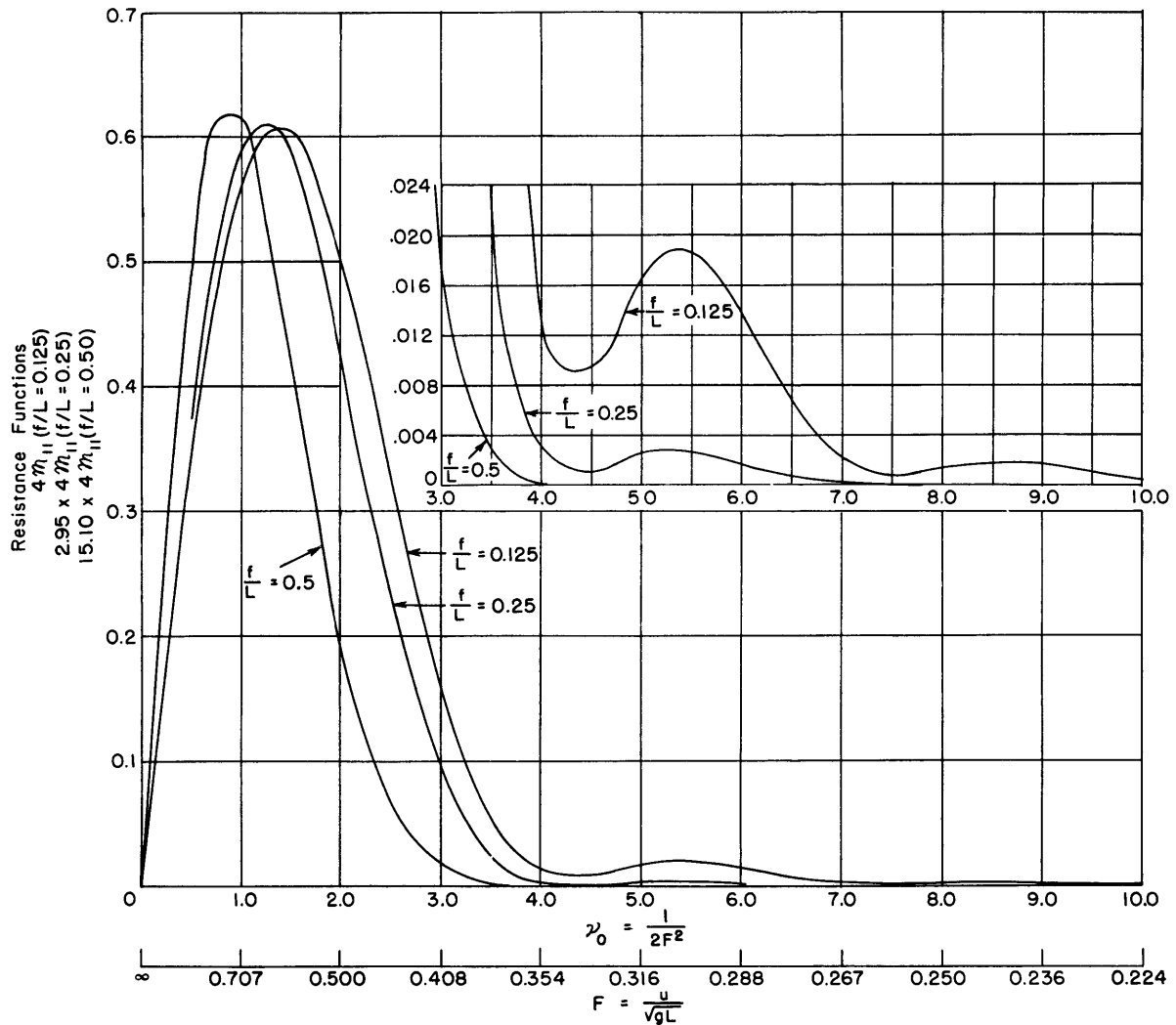


Figure 9 - Comparison of the Shape of Wave-Resistance Curves for the Spheroid $\eta(\xi) = 1 - \xi^2$; the Curves are Reduced to Approximately Equal Maxima

A. Small depths of immersion

1) Within reasonable limits, the peak value of the R/Δ curve does not depend too much on the shape of the body,* especially upon the prismatic coefficient.

2) The merits of full forms, over a wide and possibly important range of Froude numbers $0.35 \leq F \leq 0.50$, are clearly emphasized, as well as

3) The heavy penalty which has to be paid for high prismatics at lower F .

*If more elaborate results are desired they can be derived from Figures 28 through 35.

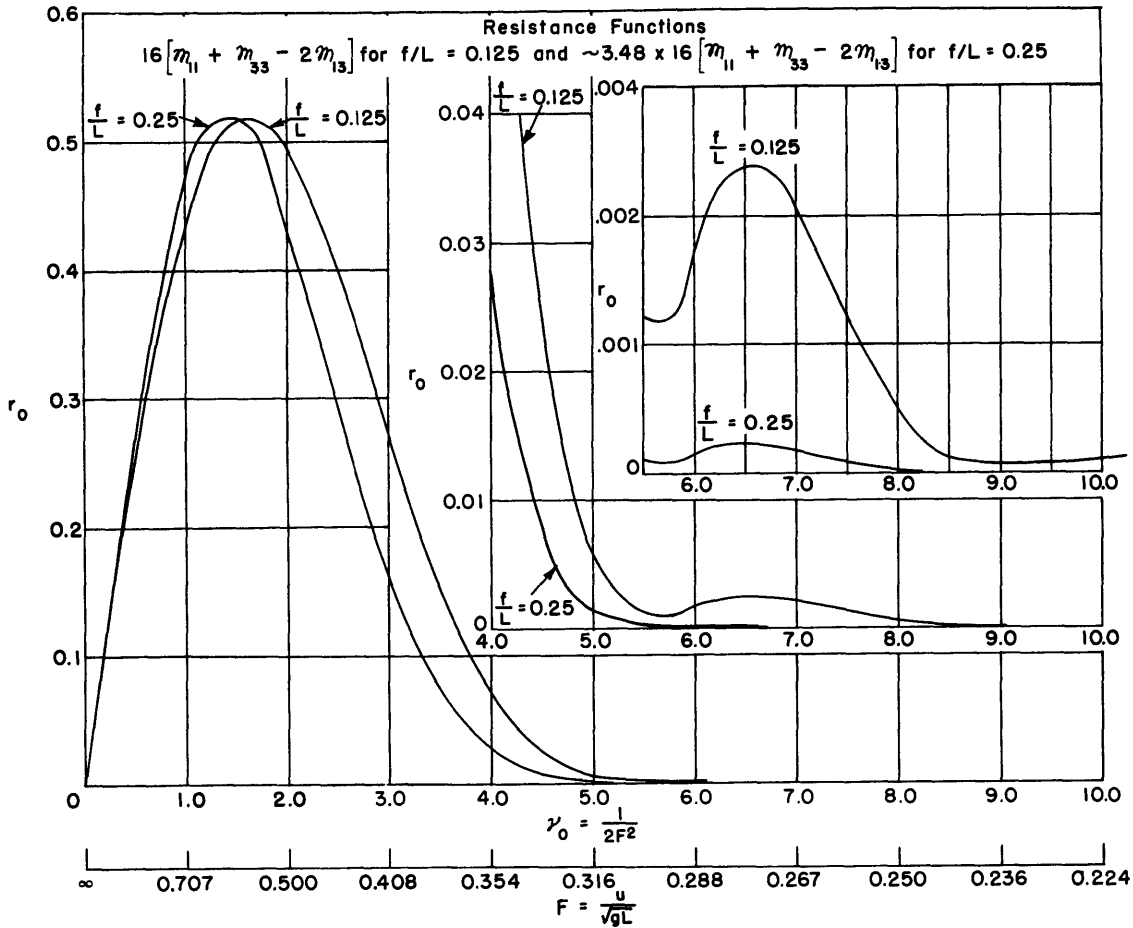


Figure 10 - Comparison of the Shape of Wave-Resistance Curves for $\eta = (1 - \xi^2)^2$ Reduced as by Figure 9

B. For larger depths of immersion the dependence of the peak values of R/Δ upon ϕ becomes more pronounced; the advantage of high prismatics in the range mentioned in A(2) is, on the average, reduced.

4.3. RESISTANCE CURVES OF ASYMMETRICAL BODIES

Further curves representing the wave-resistance coefficients of the four TMB models represented in Figures 14 and 15 are shown in Figures 16, 17 and 18. Before discussing these particular asymmetric models, however, an investigation must be made of the influence of asymmetry on the resistance.

Figure 5 represents examples of asymmetrical lines belonging to the family $\eta_a^* = \xi + b_3 \xi^3 - (1 + b_3) \xi^5$, Equation [4g].

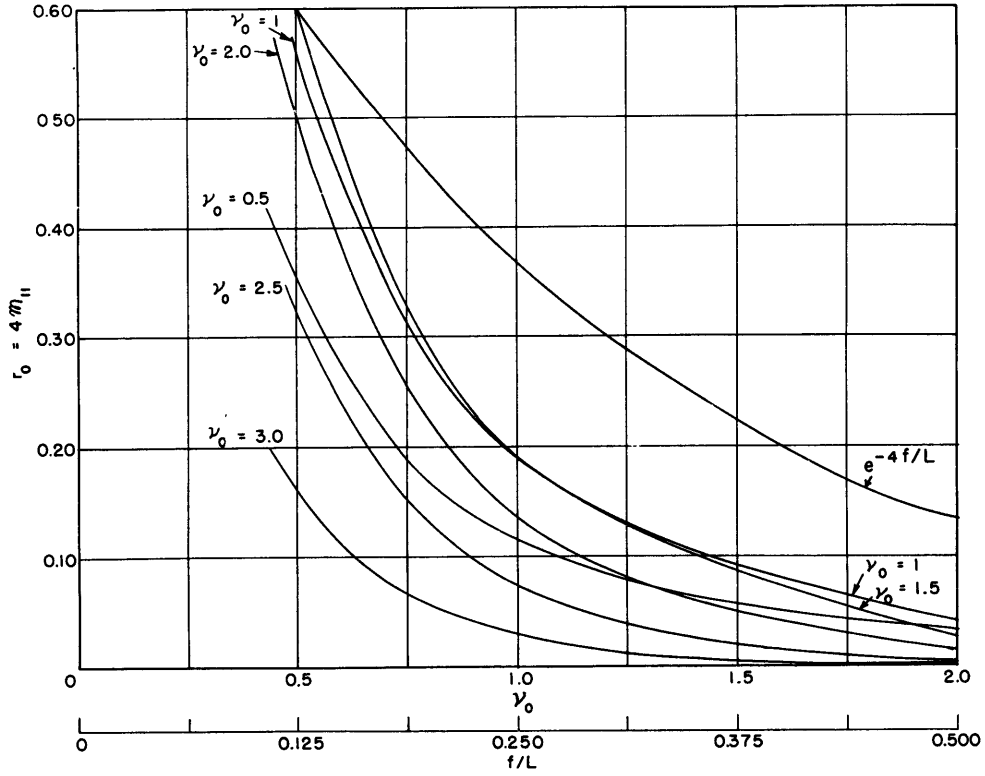


Figure 11 - Wave-Resistance Coefficients of the Spheroid as Functions of f/L with $\gamma_0 = 1/2F^2$ as Parameter

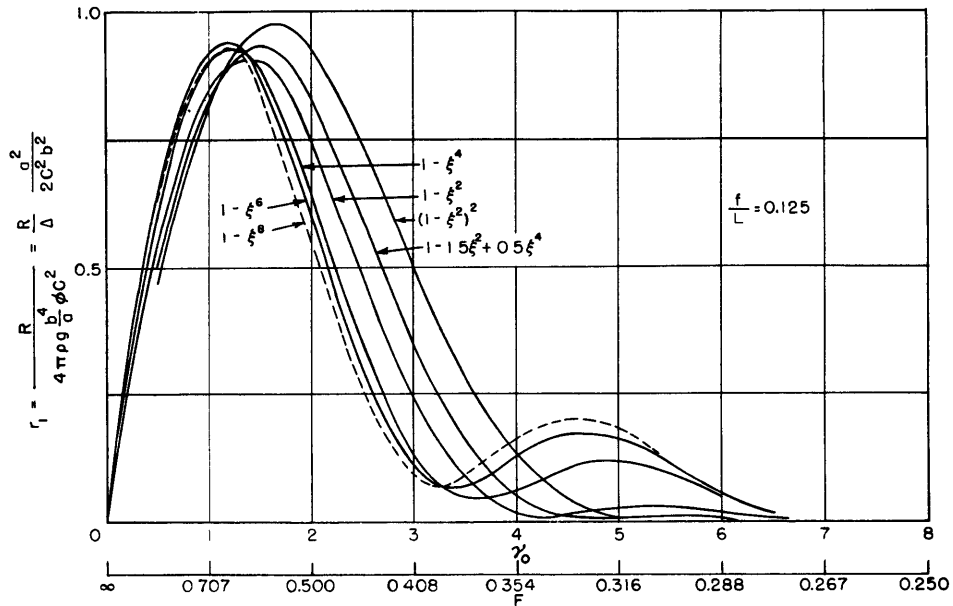


Figure 12 - Wave-Resistance Coefficients $r_1 = \frac{r_0}{\phi} = \frac{R}{\Delta} \frac{a^2}{2C^2b^2}$ of Symmetrical Bodies Shown on Figure 4, $f/L = 0.125$

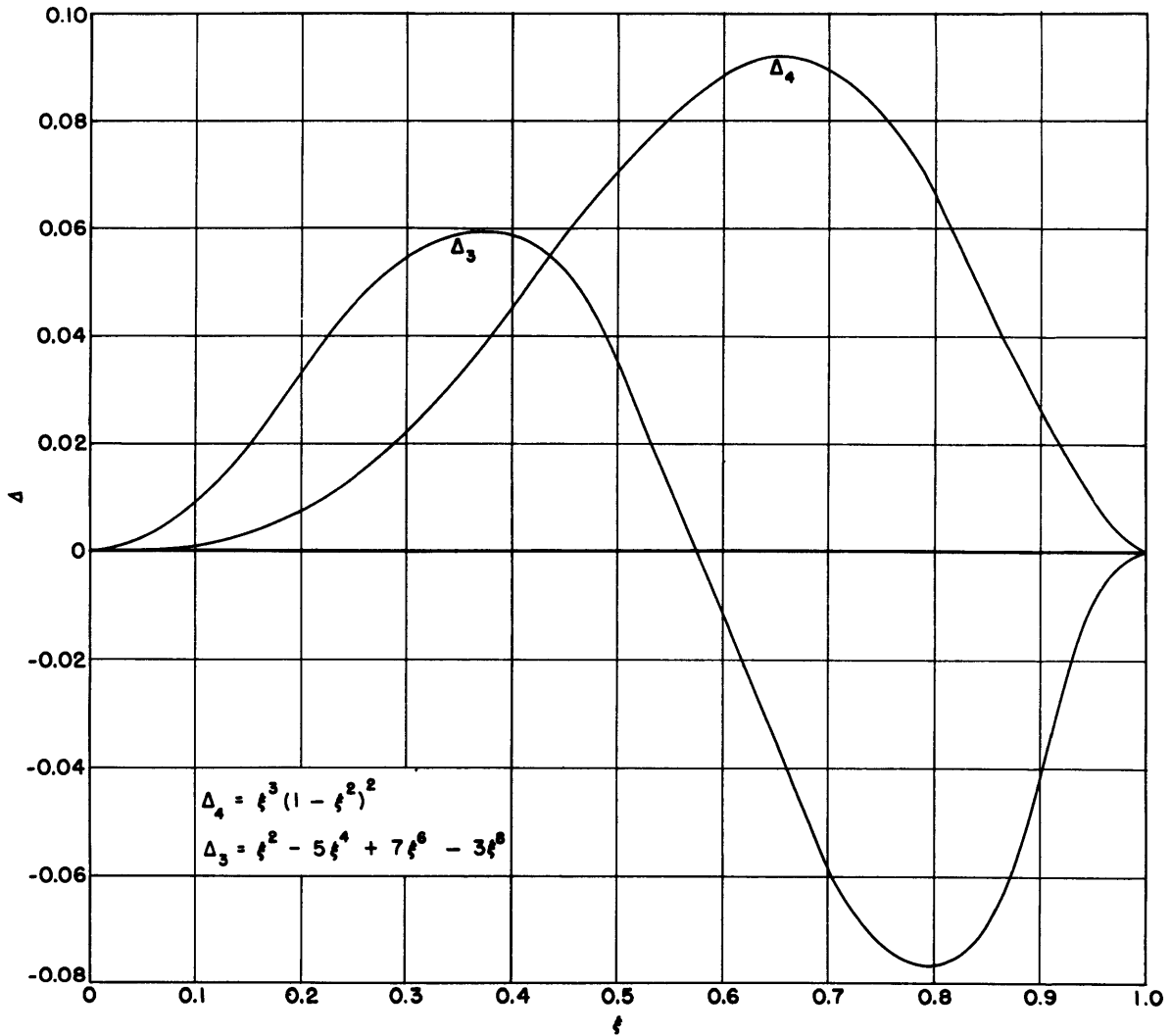


Figure 13 - Distribution Functions Following Equations [6a] and [6b]

The curves I_a to IV_a have been derived from the TMB models (Figures 14 and 15) by reducing the coefficient of ξ to unity. The procedure of obtaining the symmetric and the skew part from graphs is obvious: The first one is the arithmetic mean of the fore and afterbody ordinates $\eta_m = \frac{\eta_F + \eta_A}{2}$ and the latter one the difference $\frac{\eta_F - \eta_m}{2}$ or $\frac{\eta_m - \eta_A}{2}$ respectively.

The computation of the wave resistance due to asymmetry is based on Equation [24]:

For the trinomial

$$\eta_a = a_1 (\xi + b_3 \xi^3 + b_5 \xi^5)$$

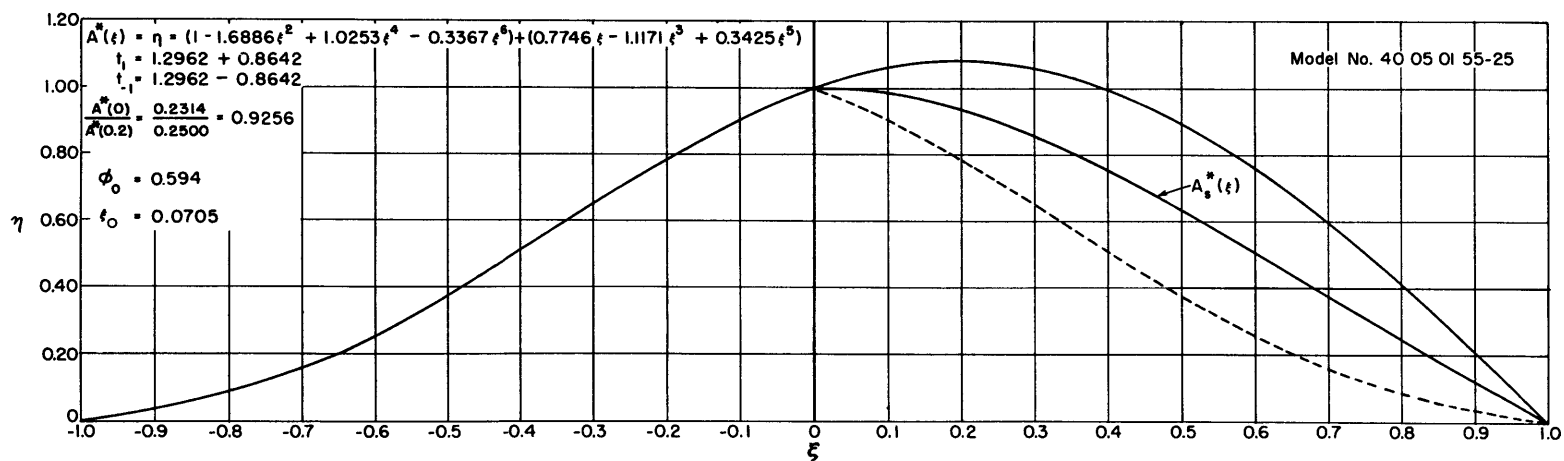
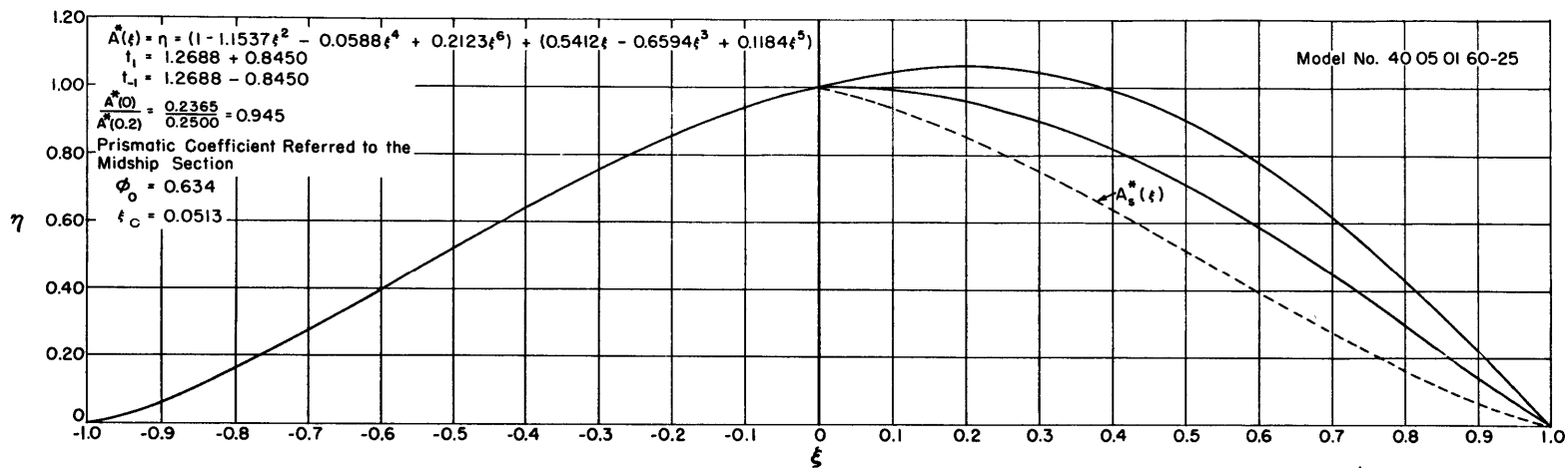


Figure 14 - Sectional-Area Curves of TMB Models

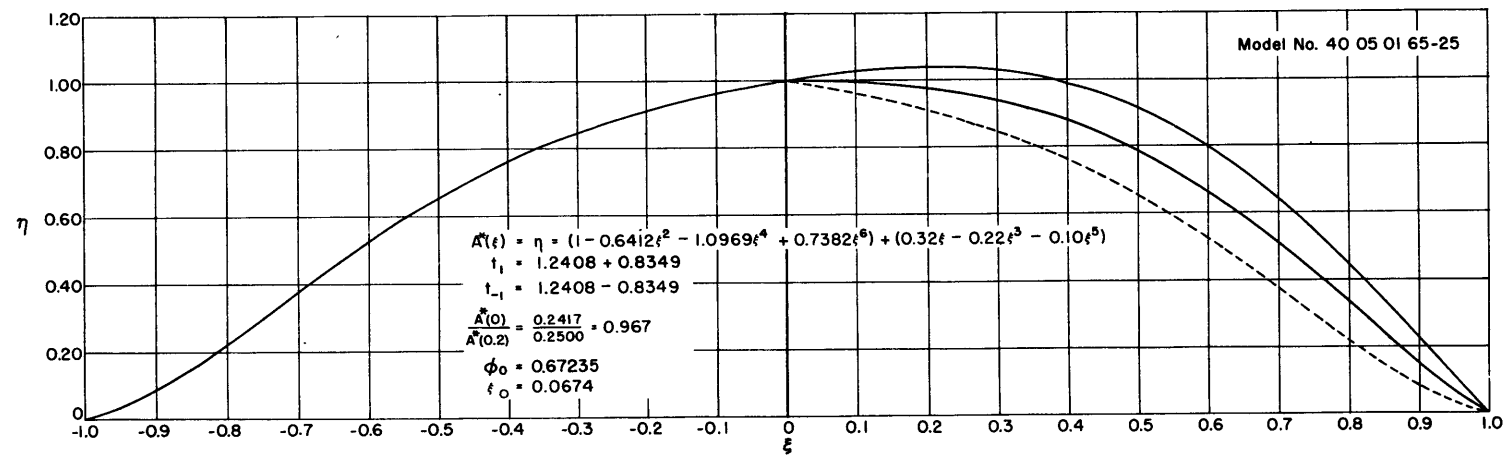
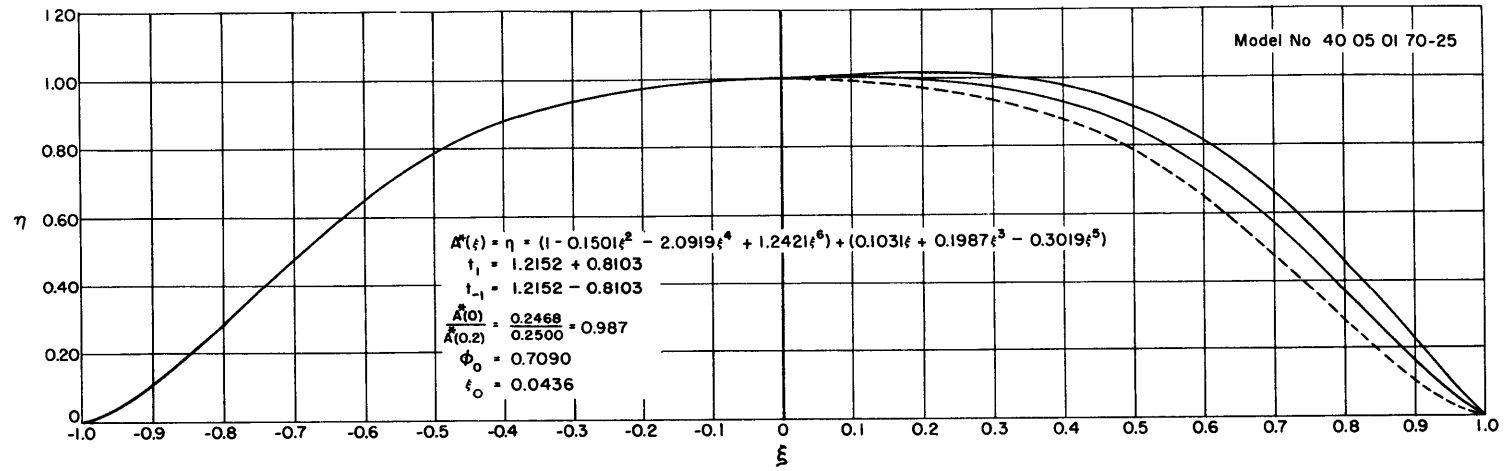


Figure 15 - Sectional-Area Curves of TMB Models

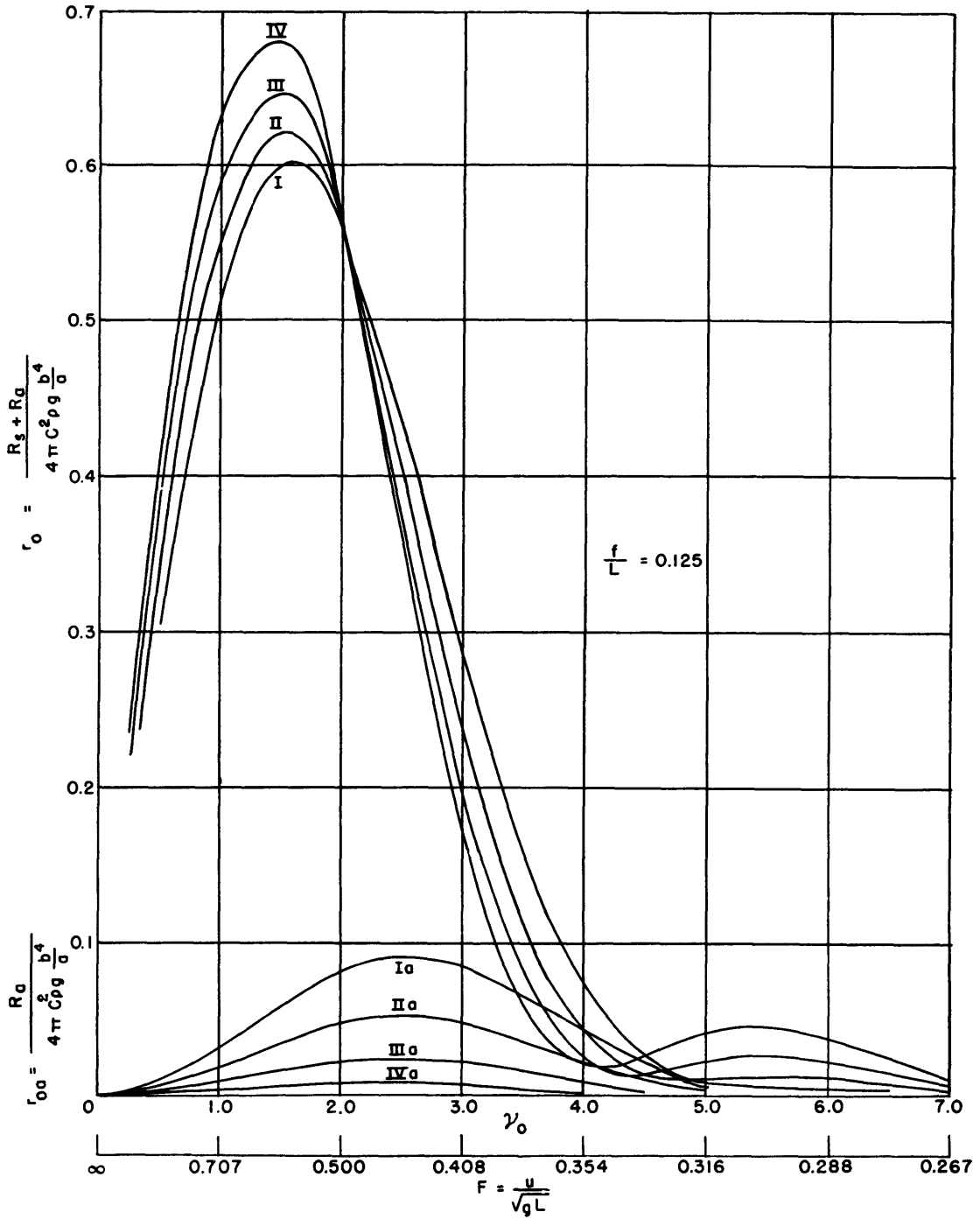


Figure 16 - Total Wave-Resistance Coefficients and Coefficients Due to Asymmetry of the Four TMB Models Shown in Figure 14 and Figure 15, $f/L = 0.125$

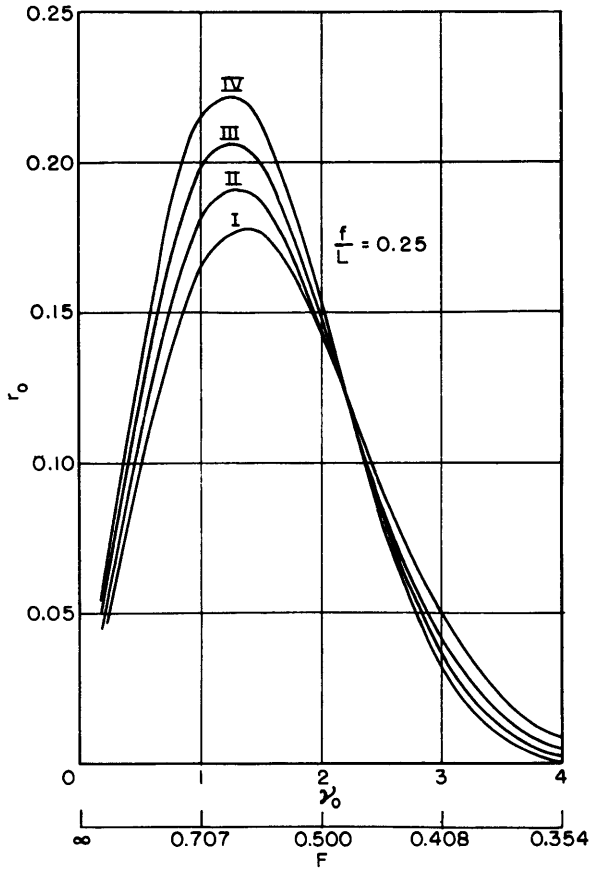


Figure 17 - Total Wave-Resistance Coefficients r_o of the TMB Models Shown in Figures 14 and 15, $f/L = 0.25$

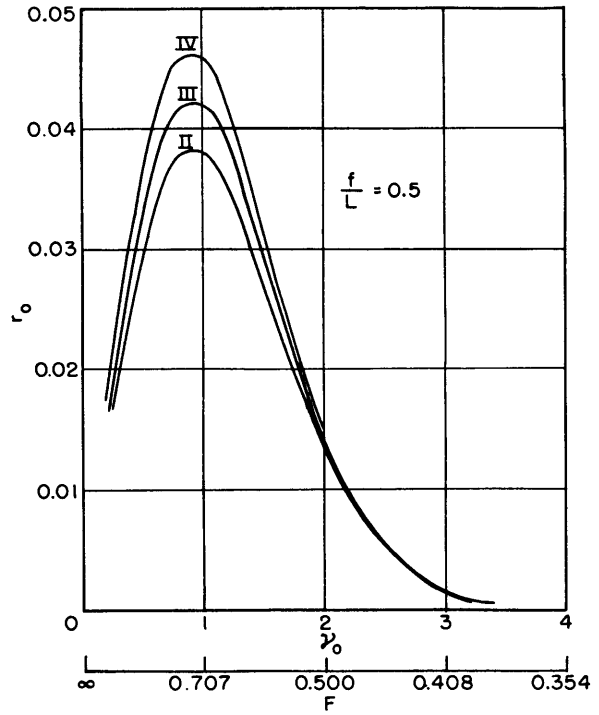


Figure 18 - Total Wave-Resistance Coefficients r_o of the TMB Models Shown in Figures 14 and 15, $f/L = 0.5$

with the derivative

$$\frac{\partial \eta_a}{\partial \xi} = a_1 (1 + 3b_3 \xi^2 + 5b_5 \xi^4)$$

we obtain

$$R_a = C_0 a^2 \left[\eta'_{00} + 9b_3^2 \eta'_{22} + 25b_5^2 \eta'_{44} + 6b_3 \eta'_{02} + 10b_5 \eta'_{04} + 30b_3 b_5 \eta'_{24} \right] \quad [33]$$

Figure 19 shows the functions

$$r_{oa} = \frac{R_a}{4\pi\rho g C^2 b^4/a}$$

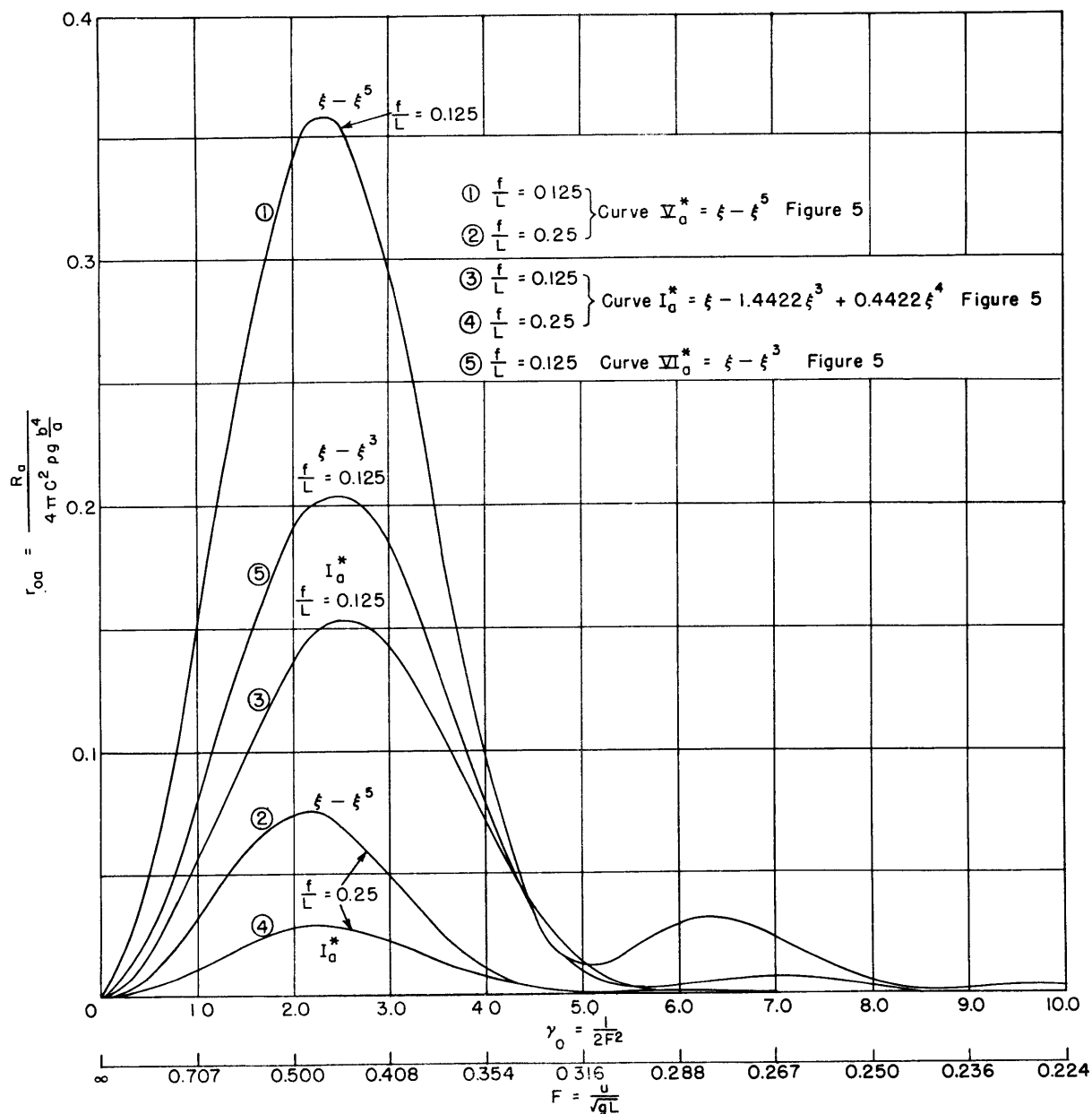


Figure 19 - Wave-Resistance Coefficients r_{0a} Due to Antisymmetrical Distributions Following Figure 5

corresponding to the distributions $\xi - \xi^5$, $\xi - \xi^3$ and I_a^* shown in Figure 5, where curve I_a^* is derived from the TMB body, Figure 14.

The "amount" of asymmetry which corresponds to the equation $\eta_a = \xi - \xi^5$ is very large, but by assuming the strength parameter $a_1 < 1$ (Equation [4e]) more usual distributions are reached; for these asymmetric terms the wave-resistance curves are obtained simply by multiplying the ordinates of Figure

19 by a_1^2 .

The resistance curves in Figure 19 corresponding to $\xi - \xi^5$ and I_a^* are somewhat similar in the range of the large hump and the ratios of their absolute values are of the order of 0.5. In the range of the second hump the ordinates of both curves are small, but it is characteristic that here a much lower resistance corresponds to the finer line I_a^* , rather than to $\xi - \xi^5$.

We return now to the four TMB models designated by I, II, III, IV shown in Figures 14 and 15. In these figures the line $A_s^*(\xi)$ shows the symmetrical part of a body. The resistance results are plotted on Figures 16, 17 and 18;* in them the lower set represents the contribution due to antisymmetry

$$r_{oa} = \frac{R_a}{4\pi\rho g C^2 b^4/a},$$

the upper set the total wave-resistance coefficient

$$r_o = \frac{R_a + R_s}{4\pi\rho g C^2 b^4/a}.$$

The computations are made under the assumption that the doublet distribution $\mu^*(\xi) = A^*(\xi)$. With the model number rising from I to IV the prismatic increases and the asymmetry decreases. In the important range of Froude numbers $0.50 \geq F \geq 0.35$ the finer models are extremely unfavorable because of the low prismatic as well as because of the very pronounced asymmetry.

When comparing the total resistance values a slight departure from symmetry generally is advantageous because of viscous effects. It has also been pointed out that small asymmetric terms do not increase appreciably the wave resistance even in the most sensitive range of Froude numbers, say $0.45 \geq F \geq 0.35$; this is well supported by our present results, for instance by Curve IV. Further, the obvious fact must be once more emphasized that an immediate comparison between symmetrical and asymmetrical bodies—as to their wave-resistance properties—is only feasible when the sectional area of the former $A_s^*(\xi)$ is the even part of the sectional area of the latter

$$A^*(\xi) = A_s^*(\xi) + A_a^*(\xi)$$

It is entirely possible to obtain asymmetrical forms with wave-resistance properties which are superior to the corresponding ones of a poorly chosen symmetrical form, equal prismatics and principal dimensions being assumed.

Similar computations have been performed for other depths of immersion; some results are listed in Table 2 of Appendix III. Obviously it is not difficult to investigate the wave resistance corresponding to any curve of the family defined by Equation [4e] at the three depths of immersion for which the integrals have been tabulated.

*There is a slight error in the resistance curves R_a of Model III due to inaccuracy in computations, but it does not invalidate the comparison.

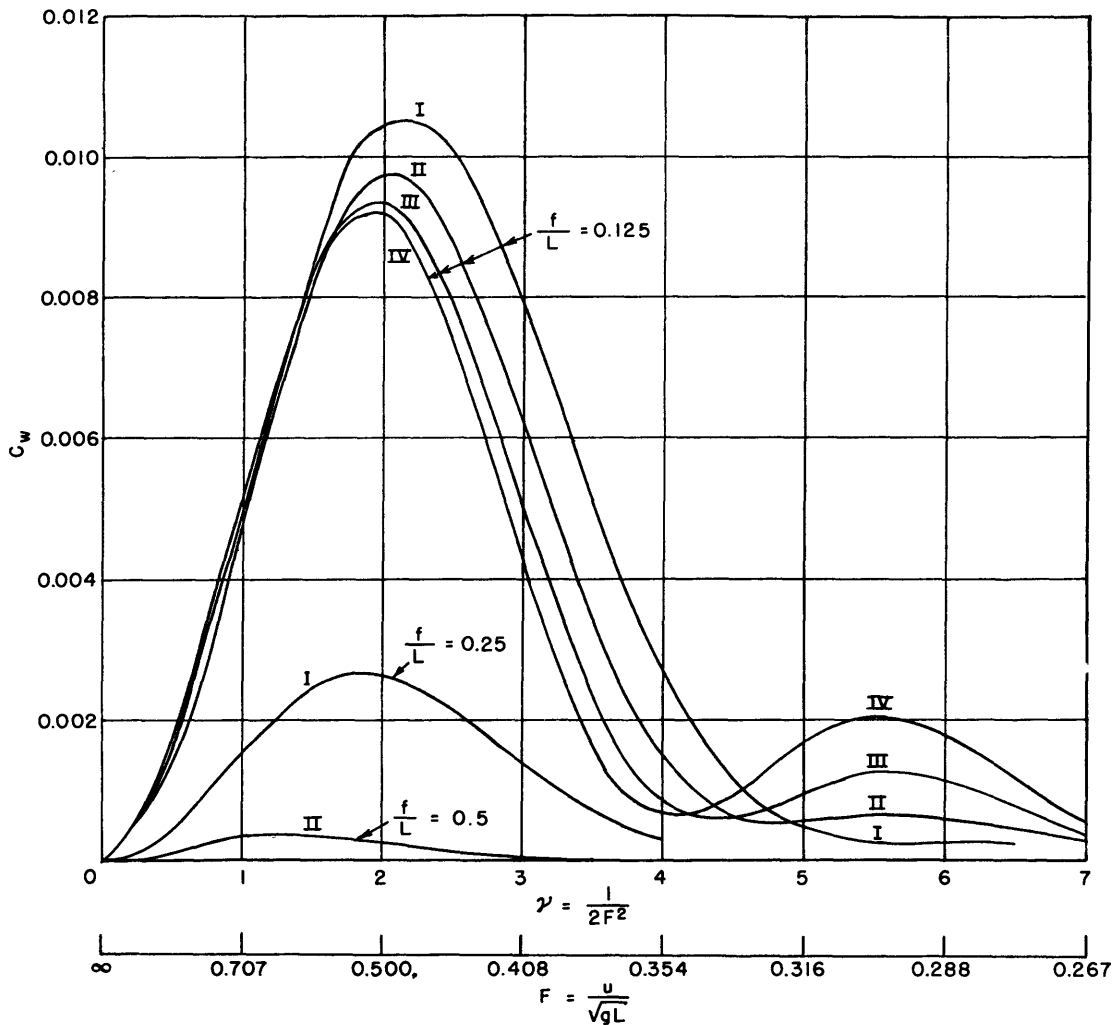


Figure 20 - Wave-Resistance Coefficients $c_w = \frac{R}{\rho/2 U^2 S}$ Referred to the Wetted Area S for the Four TMB Models I-IV, $f/L = 0.125$ (For Comparison of Range Single Curves for $f/L = 0.25$ and $f/L = 0.5$ are Shown)

To check the order of magnitude of the wave resistance and to enable a comparison with experimental data, resistance coefficients c_w of the four TMB models I to IV are shown in Figures 20 to 22, calculated for $b/a = 1/7$ and $C = 1.07$. In this case the depth of immersion ratios f/L correspond to the technically more familiar f/D ratios as follows:

f/L	0.125	0.25	0.5
f/D	0.875	1.75	3.5

Assuming a rather high viscous-drag coefficient ($c_v = 0.003$), the relative importance of the wave resistance at various depths of immersion

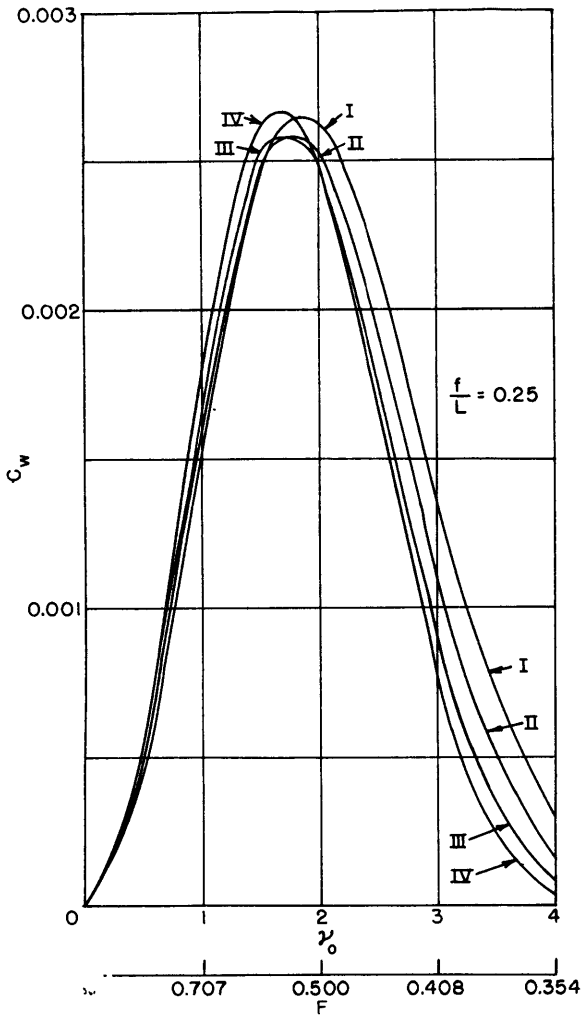


Figure 21 - Wave-Resistance Coefficients $c_w = \frac{R}{\rho/2 U^2 S}$ Referred to the Wetted Area S for the Four TMB Models I-IV, $f/L = 0.25$

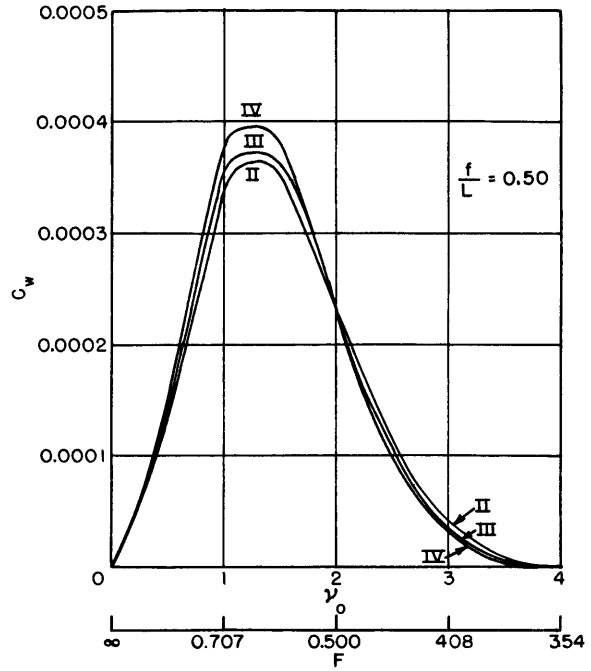


Figure 22 - Wave-Resistance Coefficients $c_w = \frac{R}{\rho/2 U^2 S}$ Referred to the Wetted Area S for the Four TMB Models I-IV, $f/L = 0.50$

and Froude numbers can be estimated for a comparatively wide span of prismatic coefficient $0.71 \geq \phi \geq 0.59$. Attention is drawn to the changes in the mutual relations between the curves in Figures 20 to 22. These changes are dependent upon f/L and upon the obvious shift of the peaks towards smaller Froude numbers as compared with Figures 16 to 18, because of the factor U^2 in the denominator of c_w .

Considerations of wave resistance may play a significant role when fixing the optimum elongation ratio D/L as long as free-surface conditions are important. Assuming both Ψ and ϕ to be constant, the surface S and therefore the viscous drag vary only with $\sqrt[3]{L/D}$ while the wave resistance varies

with $(D/L)^2$ multiplied by a complicated function r_0 of F . Restricting F to a range $\sim 0.6 \geq F \geq 0.35$, r_0 is monotonically and, on the average, heavily decreasing with decreasing F . Thus any reduction of D/L heavily reduces the wave resistance.

4.4. LIMITING DEPTH OF IMMERSION

It is important to know below what depths of immersion f_0 the wave resistance can be neglected. This limit can be established from such cross curves as shown on Figure 11; it obviously depends upon:

- a. The Froude number F or $\gamma_0 = 1/2F^2$
- b. The L/D ratio, and
- c. The dimensionless shape of the body, primarily its prismatic coefficient ϕ , especially outside of the large hump.

However, some additional simple reasoning may be helpful when curves $R = R(f/L)$ are not available. We can consider the wave resistance as negligible either when

- a. It is a small percentage of a given standard resistance, or
- b. It is less than an absolute small value δR .

Some obvious differences in results due to the different approach have sometimes been overlooked.

a. Assume that for $f \geq f_0$ the wave resistance becomes less than a given small fraction ϵ of the wave resistance R_0 at a standard depth, for instance at the immersion of one diameter; f_0 is derived from a ratio of the resistances in question. Comparing bodies of equal length, f_0 depends upon the Froude number and upon the dimensionless shape of the body, but only very slightly upon the elongation ratio $D/L \cong b/a$, since the latter influences only the constant $4\pi C^2 \rho g b^4/a$, which drops out in the comparison.

b. Assume that the limiting depth f_0 is derived from the condition that the wave resistance is less than an absolute value δR independent of the standard resistance R_0 . Comparing again bodies of equal length f_0 now becomes highly sensitive to changes in D/L .

A rough idea of the necessary limiting depth f_0 of immersion can be obtained from the decline of the water disturbance with increasing depth in a plane sinusoidal wave; this estimate normally gives exaggerated values f_0 .

Denoting the wave amplitude by h_m and the amplitude of the disturbance by h one obtains

$$h = h_m e^{-\frac{2\pi f}{\lambda}}$$

putting further

$$\lambda = \frac{2\pi U^2}{g} = 2\pi F^2 L$$

$$h = h_m e^{-\frac{f}{LF^2}}$$

and prescribing h/h_m , for instance assuming $h/h_m < 0.01$, one obtains

$$f_0 \geq \sim 0.75 \lambda$$

or

$$f_0/L \geq 1.5\pi F^2$$

This estimate is superficial for many reasons:

- a. The resistance depends rather on the square of the generated wave amplitudes,
- b. The actual problem is three dimensional, and
- c. The body shape is neglected.

However, it shows at least that in principle the limiting depth cannot be expressed as a fraction of the dimensions of the body alone, since it depends upon the length of the free wave λ or the Froude number F .

From practical considerations matters are somewhat different. As mentioned before, at very high Froude numbers the ratio of wave resistance to frictional drag is normally very small. Thus the problem of finding an accurate value of the limiting depth becomes rather unimportant since even grave errors in computing it do not lead to appreciable errors in the total resistance.

5. BODIES OF REVOLUTION OF LEAST WAVE RESISTANCE

5.1. TWO-PARAMETER FORMS

In an earlier paper⁵ endeavors were made to determine distributions of least resistance for given Froude numbers. The results varied with Froude numbers and depths of immersion, which is quite natural in the light of such resistance graphs as represented by Figures 6, 7 and 8.

An important feature is the peculiar "swan neck" form obtained for higher Froude numbers—equal to and above $F = 0.35$. Because of the limited accuracy of these former calculations the problem has been reconsidered here. The present investigation supports the earlier statements.

The formalism needed is very simple. Some controversy arose as to how far the application of exact methods of the calculus of variation is consistent when dealing with surface ships;⁵ the results obtained did not

lead to reasonable ship's forms. However, when we restrict ourselves to families of curves expressed by polynomials with few arbitrary parameters, we really obtain an ordinary minimum problem and do not need to bother about the difficulties connected with the application of the calculus of variations.

Take for instance the family (basic form)

$$\eta = 1 - \xi^6 - a_2(\xi^2 - \xi^6) - a_4(\xi^4 - \xi^6) \quad [34]$$

with two arbitrary parameters. The wave resistance R is given as a second degree function in a_2 and a_4 .

$$R = 4B_{22} a_2^2 + 4B_{44} a_4^2 + 8B_{24} a_2 a_4 + 24B_{22} a_2 + 24B_{44} a_4 + B_0 \quad [35]$$

where

$$\begin{aligned} B_{22} &= m_{11} - 6m_{15} + 9m_{55} \\ B_{44} &= 4m_{33} - 12m_{35} + 9m_{55} \\ B_{24} &= 2m_{13} - 3m_{15} + 9m_{55} - 6m_{35} \\ B_2 &= m_{15} - 3m_{55} \\ B_4 &= 2m_{35} - 3m_{55} \\ B_0 &= 36m_{55} \end{aligned}$$

differentiating R partially with respect to a_2 and a_4 , one obtains the minimum conditions

$$\begin{aligned} \frac{\partial R}{\partial a_2} &= B_{22} a_2 + B_{24} a_4 + 3B_2 = 0 \\ \frac{\partial R}{\partial a_4} &= B_{24} a_2 + B_{44} a_4 + 3B_4 = 0 \end{aligned} \quad [36]$$

whence

$$\begin{aligned} a_2 &= -\frac{3[B_{24} B_{44} - B_{44} B_{24}]}{B_{22} B_{44} - B_{24}^2} \\ a_4 &= -\frac{3[B_{44} B_{22} - B_{22} B_{44}]}{B_{22} B_{44} - B_{24}^2} \end{aligned} \quad [37]$$

These equations lead to results which are not applicable to practice when $\gamma_0 = 1$ and of restricted interest when $\gamma_0 = 2$ (f/L is assumed equal to 0.125).

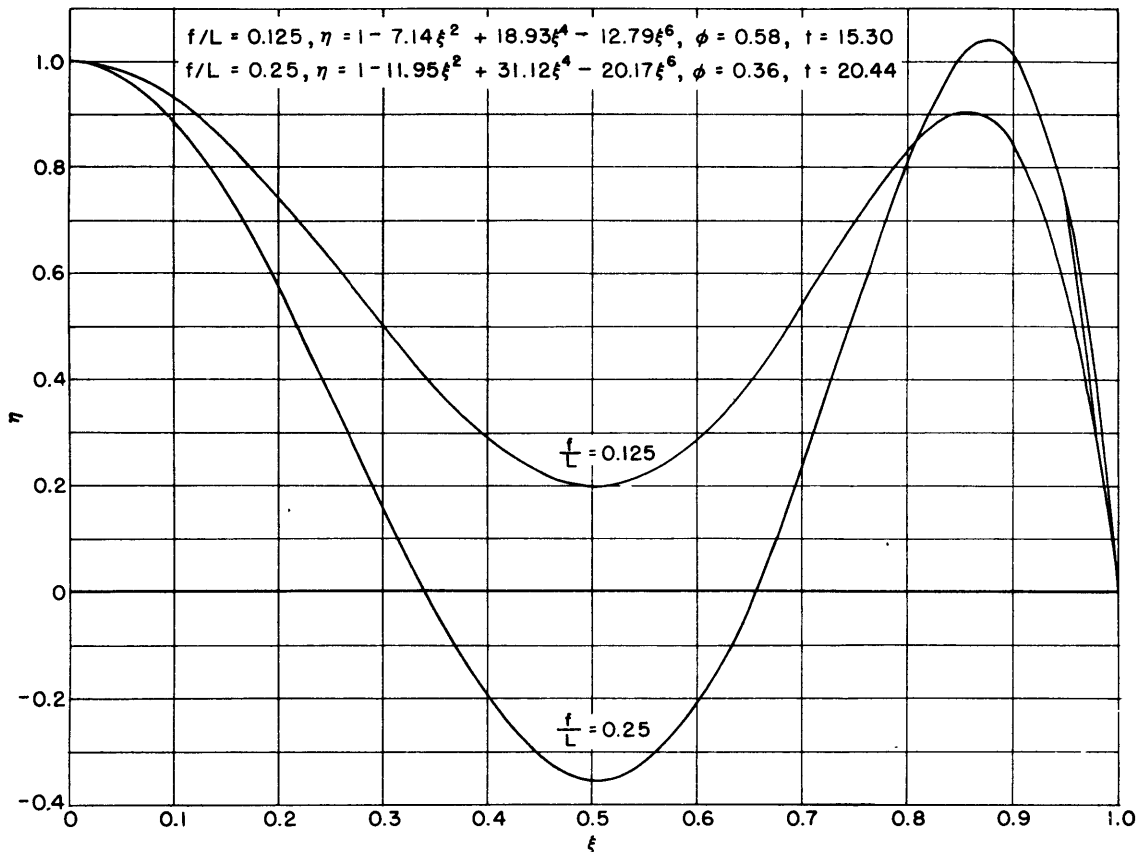


Figure 23 - Doublet Distribution for Least Resistance,
Two-Parameter Forms, $F = 0.408$, $\gamma_0 = 3$

When $\gamma_0 = 3$ the distributions shown on Figure 23 are obtained. We note again the difference in the shapes when $f/L = 0.125$ and $f/L = 0.25$. Extending the calculations to $\gamma_0 = 4$ and $\gamma_0 = 5$, curves of more and more "reasonable" character are obtained as shown in Figures 24 and 25.

The apparent failure of the theory to yield useful results in some cases, is often due to lack of suitable conditions imposed. There is no reason, for instance, to expect a solution which leads to a "normal" prismatic coefficient if no restrictions as to this coefficient are made. On the contrary, it is rather fortunate that one obtains results which meet other requirements of practice (i.e., are "reasonable"), without this restriction in certain ranges of Froude numbers.

5.2. ISOPERIMETRIC PROBLEMS, ONE-PARAMETER FORMS

Introducing a condition $\phi = \text{const}$ we obtain an isoperimetric problem. Then Equation [34] retains only one arbitrary parameter. This can be

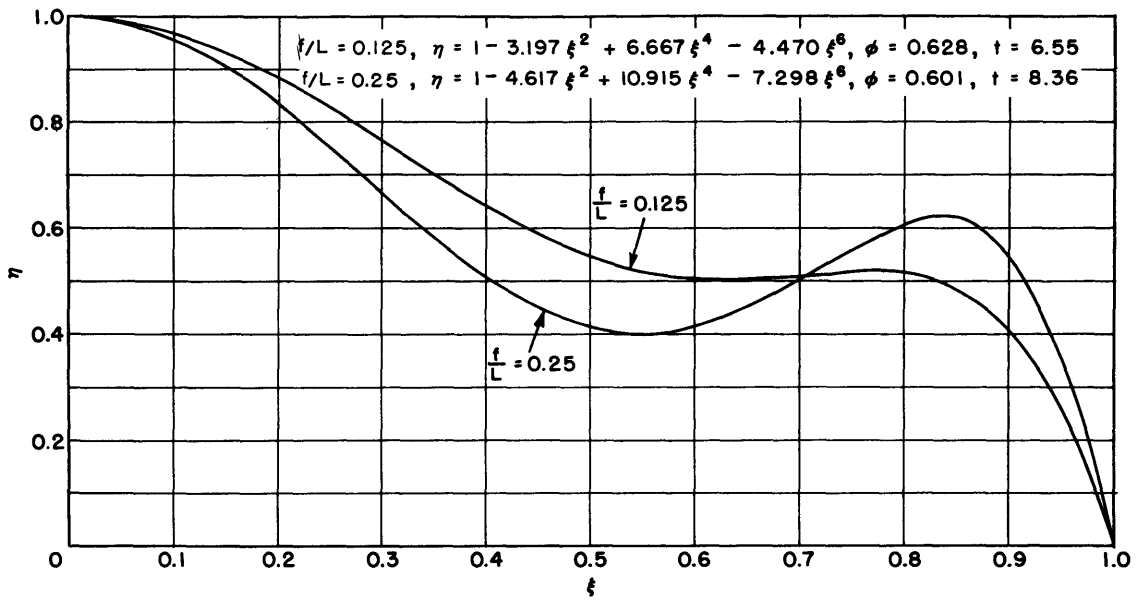


Figure 24 - Doublet Distribution for Least Resistance,
Two-Parameter Forms, $F = 0.354, \gamma_0 = 4$

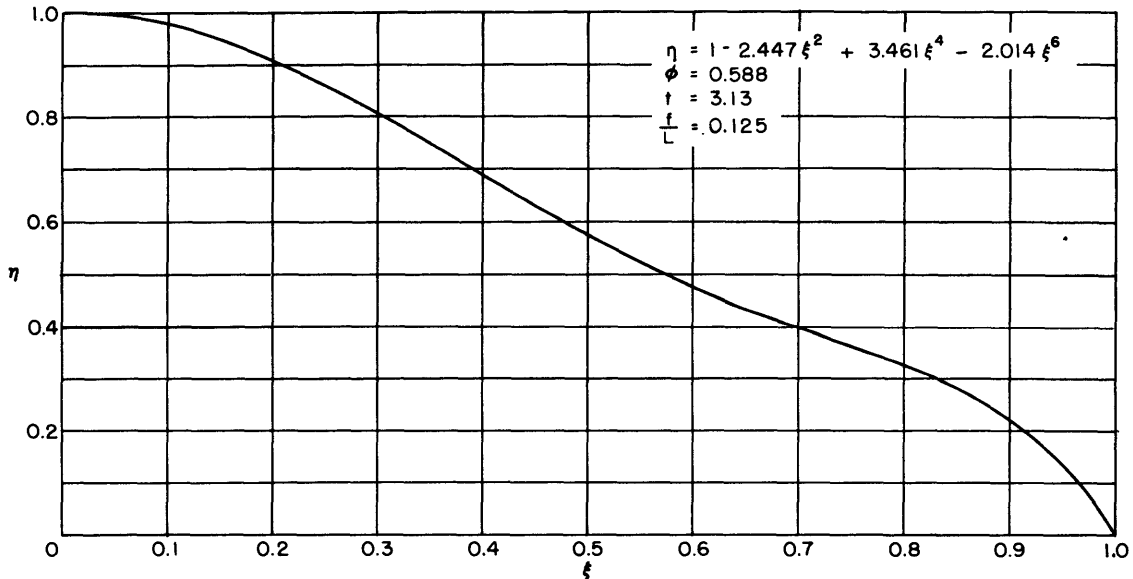


Figure 25 - Doublet Distribution for Least Resistance,
Two-Parameter Form, $F = 0.316, \gamma_0 = 5$

interpreted, for example, as Taylor's tangent value t . The resulting equation is of the type

$$\eta(\xi) = \eta_0(\xi) - \frac{3}{8}t' \left[\xi^2 - \frac{10}{3}\xi^4 + \frac{7}{3}\xi^6 \right] \quad [38]$$

Here $\eta_0(\xi)$ is a given polynomial complying with the condition $\phi = \text{const}$; its tangent value t_0 may be chosen in such a way that the equation η_0 is as simple as possible. The function

$$-\frac{3}{8} \left[\xi^2 - \frac{10}{3}\xi^4 + \frac{7}{3}\xi^6 \right] = \Delta_2 \eta(\xi) \quad [38a]$$

has the properties:

1. $\frac{\partial \Delta_2 \eta(1)}{\partial \xi} = -1$
2. $\Delta_2 \eta(0) = \Delta_2 \eta(1) = 0$
3. $\int_0^1 \Delta_2 \eta(\xi) d\xi = 0$

t' is the variable tangent parameter, the resulting t of the Equation [38] being obviously $t = t' + t_0$.

$$\text{Assuming } \phi = 2/3, \eta_0 = 1 - \xi^2$$

$$\frac{\partial \eta}{\partial \xi} = -2\xi - \frac{3}{4}t' \left[\xi - \frac{20}{3}\xi^3 + 7\xi^5 \right]$$

one obtains

$$R = \frac{9}{16} t'^2 A_2 + 3t' A_1 + 4m_{11} \quad [39]$$

$$\frac{\partial R}{\partial t'} = \frac{9}{8} t' A_2 + 3A_1 = 0 \quad [39a]$$

with

$$A_2 = m_{11} + \frac{400}{9} m_{33} + 49m_{55} - \frac{40}{3} m_{13} + 14m_{15} - \frac{280}{3} m_{35}$$

$$A_1 = m_{11} - \frac{20}{3} m_{13} + 7m_{15}$$

hence

$$t' = -\frac{8}{3} \frac{A_1}{A_2} \quad [39b]$$

Another isoperimetric problem is given by $t = \text{const}$ and ϕ variable. Although this problem looks somewhat artificial since there are no technical reasons to keep the tangent of the sectional-area curve rigidly fixed the

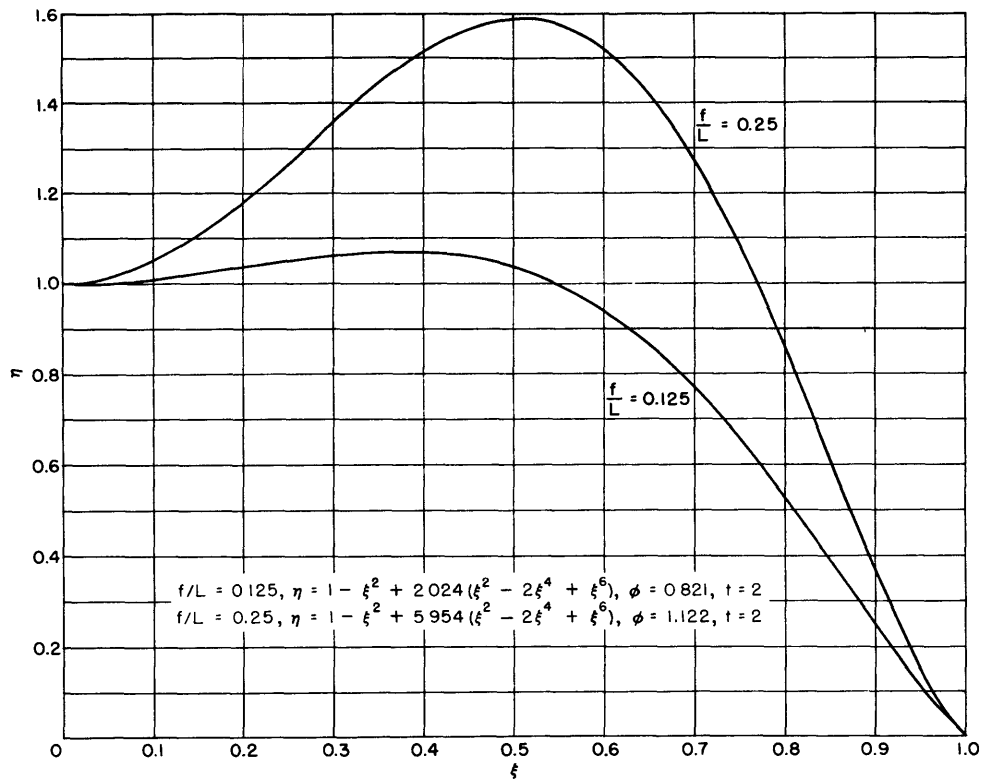


Figure 26 - Doublet Distribution for Least Resistance, One-Parameter Forms, $F = 0.408$, $\gamma_0 = 3$

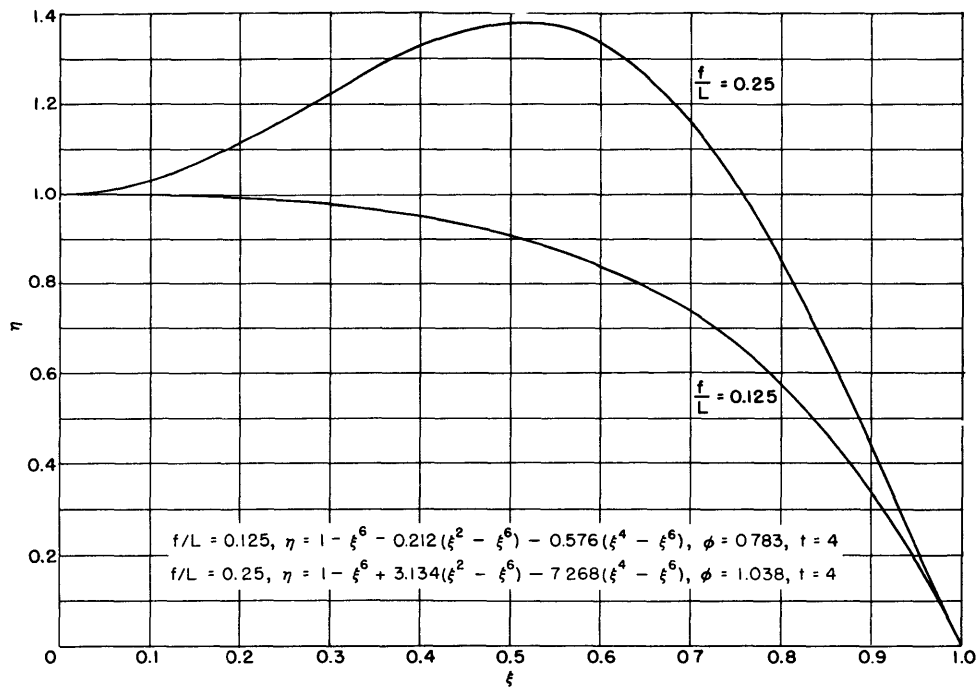


Figure 27 - Doublet Distribution for Least Resistance, One-Parameter Forms, $F = 0.408$, $\gamma_0 = 3$

results are interesting. Figures 26 and 27 show that assuming rather different t values optimum ship lines with a similar trend may be obtained.

We notice that the optimum area coefficient ϕ for a medium depth of immersion $f/L = 0.25$ is much higher than for a slight immersion $f/L = 0.125$. This might have been inferred from the shift of the resistance curves following Figures 6, 7 and 8.

The necessary formalism is again very simple: assuming as before a curve η_0 with the fixed $t = t_0$ value, for example as before, $\eta_0 = 1 - \xi^2$, $t_0 = 2$, and denoting $\phi = \phi_0 + \phi'$,

$$\eta = 1 - \xi^2 + 13.125\phi'(\xi^2 - 2\xi^4 + \xi^6) \quad [40]$$

$$\Delta_1 \eta(\xi) = 13.125(\xi^2 - 2\xi^4 + \xi^6) \quad [40a]$$

complies with

$$1. \quad \Delta_1 \eta(0) = \Delta_1 \eta(1) = 0$$

$$2. \quad \int_0^1 \Delta_1 \eta(\xi) d\xi = 1$$

$$3. \quad \frac{\partial \Delta_1 \eta(1)}{\partial \xi} = 0$$

from

$$\frac{\partial \eta}{\partial \xi} = -2\xi + 26.25\phi'[\xi - 4\xi^3 + 3\xi^5]$$

we obtain

$$\phi' = \frac{2}{26.25} \frac{A'_1}{A'_2} \quad [41]$$

with

$$A'_2 = m_{11} + 16m_{33} + 9m_{55} - 8m_{13} + 6m_{15} - 24m_{35}$$

$$A'_1 = m_{11} - 4m_{13} + 3m_{15}$$

6. RESISTANCE CURVES OF THE FAMILY (2, 4, 6; ϕ ; t)

A systematic survey of resistance properties of ship forms can be obtained by a different approach, i.e., varying the parameters of a given family of ship lines and plotting the corresponding resistance curves. Restricting ourselves to a two-parameter equation

$$(2, 4, 6; \phi; t) = 1 - \sum_{2,4,6} a_n \xi^n \quad [34]$$

Equation [35] can be used for calculating the resistance, or still simpler,

$$R = 4[a_2^2 m_{11} + 4a_4^2 m_{33} + 9a_6^2 m_{55} + 4a_2 a_4 m_{13} + 6a_2 a_6 m_{15} + 12a_4 a_6 m_{35}] \quad [42]$$

The parameters a_2 , a_4 and a_6 are connected with the basic form coefficients ϕ and t by the equations

$$\begin{aligned} a_2 &= 9 - \frac{105}{8} \phi + \frac{3}{8} t \\ a_4 &= -15 + \frac{105}{4} \phi - \frac{5}{4} t \\ a_6 &= 1 - a_2 - a_4 \end{aligned} \quad [43]$$

Table 3 contains wave-resistance coefficients r_0 for $t = 0, 1, 2, 3$ and $0.68 \geq \phi \geq 0.56$ with an interval of $\Delta\phi = 0.02$ within a range of Froude numbers $1 \geq F \geq 0.25$ (for $t = 0$ additionally $= 0.50, 0.52, 0.54$) at a depth of immersion ratio $f/L = 0.125$.

The corresponding curves spaced $\Delta\phi = 0.04$ are shown on Figures 28 to 35 grouped following t and ϕ . The main purpose of these plots is to demonstrate the dependence of the wave resistance upon t for $\phi = \text{const}$; it is interesting to note that the peak values (cf page 24) differ as much as ~ 15 percent for $t = 0$ and $t = 3$, in close agreement with results known from studies of surface ships and the tendency exposed by the minimum calculations. One should, however, remember that theory tends to overestimate the favorable interference effects and that viscosity precludes the realization of excessive angles of run. On the other hand, for very high Froude numbers the relative importance of asymmetry decreases, so that forms with steep slopes at the bow and moderate slopes at the stern may be advantageous.

SUMMARY

Using Havelock's basic work and some former investigations by the present author, a systematic synopsis is made on the wave resistance of bodies of revolution. Tables evaluated by the Bureau of Standards and graphs are given which allow the investigator to estimate immediately the wave resistance of a wide class of bodies of revolution defined by doublet distributions along the axis expressed by polynomials.

Some discussions refer to the relations between this distribution $\mu^*(\xi)$ and the sectional area of the body $A^*(\xi)$. For "normal" shapes of distribution the usual assumption is made that there is affinity between $\mu^*(\xi)$

and $A^*(\xi)$. In extreme cases the shape of the body can be calculated by methods due to Landweber and Amtsberg; no corrections, however, are given for the influence of the free surface on the shape.

Within the first-order theory the resistance can be split up into a main part due to a symmetric distribution with respect to the midship section and a part due to asymmetry, which can be investigated independently. Large amounts of asymmetry can influence the resistance detrimentally in some ranges of the Froude number.

The investigation of the resistance as a function of the body form leads to conclusions which sometimes are contrary to those derived for surface ships. The choice of appropriate prismatic coefficients varies decisively with the range of the Froude number, as is clearly illustrated by the numerous graphs. The same applies to the influence of the tangent value t . Ceteris paribus the resistance is approximately proportional to the square of the midship section.

The dependence of the resistance upon the depth of immersion is investigated; this dependence is best explained by the ratio f/λ , where $\lambda = \frac{2\pi U^2}{g}$ is the length of the free wave. Thus for common prismatic coefficients the wave resistance decreases rapidly with increasing f except in the range of high Froude numbers (large λ values). In the range of high F the calculation of forms (distributions) of least resistance leads sometimes to results bare of practical applicability; by introducing suitable restrictions such difficulties are avoided. These investigations show important peculiarities of the distributions.

A set of resistance diagrams calculated for the family $(2,4,6;\phi;t)$ gives a survey of the resistance properties of a class of normal bodies.

Acknowledgment is made of the valuable help provided by Messrs. Samuel Lum and David Rego and Miss Janet Kendrick of the Taylor Model Basin. The author further wishes to express his gratitude to Dr. Alt, Dr. Levin and Mr. Blum of the National Bureau of Standards. Finally, it is a pleasure for the author to thank his colleagues, Mr. Cummins and Mr. Landweber, for reviewing the present report.

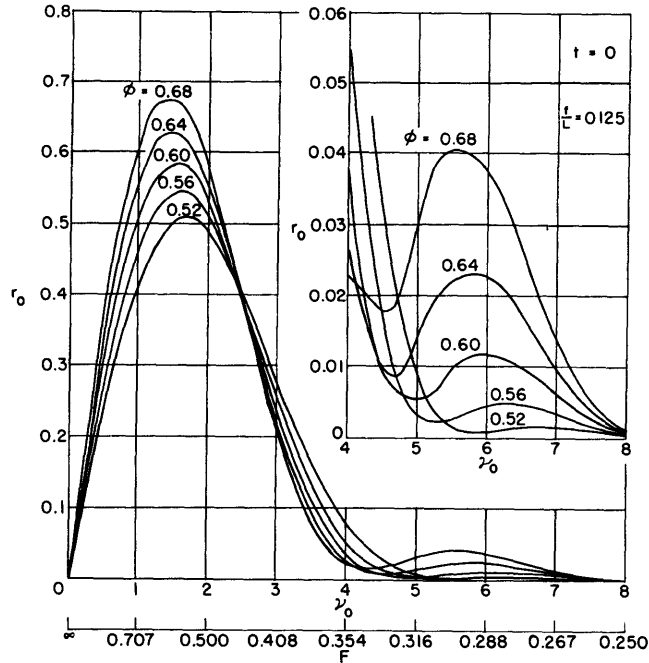


Figure 28 - Wave-Resistance Coefficients $r_0 = \frac{R}{4\pi C^2 \rho g b^4 / a}$,
of Symmetrical Bodies Belonging to the Class
 $(2,4,6;\phi;t) = 1 - a_2 \xi^2 - a_4 \xi^4 - a_6 \xi^6$ Over $\gamma_0 = 1/2F^2$ and $F = U/\sqrt{gL}$
 $t = 0$

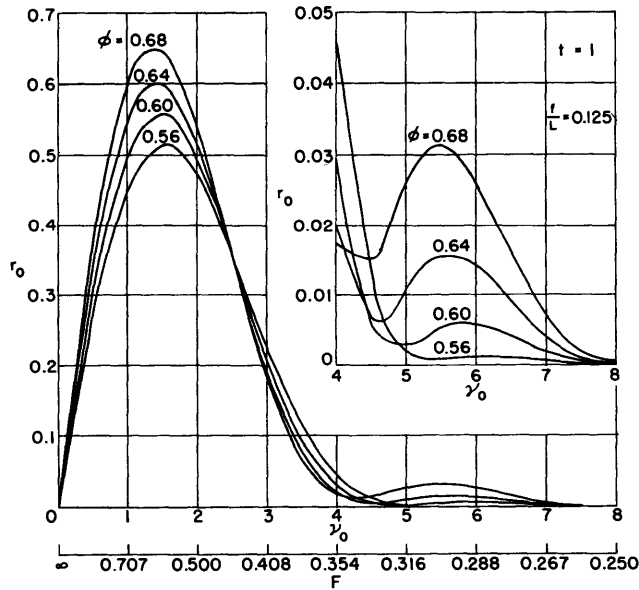


Figure 29 - Wave-Resistance Coefficients $r_0 = \frac{R}{4\pi C^2 \rho g b^4 / a}$,
of Symmetrical Bodies Belonging to the Class
 $(2,4,6;\phi;t) = 1 - a_2 \xi^2 - a_4 \xi^4 - a_6 \xi^6$ Over $\gamma_0 = 1/2F^2$ and $F = U/\sqrt{gL}$
 $t = 1$

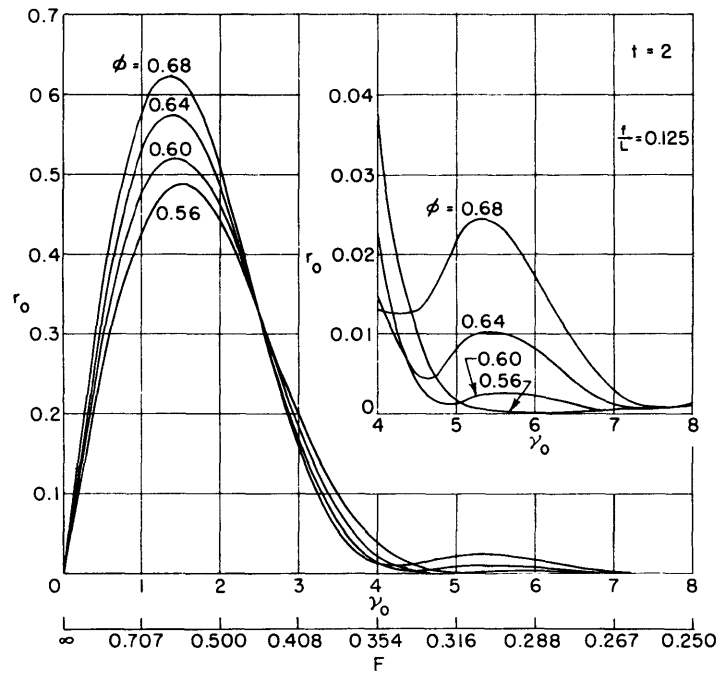


Figure 30 - Wave-Resistance Coefficients $r_0 = \frac{R}{4\pi C^2 \rho g b^4/a}$ of Symmetrical Bodies Belonging to the Class $(2,4,6;\phi;t) = 1 - a_2 \xi^2 - a_4 \xi^4 - a_6 \xi^6$ Over $\gamma_0 = 1/2F^2$ and $F = U/\sqrt{gL}$
 $t = 2$

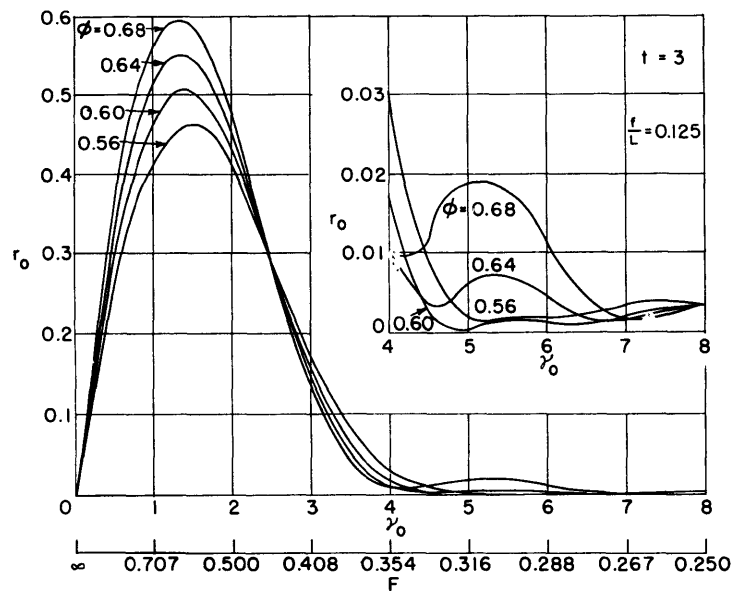


Figure 31 - Wave-Resistance Coefficients $r_0 = \frac{R}{4\pi C^2 \rho g b^4/a}$ of Symmetrical Bodies Belonging to the Class $(2,4,6;\phi;t) = 1 - a_2 \xi^2 - a_4 \xi^4 - a_6 \xi^6$ Over $\gamma_0 = 1/2F^2$ and $F = U/\sqrt{gL}$
 $t = 3$

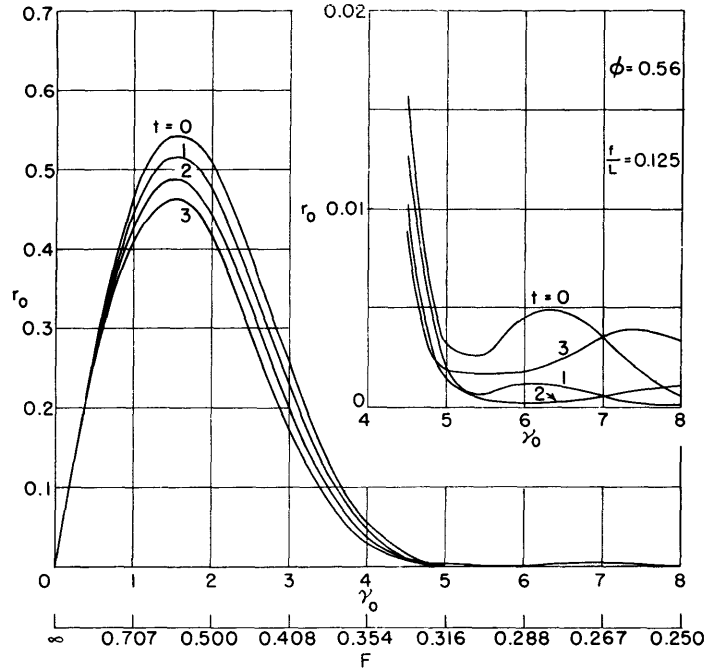


Figure 32 - Wave-Resistance Coefficients $r_0 = \frac{R}{4\pi C^2 \rho g b^4/a}$,
of Symmetrical Bodies Belonging to the Class
 $(2,4,6;\phi;t) = 1 - a_2 \xi^2 - a_4 \xi^4 - a_6 \xi^6$ Over $\gamma_0 = 1/2F^2$ and $F = U/\sqrt{gL}$
 $\phi = 0.56$

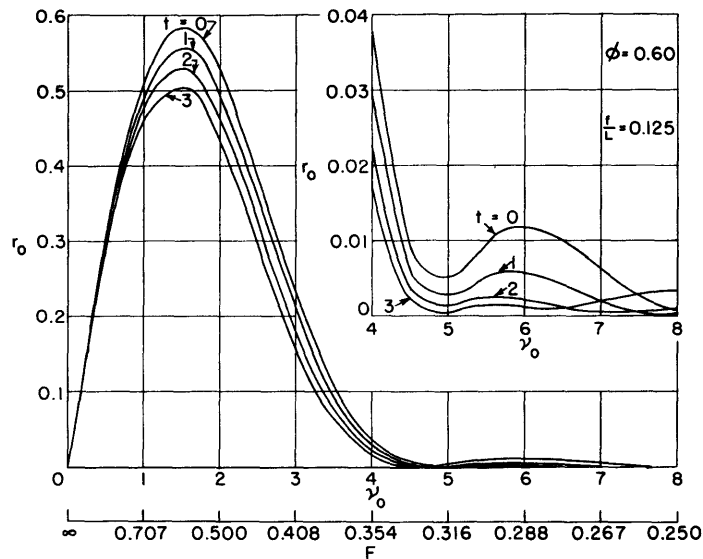


Figure 33 - Wave-Resistance Coefficients $r_0 = \frac{R}{4\pi C^2 \rho g b^4/a}$,
of Symmetrical Bodies Belonging to the Class
 $(2,4,6;\phi;t) = 1 - a_2 \xi^2 - a_4 \xi^4 - a_6 \xi^6$ Over $\gamma_0 = 1/2F^2$ and $F = U/\sqrt{gL}$
 $\phi = 0.60$

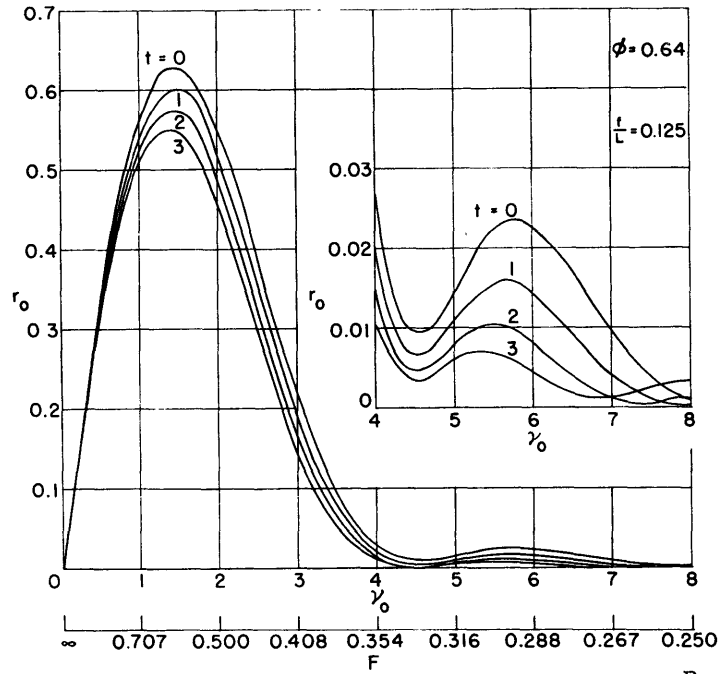


Figure 34 - Wave-Resistance Coefficients $r_0 = \frac{R}{4\pi C^2 \rho g b^4/a}$,
of Symmetrical Bodies Belonging to the Class
 $(2,4,6;\phi;t) = 1 - a_2 \xi^2 - a_4 \xi^4 - a_6 \xi^6$ Over $\gamma_0 = 1/2F^2$ and $F = U/\sqrt{gL}$
 $\phi = 0.64$

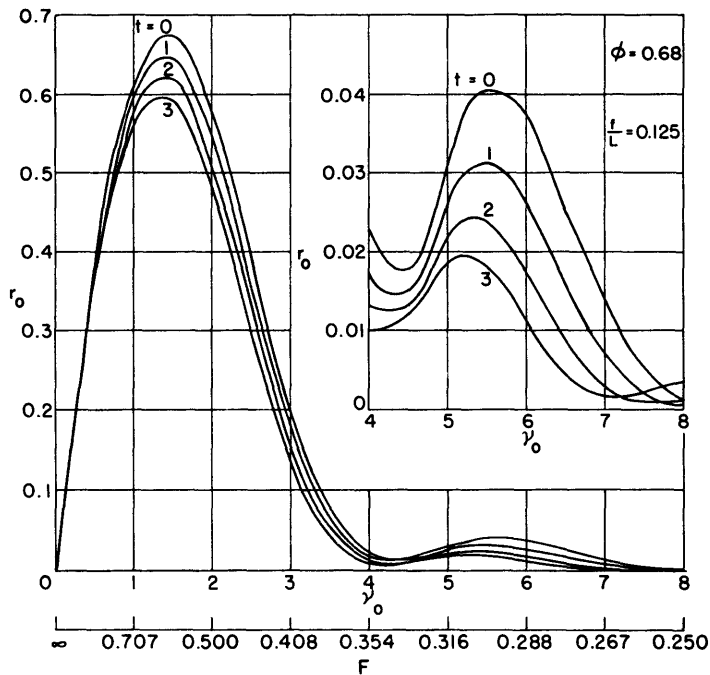


Figure 35 - Wave-Resistance Coefficients $r_0 = \frac{R}{4\pi C^2 \rho g b^4/a}$,
of Symmetrical Bodies Belonging to the Class
 $(2,4,6;\phi;t) = 1 - a_2 \xi^2 - a_4 \xi^4 - a_6 \xi^6$ Over $\gamma_0 = 1/2F^2$ and $F = U/\sqrt{gL}$
 $\phi = 0.68$

APPENDIX I

APPROXIMATE CALCULATION OF THE SURFACE S OF
A CLASS OF ELONGATED BODIES OF REVOLUTION

From Guldin's rule

$$S = 2\pi \int y ds = 2\pi \int_{-a}^{+a} y \sqrt{1 + (y')^2} dx$$

$$S \cong 2\pi \int_{-a}^{+a} y dx + \pi \int_{-a}^{+a} y y'^2 dx = \pi A_m + \pi \int_{-a}^{+a} y y'^2 dx \quad [29]$$

the main part of the surface is given by π times area of the meridian section A_m plus a correction term neglecting higher order terms.

With $y = bH$

$$y' = \frac{b}{a} \frac{\partial H}{\partial \xi}$$

the correction term becomes

$$\pi \int_{-a}^{+a} y y'^2 dx = \pi ab \frac{b^2}{a^2} \int_{-1}^{+1} H \left(\frac{\partial H}{\partial \xi} \right)^2 d\xi = \pi ab \frac{b^2}{a^2} I \quad [30]$$

i.e., the correction term is equal to the area of an ellipse with the axes a , b multiplied by the square of the elongation ratio and a numerical value I dependent upon the equation of the curve. To get an idea, with obvious denotations,

$$I_2 = 16/15 \quad H = 1 - \xi^2$$

$$I_4 = 128/77 \quad H = 1 - \xi^4$$

$$I_n = \frac{2n^3}{(2n-1)(3n-1)} \quad H = 1 - \xi^n$$

The next term in the expansion of S

$$- \frac{\pi}{4} \int_{-a}^{+a} y y'^4 dx = \frac{\pi ab}{4} \frac{b^4}{a^4} \int_{-1}^{+1} HH'^4 d\xi \quad [31]$$

with $H' = \partial H / \partial \xi$ is obviously of the order b^4/a^4 . However, taking $H = 1 - \xi^n$ the factor

$$\int_{-1}^{+1} HH'^4 d\xi = K = \frac{2n^5}{(4n-3)(5n-3)}$$

grows with n^5 when n is large. Provided b/a is not too small, say $\sim 1/7$, the error in neglecting all terms except the first (Equation [29]) is only permissible as long as $n \leq \sim 5$.

Using Equation [30], various changes in S can be easily estimated within the range of validity of the formula. For instance, the influence of an asymmetric term can be discussed as follows:

$$H_t = H_s + H_a$$

$$I_s = \int_{-1}^{+1} (H_s + H_a)(H'_s + H'_a)^2 d\xi = I_s + \int_{-1}^{+1} H_s H_a'^2 d\xi + \int_{-1}^{+1} H_a H_s' H_a' d\xi$$

[32]

Where I_s refers to the even part following [30]. When the meridian curve has vertical tangents at the bow and stern (or bow or stern) the preceding reasoning can be applied in principle to a range $1 - \epsilon_F \geq \xi \geq -(1 - \epsilon_A)$, and the remainder is calculated as the surface area of a segment of the sphere generated by the radius of curvature at the nose or stern. Such an approach is, however, only useful when the integrals involved are of simple type.

APPENDIX II

EVALUATION OF THE AUXILIARIES INTEGRALS*

The integral to be computed is given by:

$$m_{ij} = I = C_0 \int_{\gamma_0}^{\infty} e^{-\frac{k\gamma^2}{\gamma_0}} \frac{(\gamma/\gamma_0)^2}{\sqrt{(\gamma/\gamma_0)^2 - 1}} M_i(\gamma) M_j(\gamma) d\gamma$$

The functions $e^{-\frac{k\gamma^2}{\gamma_0}}$ and $M_i(\gamma)M_j(\gamma)$ are well-behaved in the entire interval of integration. However, the algebraic function $(\gamma/\gamma_0)^2 / \sqrt{(\gamma/\gamma_0)^2 - 1}$ causes some difficulty at the lower limit of integration, i.e., at $\gamma = \gamma_0$. In the neighborhood of $\gamma = \gamma_0$, the contribution of I is far from negligible and therefore an investigation was carried out to determine the asymptotic behavior of the integral as a function of the upper limit. Specifically, the following function was examined:

$$I(\epsilon) = \int_{\gamma_0}^{\gamma_0(1+\epsilon)} M(\gamma)f(\gamma)d\gamma \quad \epsilon > 0$$

where

$$M(\gamma) = e^{-\frac{k\gamma^2}{\gamma_0}} M_i(\gamma)M_j(\gamma)$$

and

$$f(\gamma) = \frac{(\gamma/\gamma_0)^2}{\sqrt{(\gamma/\gamma_0)^2 - 1}}$$

It was found that:

$$I(\epsilon) \sim e^{-k\gamma_0} M_i(\gamma)M_j(\gamma) \gamma_0 \sqrt{2\epsilon} \left\{ 1 + \frac{7}{12}\epsilon + O(\epsilon^2) \right\}$$

This asymptotic expression was used to determine the interval of integration, $\Delta\gamma$ for a numerical integration. This interval was too small to be practicable, even allowing for subsequent changes in $\Delta\gamma$.

A new approach to the problem was sought in a suitable transformation. The following transformation very quickly presented itself:

$$\gamma = Z^2 + \gamma_0$$

$$d\gamma = 2Z dZ$$

The original integral was transformed as given by:

*By J. Blum, National Bureau of Standards

$$I = \frac{2}{\gamma_0} \int_0^\infty e^{-\frac{k}{\gamma_0}(Z^2 + \gamma_0)^2} \frac{(Z^2 + \gamma_0)^2}{\sqrt{Z^2 + 2\gamma_0}} M_1(\gamma) M_j(\gamma) (Z^2 + \gamma_0) dZ$$

In this form, the integrand behaves properly, (there is no longer a singularity at $\gamma = \gamma_0$) and the integral converges rapidly.

The integral was actually computed by using the form in [5]. The numerical integration was performed once using Simpson's rule and a second time using the trapezoidal rule—for checking purposes. The interval ΔZ was taken as 0.1 and the range extended from 0.0 to approximately 3.5. The M functions were computed from previous tables by using 4-point Lagrangian interpolation. The exponential function was computed from tables and the use of the approximation $e^{-x} = 1 - x + x^2/2$, $x < 0.01$. The algebraic function in the integrand was computed in straight form and fashion. All of this work was done on the IBM electronic calculator (type 604) and the auxiliary IBM punch card equipment. All the IBM operations were checked—independently wherever possible.

TABLE 2

Resistance Coefficients r_{os} , r_{oa} , r_o and c_w of the
Four TMB Models I, II, III, IV; see Figures 14 and 15

γ_0	r_{os}	r_{oa}	r_o	c_w	γ_0	r_{os}	r_{oa}	r_o	c_w
f/L = 0.125 Model I					f/L = 0.125 Model III				
.5	0.29452	0.0104	0.3049	0.001409	.5	0.36498	0.002771	0.36775	0.001559
1.0	.48255	.0328	.5153	.004761	1.0	.58143	.009204	.59063	.005006
1.5	.54304	.0594	.6024	.008349	1.5	.63080	.016713	.64751	.008232
2.0	.48218	.0817	.5639	.01042	2.0	.52910	.022700	.55180	.009354
2.5	.34676	.0918	.4386	.01013	2.5	.34891	.024644	.37355	.007916
3.0	.20136	.0859	.2873	.007964	3.0	.17596	.021705	.19767	.005026
3.5	.09112	.0669	.1580	.005110	3.5	.06278	.015373	.07815	.002318
4.0	.02937	.0428	.0722	.002669	4.0	.01623	.008461	.02469	.000837
4.5	.00572	.0217	.0274	.001131	4.5	.01234	.003367	.01571	.000601
5.0	.00184	.0081	.0099	.000457	5.0	.02159	.000940	.02253	.000955
5.5	.00335	.0020	.0054	.000274	5.5	.02589	.000562	.02645	.001233
6.0	.00370	.0007	.0044	.000246	6.0	.02129	.000997	.02229	.001134
6.5	.00244	.0012	.0036	.000216	6.5	.01252	.001286	.01381	.000761
7.0	0.00096	0.0016			7.0	0.00500	0.001118	0.00612	0.000363
f/L = 0.125 Model II					f/L = 0.125 Model IV				
.5	0.32962	0.006262	0.335882	0.001478	.5	0.40102	0.001320	0.40234	0.001643
1.0	.53257	.019503	.552073	.004858	1.0	.62996	.003790	.63375	.005192
1.5	.58729	.034835	.622125	.008211	1.5	.67440	.006386	.68079	.008367
2.0	.50553	.047328	.552858	.009729	2.0	.55349	.008096	.56159	.009202
2.5	.34728	.052235	.399515	.008788	2.5	.35194	.008092	.36003	.007374
3.0	.18718	.047648	.234828	.006199	3.0	.16756	.006369	.17393	.004275
3.5	.07449	.035789	.110279	.003396	3.5	.05549	.003822	.05931	.001707
4.0	.01955	.021718	.041268	.001452	4.0	.01863	.001663	.02029	.000665
4.5	.00552	.010117	.015637	.000619	4.5	.02534	.000632	.02597	.000956
5.0	.00855	.003285	.011835	.000521	5.0	.04020	.000668	.04087	.001674
5.5	.01212	.000792	.012912	.000625	5.5	.04408	.001156	.04524	.002039
6.0	.01086	.000731	.011591	.000612	6.0	.03429	.001473	.03576	.001758
6.5	.00657	.001227	.007797	.000446	6.5	.02006	.001343	.02140	.001140
7.0	0.00261	0.001340	0.003950	0.000243	7.0	0.00803	0.000912	0.00894	0.000513
f/L = 0.25 Model I					f/L = 0.25 Model III				
.5	0.093464	0.0018	0.0952	0.000440	.5	0.117864	0.000380	0.118244	0.0005011
1.0	.158660	.0066	.1652	.001526	1.0	.196046	.001796	.197842	.0016769
1.5	.163934	.0127	.1766	.002448	1.5	.195792	.003625	.199417	.0025354
2.0	.125729	.0167	.1424	.002632	2.0	.142235	.004787	.147022	.0024923
2.5	.075703	.0168	.0925	.002137	2.5	.078642	.004667	.083309	.0017653
3.0	.036196	.0134	.0495	.001372	3.0	.032522	.003527	.036049	.0009167
3.5	.013347	.0088	.0221	.000715	3.5	.009079	.002087	.011166	.0003312
4.0	0.003449	0.0046	0.0080	0.000296	4.0	0.001301	0.000941	0.002242	0.0000760
f/L = 0.25 Model II					f/L = 0.25 Model IV				
.5	0.105547	0.001054	0.106601	0.0004690	.5	0.130528	0.000229	0.130757	0.0005356
1.0	.177413	.003961	.181374	.0015959	1.0	.214810	.000823	.215633	.0017667
1.5	.180062	.007542	.187604	.0024760	1.5	.211405	.001496	.212901	.0026164
2.0	.134025	.009821	.143846	.0025315	2.0	.150538	.001820	.152358	.0024964
2.5	.077166	.009683	.086849	.0019105	2.5	.080224	.001621	.081845	.0016764
3.0	.034261	.007564	.041825	.0011041	3.0	.030993	.001086	.032079	.0007884
3.5	.011006	.004751	.015757	.0004853	3.5	.007526	.000532	.008058	.0002311
4.0	0.002118	0.002371	0.004389	0.0001545	4.0	0.000940	0.000173	0.001113	0.0000365
f/L = 0.5 Model I					f/L = 0.5 Model III				
.5	0.025894				.5	0.032826	0.000052	0.032878	0.0001393
1.0	.033468				1.0	.041753	.000254	.042007	.0003561
1.5	.023467				1.5	.028431	.000413	.028844	.0003667
2.0	.011701				2.0	.013493	.000385	.013878	.0002353
2.5	.004499				2.5	.004794	.000250	.005044	.0001069
3.0	.001366				3.0	.001267	.000122	.001389	.0000353
3.5	.000319				3.5	.000226	.000046	.000272	.0000081
4.0	0.000052				4.0	0.000010	0.000013	0.000023	0.0000008
f/L = 0.5 Model II					f/L = 0.5 Model IV				
.5	0.029348	0.000207	0.029555	0.0001300	.5	0.036364	0.000037	0.036401	0.0001491
1.0	.037590	.000597	.038187	.0003360	1.0	.046002	.000128	.046130	.0003779
1.5	.025958	.000868	.026826	.0003541	1.5	.030924	.000178	.031102	.0003822
2.0	.012605	.000787	.013392	.0002357	2.0	.014384	.000151	.014535	.0002382
2.5	.004650	.000513	.005163	.0001136	2.5	.004938	.000090	.005028	.0001030
3.0	.001315	.000259	.001574	.0000415	3.0	.001223	.000039	.001262	.0000310
3.5	.000269	.000104	.000373	.0000115	3.5	.000188	.000012	.000200	.0000057
4.0	0.000033	0.000033	0.000066	0.0000023	4.0	0.000010	0.000003	0.000013	0.0000004

TABLE 3

Resistance Coefficients $r_0 = \frac{R}{4\pi C^2 \rho g b^4/a}$ of Symmetrical Bodies Belonging to the Class

$$\eta = 1 - a_2 \xi^2 - a_4 \xi^4 - a_6 \xi^6 \quad \frac{\partial \eta}{\partial \xi} = -2(a_2 \xi + 2a_4 \xi^3 + 3a_6 \xi^5)$$

$$r_0 = 4 \left(a_2^2 m_{11} + 4a_4^2 m_{33} + 9a_6^2 m_{55} + 4a_2 a_4 m_{13} + 6a_2 a_6 m_{15} + 12a_4 a_6 m_{35} \right)$$

$\psi \backslash \gamma_0$	0.5	1.0	1.5	2.0	2.5	3.0	3.5	4.0	4.5	5.0	5.5	6.0	6.5	7.0	7.5	8.0
t = 0																
.50	0.2262167	0.395227	0.482176	0.478585	0.399765	0.287017	0.177414	0.0931007	0.0399619	0.0130724	0.00291654	0.000501923	0.000654186	0.000906827	0.000754301	0.000409008
.52	.241061	.417347	.501587	.487737	.397167	.275175	.161702	.0787014	.0299938	.00802265	.00142954	.000915184	.00153311	.00154011	.00101411	.000444701
.54	.256458	.439875	.521448	.497324	.394953	.264013	.147151	.0659474	.0219018	.00472942	.00135409	.00224750	.00289584	.00237037	.00132932	.000493900
.56	.272409	.462811	.541757	.507347	.393122	.253531	.133762	.0548385	.0156858	.00319270	.00269019	.00449889	.00474239	.00339760	.00169992	.000556605
.58	.288913	.486154	.562515	.517805	.391676	.243731	.121534	.0453746	.0113457	.00341247	.00543785	.00766933	.00707276	.00462181	.00212591	.000632815
.60	.305971	.509906	.583722	.528699	.390614	.234610	.110468	.0375558	.00888162	.00538875	.00959706	.0117588	.00988694	.00604300	.00260729	.000722531
.62	.323582	.534066	.605378	.540029	.389936	.226170	.100563	.0313821	.00829351	.00912153	.0151678	.0167674	.0131849	.00766116	.00314406	.000825753
.64	.341747	.558634	.627483	.551794	.389642	.218411	.0918200	.0268536	.00958139	.0146108	.0221501	.0226950	.0169668	.00947630	.00373623	.000942480
.66	.360465	.583609	.650037	.563994	.389732	.211332	.0842379	.0239701	.0127452	.0218566	.0305440	.0295417	.0212324	.0114884	.00438379	.00107271
.68	0.379736	0.608993	0.673040	0.576630	0.390207	0.204933	0.0778173	0.0227317	0.0177851	0.0308589	0.0403494	0.0373074	0.0259818	0.0136975	0.00508674	0.00121645
t = 1																
.56	0.267895	0.446802	0.515401	0.474195	0.358427	0.224501	0.114702	0.0456125	0.0126115	0.00194853	0.000726062	0.00116444	0.00106146	0.000538598	0.000167800	0.000108211
.58	.284159	.470487	.536077	.484420	.357237	.215331	.103345	.0367938	.00833174	.00157001	.00227915	.00302235	.00231546	.00108809	.000313147	.000156728
.60	.300976	.494580	.557203	.495080	.356432	.206841	.0931487	.0296200	.00592792	.00294800	.00524380	.00579932	.00405329	.00183479	.000513887	.000218750
.62	.318347	.519081	.578777	.506176	.356011	.199032	.0841138	.0240914	.00540008	.00608246	.00962000	.00949529	.00627493	.00277833	.000770019	.000294278
.64	.336271	.543990	.600799	.517707	.355974	.191904	.0762402	.0202079	.00674822	.0109735	.0154077	.0141104	.00898039	.00391889	.00108154	.000383311
.66	.354748	.569307	.623271	.529674	.356321	.185456	.0695280	.0179695	.00997234	.0176210	.0226071	.0196446	.0121697	.00525641	.00144846	.000485850
.68	0.373780	0.595031	0.646192	0.542075	0.357052	0.179688	0.0639773	0.0173762	0.0150724	0.0260250	0.0312179	0.0260978	0.0158427	0.00679090	0.00187077	0.000601895
t = 2																
.56	0.263667	0.429466	0.489245	0.442482	0.325335	0.197385	0.0972121	0.0375030	0.0103302	0.00150426	0.000423770	0.000271083	0.000301165	0.000553898	0.000882234	0.00102788
.58	.279690	.453492	.509839	.452473	.324402	.188846	.0867242	.0293293	.00611066	.000527452	.000782298	.000816457	.000478817	.000428905	.000746938	.00104870
.60	.296267	.477926	.530882	.462899	.323854	.180987	.0773976	.0228007	.00376711	.00130715	.00255238	.00228089	.00114028	.000500888	.000667035	.00108303
.62	.313397	.502768	.552374	.473761	.323690	.173809	.0692325	.0179172	.00329953	.00384335	.00573401	.00466439	.00228557	.000769848	.000642525	.00113087
.64	.331081	.528019	.574315	.485059	.323909	.167312	.0622288	.0146788	.00470793	.00813606	.0103272	.00796694	.00391467	.00123578	.000673406	.00119221
.66	.349318	.553677	.596705	.496792	.324513	.161495	.0563865	.0130855	.00799232	.0141853	.0163319	.0121886	.00602758	.00189870	.000759681	.00126705
.68	0.368109	0.579743	0.619544	0.508961	0.325501	0.156358	0.0517057	0.0131373	0.0131527	0.0219910	0.0237482	0.0173292	0.00862431	0.00275892	0.000901347	0.00135540
t = 3																
.56	0.259724	0.410802	0.463289	0.412207	0.293847	0.172184	0.0812897	0.0305101	0.00884174	0.00185989	0.00178332	0.00181881	0.00246152	0.00344350	0.00384322	0.00331561
.58	.275507	.435169	.483801	.421964	.293171	.164276	.0716716	.0229815	.00468247	.000284792	.000947282	.00105165	.00156282	.00264391	.00342728	.00330874
.60	.291843	.459945	.504762	.432158	.292880	.157049	.0632150	.0170980	.00239918	.000466200	.00152280	.00120355	.00114793	.00204129	.00306673	.00331538
.62	.308733	.485128	.526172	.442786	.292972	.150501	.0559197	.0128596	.00199186	.00240411	.00350987	.00227450	.00121685	.00163565	.00276158	.00333552
.64	.326176	.510720	.548031	.453850	.293449	.144635	.0497859	.0102663	.00346053	.00609853	.00690849	.00426453	.00176959	.00142698	.00251182	.00336916
.66	.344173	.536719	.570338	.465349	.294310	.139449	.0448135	.00931806	.00680518	.0115494	.0117187	.00717361	.00280615	.00141529	.00231745	.00341631
.68	0.362723	0.563126	0.593095	0.477284	0.295555	0.134943	0.0410024	0.0100149	0.0120258	0.0187569	0.0179404	0.0110018	0.00432652	0.00160058	0.00217848	0.00347697

REFERENCES

1. Hoerner, S., Jahrb. Luftfahrtforsch (Berlin), Vol. 5, 1942
2. Landweber, L., and Gertler, M., "Mathematical Formulation of Bodies of Revolution," TMB Report 719, September 1950.
3. Havelock, T., Proc. Royal Soc. A., Vol. 131, 1931
4. Havelock, T., Proc. Royal Soc. A., Vol. 132, 1932
5. Weinblum, G., Ingenieurarchiv, Vol. 7, pp. 104-117, 1936
6. Weinblum, G., Amtsberg, H., and Bock, W., "Tests on Wave Resistance of Immersed Bodies of Revolution" (Versuche über den Wellenwiderstand Getauchter Rotationskörper), Mitteilungen der Preussischen Versuchsanstalt für Wasserbau und Schiffbau, Berlin, 1936. TMB Report T-234, September 1950.
7. Weinig, F., Zeitschrift Techn. Physik, 1928
8. Munk, M.M., "Fluid Mechanics, Part 2," in Durand W.F. ed. Aerodynamic Theory, Vol. 1, 1934.
9. Havelock, T., Quart. Journ. Mech. Appl. Math., Vol. 2, 1949.
10. Amtsberg, H., Jahrb. Schiffb. Ges., Vol. 38, 1937.
11. Taylor, D.W., Schiffbau, 1904.
12. Taylor, D.W., Trans. Inst. Engineering Congress, San Francisco, 1915.
13. Weinblum, G., Schiffbau, Vol. 35, No. 6, March 1934, pp. 83-85.
14. Weinblum, G., Werft-Reederei-Hafen, Vol. 10, 1929, pp. 462-466, 489-493.
15. Weinblum, G., "Analysis of Wave Resistance," TMB Report 710, September 1950.
16. Weinstein, A., Quart. Appl. Math., Vol. 5, No. 4, January 1948.
17. Lamb, H., Hydrodynamics, VI ed., 1932.
18. Havelock, T., Proc. Royal Soc. A., Vol. 95, 1919.

MIT LIBRARIES

DUPL



3 9080 02754 1090

SEP 6 1983